Towards the development of an in-vitro test to better predict fibrotic tendency of biomaterials prior to implantation.

By:

Mr.Sanad Saad

190296731

A thesis submitted to the University of Sheffield for the degree of Doctor of Philosophy.

The University of Sheffield

Faculty of Engineering

Department of Materials Science and Engineering

July 2024

TABLE OF CONTENTS

Chapter 1. Introduction……16
1.1 Pelvic floor anatomy……16
1.1.1 Pelvic musculature……17
1.1.2 Fasciae and ligaments……17
1.2 Pelvic Organ Prolapse and Stress Urinary Incontinence……19
1.2.1 Definition……19
1.2.2 Epidemiology……19
1.2.3 Impact……20
1.2.4 Risk Factors……20
1.2.5 Pathophysiology……21
1.2.5.1 Alterations in urethra-vesical axis. ……22
1.2.5.2 Intrinsic Sphincter Deficiency……22
1.2.5.3 Hammock Theory……23
1.2.5.4 Integral Theory……23
1.2.6 Treatment modalities……23
1.3 Biomaterial development and use in the pelvic floor ……24
1.3.1 Biological grafts……24
1.3.2 Synthetic grafts……25
1.3.3 Complications and current regulations……27
1.4 Wound healing……29
1.5 Fibrosis……33
1.5.1 Biomaterial-induced fibrosis……34
1.5.1.1 Macrophage recruitment and adhesion……35
1.5.1.2 Macrophage fusion and fibrous encapsulation……35
1.5.1.3 Macrophage phenotypes in wound healing and fibrosis……36
1.5.1.4 Role of myofibroblasts……38
1.6 In-vitro models of fibrosis……41
1.6.1 Why is an in-vitro model required? ……41

1.6.2 The ideal model……41
1.6.3 Current in-vitro models of fibrosis……42
1.6.4 Lessons learned from explanted mesh……45
1.7 Aims and objectives……51

Chapter 2. Materials and Methods……53
2.1 Preparation of polypropylene mesh scaffolds……53
2.2 Monocyte isolation and culture……53
2.3 Fibroblast isolation and culture……54
2.4 Cell seeding optimisation……55
2.4.1 Seeding volume……55
2.4.2 Seeding density……55
2.4.3 Stainless steel rings for anchoring……55
2.4.4 Cell protect buffer vs no cell protect buffer……56
2.4.5 Elution of lysate separately vs together……56
2.4.6 Trizol vs lysis buffer……56
2.4.7 Homogenisation……57
2.5 Extraction and quantification of macrophage/fibroblast mRNA……57
2.5.1 RNA extraction……57
2.5.2 Transcription into cDNA……58
2.5.3 Quantification of cDNA ……59
2.6 Immunostaining to assess α-SMA expression……60
2.7 Imaging……62
2.7.1 Live dead staining……62
2.7.2 Microscopy……62
2.8 Statistical analysis……62
Chapter 3. Development of optimal cell seeding strategy for macroporous biomaterials to extract sufficient RNA for downstream applications……63
3.1 Introduction ……63
3.2 Results……64
3.2.1 Seeding volume……65
3.2.2 Seeding density……67

3.2.3 Ring vs no ring……68
3.2.4 Cell protect buffer vs no cell protect buffer……69
3.2.5 Elution of lysate separately vs together……70
3.2.6 Trizol vs lysis buffer……71
3.2.7 Homogenisation……72
3.3 Discussion……72
Chapter 4. Assessing the effect of mechano-chemical stress on the surface changes and the biological response to polypropylene mesh……76
4.1 Introduction……76
4.2 Results……78
4.2.1 Does SEM/AFM reveal any surface changes on the mesh? ……78
4.2.2 Do macrophages respond differently to mechano-chemically stressed mesh vs non-stressed mesh?……82
4.2.3 Fibroblast response to conditioned media from non-distressed and mechanochemically distressed mesh……84
4.3 Discussion……89
Chapter 5. General discussion……95
5.1 Discussion……95
5.2 Limitations ……101
5.3 Future work……102
5.4 Conclusions ……105
References……106

ABSTRACT

Synthetic meshes used for pelvic floor repair have been associated with the complications of pain and erosion. Polypropylene is the most used biomaterial in pelvic floor repair and currently is the subject of significant morbidity and litigation. Biomaterial-induced fibrosis remains a challenging issue and has been suggested as a potential reason for biomaterial failure. Macrophages and fibroblasts play a central role in the body's immunological response to implanted biomaterials.

During the healing process after implantation, macrophage phenotype ranges from pro-inflammatory (M1) to anti-inflammatory/pro-fibrotic (M2) phenotypes. Mesh implanted in the pelvic floor is subject to mechano-chemical stress which our group has shown induces surface changes. The study aimed to develop an in vitro model to measure macrophage and fibroblast response to biomaterials to help predict the risk of biomaterial induced fibrosis. A method was developed to culture macrophages on polypropylene mesh. This was combined with methods developed in our lab to simulate the mechano-chemical stress in vitro to assess macrophage response before and after application of these stresses. Genetic response of macrophages was assessed using qPCR. Fibroblasts were separately cultured in conditioned media collected from macrophage experiments and studied their response using qPCR and immunohistochemistry.

Surface changes were demonstrated on the mesh after exposure to mechano-chemical stress. Surface oxidation and helical defects were seen in the polymer. At the genetic level, macrophages cultured on mechano-chemically stressed mesh upregulated pro-inflammatory as well as pro-fibrotic genes. Fibroblasts cultured in conditioned media from macrophages cultured on mechano-chemically stressed mesh demonstrated increased alpha smooth muscle actin (α-SMA) production, a marker of myofibroblast differentiation. The results demonstrate a changing macrophage response as polypropylene is mechanochemically distressed. This is the first study that attempts to develop a novel in-vitro test combining mechanochemical stress testing with macrophages and fibroblasts to better understand biomaterial induced fibrosis.

PRESENTATIONS AND PUBLICATIONS

PRESENTATIONS:

Saad S, Murdoch C, Workman V, Hearnden V, Macneil S, Chapple CR. Developing better materials for the pelvic floor by early detection of materials likely to promote fibrosis. BioSheffield Conference, The Diamond, University of Sheffield, UK. (2022)

Saad S, Murdoch C, Workman V, Hearnden V, Macneil S, Chapple CR. In-vitro evaluation of macrophage response to polypropylene mesh before and after application of mechano-oxidative stress. European Association of Urology (EAU) Annual meeting, Milan, Italy. (2023)

PUBLICATIONS:

Farr NTH, Workman VL, **Saad S**, Roman S, Hearnden V, Chapple CR, et al. Uncovering the relationship between macrophages and polypropylene surgical mesh. Biomater Adv. 2024;159:213800.

ACKNOWLEDGEMENTS

I would like to start by thanking Allah, the Most Beneficient and the Most Merciful for all His blessings.

As the saying goes, it takes a village to raise a child. As an academic, I certainly was a child back in 2019 when I came to Sheffield. This amazing “village” took me in, helped me grow as a researcher and as a person, and helped get me through my PhD despite various trials and tribulations. Without them, this PhD would never have been possible. I am not sure if any amount of thanks I say would be enough but I will give it a go. In no particular order:

Dr.Vanessa Hearnden, thank you for everything you have done for me. Right from the registration to grant writing and thesis submission, my PhD has been challenging and I am very grateful to you for your support throughout, especially the final push to get things across the line.

Dr.Victoria Workman, you took over my supervision when I had a year left and minimal relevant experimental data. If it was not for your calm direction and pastoral support during a very difficult phase in my journey, I would not have been able to finish. I am immensely grateful for your support.

Professor Craig Murdoch, your expertise, counsel and support is the reason we were able to even dream about this project. You guided me every step of the way to understand macrophage biology as well as setting up PCR and macrophage culture in Kroto institute. Your advice was also pivotal in my decision to go for a PhD rather than MSc/MD. I always believed in looking at the mesh problem biologically and you made that happen. Thank you.

Dr.Inmaculada Vazquez, Dr.Bethany Ollington and Ms Brenka McCabe, thank you for your patience, technical support and showing me how to culture macrophages and set up PCR in Kroto. And being so generous with your master mix whenever I ran out! You have a wonderful department at the Dental School and I will always remember my time training there.

Dr.Sabiniano Roman Regueros (or Sabi, as he is known in Kroto), we went through a lot of ups and downs trying to navigate through supervision during COVID and optimising experiments but I am glad you stuck with me! Thank you for your supervision and friendship throughout my PhD. I am very grateful to have worked with you and learned from you.

Dr.Anthony Bullock – the Yoda of the department! I kept coming to you with my frustrations when my experiments did not work or I was particularly down on certain days. Your encouragement and guidance kept me on track. I am thankful to have worked with you, benefitted from your tremendous experience and got to enjoy your humorous take on life!

Professor Gwendolen Reilly and Professor Cornelia Rodenburg, you are one of the prime reasons I continued with my PhD. My head was full of doubts right up to my confirmation review. We were going through the pandemic and nothing was going right. Your comments and advice lifted my spirits and gave me the boost I needed to readjust and re-acquire focus. Thank you.

Dr.Nicholas Farr, it is rightfully said “If you want to go fast, go alone. If you want to go far, go together.” I am glad we met and I was able to collaborate with you. Thank you for your insights into biomaterial degradation and taking the time to meet and collaborate on this project. I will remember our collaboration, our talks on particles and hopefully our paths will cross again in the future.

Dr.Mina Aleemardani, a big thank you for coming to my rescue when the lab freezer broke down and I lost all my fibroblasts, a few months before my PhD end date. You generously shared your three batches of fibroblasts which enabled me to finish my project in time.

Dr.Naside Mangir, thank you for guiding me through the early phases and sharing your experience with me. It helped me make the decision to pursue research in Kroto.

I have left my two guiding lights for last. Professor Christopher Chapple and Professor Sheila MacNeil. Both of you showed faith in me and provided me an opportunity of a lifetime to do

research in your esteemed lab. Your support throughout this PhD has been immense. Your translational approach gave direction to my random bursts of ideas. Both of you are the kindest human beings I have ever met in my life and I am so grateful I got to meet you, work with you and benefit from your wisdom.

Although the entire Materials Science and Engineering group is too big to name, I would like to thank every single one of them for their friendship and support. Being a clinician, I was the outsider but they took me in and made me feel part of a family. I will fondly remember my time with all of them.

I would also like to say thanks to The Urology Foundation and The Robert Luff Foundation for being so generous with their funding and helping clinicians like me to do scientific research. Without your generosity, this work would not have seen the light of day, so thank you!

I would like to say thanks to my family. My dad for all his support not just now but throughout my life. I would not be here without the sacrifices he made for his children to progress. To my wife for being so patient and caring. I would not be able to pursue my passions if I was not married to a woman who understood why I do the things I do. To my son Zaviyar who will one day grow up, read this and hopefully be proud of what his dad achieved. To my brother and sisters, my extended family and my nephew and nieces (Musa, Huda, Dua and Zuha) for their prayers, love and support.

Lastly, I would like to thank my mother, Yasmeen. You shaped me into the person I am today. When I told you I am going to do a PhD, you told me I need to buckle down as it's a big task. You knew my struggles with ADHD well but every time I got distracted, you would keep me on track. You always taught me to "finish what you start". Your voice would be in my head whenever I lost my way. I lost my anchor when you went to heaven but you left me in this "village" of kind, supportive people who looked after me. I am now at the finish line. I wish you were with me now but I know you are watching proudly from heaven that your boy has managed to finish what he started.

ABBREVIATIONS:

α-SMA	alpha-smooth muscle actin
AFM	atomic force microscopy
BSA	Bovine Serum Albumin
DAPI	4',6-diamidino-2-phenylindole dihydrochloride
DMEM	dulbecco's modified eagle medium
EGF	epithelial growth factor
ECM	extracellular matrix
ELISA	enzyme-linked immunosorbent assay
FN-EDA	fibronectin extra domain A
GM-CSF	granulocyte macrophage colony stimulating factor
ICS	international continence society
IFN-γ	interferon gamma
IL-1	interleukin-1
IL-1β	interleukin-1β
IL-4	interleukin-4
IL-6	interleukin-6
IL-10	interleukin-10
IL-13	interleukin-13
IL-18	interleukin-18
IMDM	inveco's modified dulbecco's medium
ISO	international standardisation office
IUGA	international uro-gynaecological association
LPS	lipopolysachharide
M-CSF	macrophage colony-stimulating factor
MMP	matrix metalloproteinases
NIH	national institute of health
NTR	native tissue repair
PBS	phosphate buffered solution
PDGF-BB	platelet derived growth factor-BB

PDGF	platelet-derived growth factor
PF4	platelet factor 4
PLGA	poly (lactic -*co*-glycolic acid)
POP	pelvic organ prolapse
PP	polypropylene
PTFE	polytetrafluoroethylene
ROS	reactive oxygen species
SAM	self-assembled monolayers
SEM	scanning Electron Microscopy
SIS	small intestinal submucosa
SUI	stress urinary incontinence
SEHI	secondary electron hyperspectral imaging
TGF-β	transforming growth factor – beta
TIMP	tissue inhibitors of metalloproteinases
TNF-α	tumour necrosis factor-alpha

LIST OF FIGURES

Fig 1.1 Female pelvic floor showing the four main muscles comprising the pelvic floor. …… 18

Fig 1.2 DeLancey's three levels of support in the female pelvic floor. …….. 19

Fig 1.3 Three different phases of wound healing shown with key cells involved in each phase. ……..31

Fig 1.4 Cellular and molecular events during different phases of wound healing. ….32

Fig 1.5 An overview of the foreign body reaction in response to biomaterial implantation. ……34

Fig 1.6 An overview of macrophage phenotypes with triggers leading to M1 or M2 activation. ……..38

Fig 1.7 Macrophage-fibroblast crosstalk in fibrosis. ……40

Fig 1.8 Histological examination of explanted mesh showing foreign body giant cell reaction and fibrosis. ……46

Fig 2.1: Fibroblasts treated with TGF-β showing myofibroblast morphology with α-SMA expression. ……..…61

Fig 3.1 Cells seeding at a volume of 150µl stay on the top surface of the mesh without seeping through to the bottom of the well plate. ……64

Fig 3.2 Epifluorescence microscopy at 10x showing macrophage attachment to mesh. ……..…65

Fig 3.3 Graph showing concentration of RNA extracted from different seeding volumes. ……66

Fig 3.4 Graph showing concentration of RNA extracted from different cell seeding densities. ……67

Fig 3.5 Graph showing concentration of RNA extracted from group with stainless steel ring vs without. ……68

Fig 3.6 Graph showing concentration of RNA extracted from group using Cell Protect buffer vs no Cell Protect buffer. ……69

Fig 3.7 Graph showing concentration of RNA extracted from group where cell lysate is eluted separately vs where cell lysate is eluted together. ……..70

Fig 3.8 Graph showing concentration of RNA extracted from group using Trizol vs group using QEB Lysis Buffer. ……71

Fig 3.9 Graph showing concentration of RNA extracted from group homogenised with beads prior vs group where cells are lysed in the well plate. ……72

Fig 4.1. SEM images of mechanochemically distressed and non-distressed mesh. ….80

Fig 4.2 AFM images of mechanochemically distressed and non-distressed mesh. ….81

Fig 4.3 Expression of selected genes in macrophages exposed to control non-distressed mesh or mechanochemically distressed mesh. ……83

Fig 4.4 Comparison of genetic expression of a-SMA, COL1A1, COL3A1, COL5A1 and Fibronectin in human dermal fibroblasts when cultured in DMEM and IMDM (negative control), TGF-b (positive control), conditioned media from non-stressed mesh group (NSM) and conditioned media from mechano-chemically stressed mesh group (SM). ……86

Fig 4.5 Epifluorescence images of fibroblasts grown in different conditioned media vs control. ……88

Fig 4.6 Analysis of staining intensity in the red channel as a measure of α-SMA production in fibroblasts cultured in various media. ……..89

Fig 5.1 Schematic depicting the canonical TGF-b pathway. ……..100

Fig 5.2 A schematic showing the inflammasome activation pathway. ……..101

Fig 5.3 A summary of significant results. ……102

Fig 5.4 Schematic depicting different co-culture models of macrophages and fibroblasts on biomaterials. ……104

LIST OF TABLES

Table 1.1 Biological grafts used in pelvic floor surgery. ……25

Table 1.2 *In vitro* models studying the inflammatory response to biomaterials. ……..42

Table 1.3 Summary of studies on mesh explants. ……49

Table 1.4 Most common genetic expression markers specific to M1 and M2 macrophages as identified from literature. ……..51

Table 2.1 Amount of different components for genomic DNA elimination reaction. All reactions are normalised to the sample containing least amount of RNA. ……58

Table 2.2 Amount of different components for reverse-transcription reaction. ……..59

Table 2.3. A list of primers used for qPCR. ……59

Table 2.4 List of components used in a standard reaction mixture for qPCR. ……..59

Table 2.5 qPCR thermocycler standard settings for qPCR using TaqMan primers. ……..60

CHAPTER 1

Introduction

1.1– PELVIC FLOOR ANATOMY

One of the most complex anatomical and functional areas in uro-surgical anatomy is the female pelvic floor. The description here, though overly simplistic, is meant to give the reader a basic overview to better understand where the weaknesses in the pelvic floor occur and the role biomaterials can play to strengthen it.
The pelvic floor is made up of muscles (levator ani, obturator internus, coccygeus and piriformis), ligaments, the endopelvic fascia, pelvic organs with overlying peritoneum and the perineal membrane (Ashton-Miller and DeLancey, 2007). The pelvic floor separates the pelvic cavity above it from the perineal membrane below (Drake, 2020). All the components of the pelvic floor act together to provide support to the abdominal and pelvic organs. They are arranged in such a manner that the load generated on the pelvic floor by normal everyday activities is shared across all the components (Scarpero, 2007). The components of the pelvic floor are briefly described below.

1.1.1 – PELVIC MUSCULATURE

The muscles forming the pelvic floor are the pubococcygeus, iliococcygeus, puborectalis (the three collectively known as the levator ani), obturator internus, coccygeus and piriformis (figure 1.1). These muscles constitute a “floor” across the pelvic cavity with outlets for the urethra, vagina and rectum. Physiological studies show that the levator ani are constantly active which enables them to provide a shelf-like support for the pelvic organs (Parks et al.,

1962). The pubococcygeus part of the levator ani has both fast and slow twitch fibres and it is this component that not only maintains the tone of the pelvic floor but also actively closes the urethra, vagina and rectum (Koelbl et al., 1989). The levator ani muscles are involved in mechanisms controlling urination, defecation as well as providing pelvic organ support so any damage to these muscles e.g., during prolonged labour, vaginal delivery, multiparity etc can lead to decreased pelvic organ support, faecal or urinary incontinence (Scarpero, 2007). The obturator muscles arise from bony points in the pelvis but insert into the femur. The obturator foramen and the obturator canal within the muscles is of particular importance as the neurovascular bundle runs through it. This is at risk of damage during placement of the trans-obturator variant of the mid-urethral polypropylene sling (Scarpero, 2007).

1.1.2 – FASCIAE AND LIGAMENTS:

The important fasciae in the pelvic floor are the endopelvic fascia and the fascial covering of the levator ani muscle group, known as the levator fascia. These fasciae are subdivided into the pubocervical fascia, pubourethral ligaments, urethropelvic ligaments and urethrosacral ligaments (Scarpero, 2007). These are shown in fig 1.1. Even though some of these structures are called ligaments, they are actually condensations of the levator fascia with loosely organised connective tissue and smooth muscle (Walters, 2007). The mid-urethra and anterior vaginal wall are supported and stabilised by the pubourethral ligaments. If these ligaments become lax due to any reason, they can partly cause stress urinary incontinence, as explained later in the integral theory in section 1.2.5.4 (Petros and Ulmsten, 1993). The mid-urethral sling provides support to this area. The periurethral fascia fuses with the endopelvic fascia thereby fusing the urethropelvic ligaments with the tendinous arch. These provide support to the bladder neck and proximal urethra (Scarpero, 2007). There are three different levels of support in the pelvic floor as described by O'Lancey (Ashton-Miller and DeLancey, 2007) and shown in fig 1.2. These are:

Level 1 – At the apex of the vagina, support is provided by upper divisions of endopelvic fascia, collectively known as the paracolpium.

Level 2 – At the midportion of the vagina connected laterally by the paracolpium to the pelvic sidewalls.

Level 3 – At the distal vagina, support is provided by direct attachment to the surrounding organs and muscle without any intervening fascia.

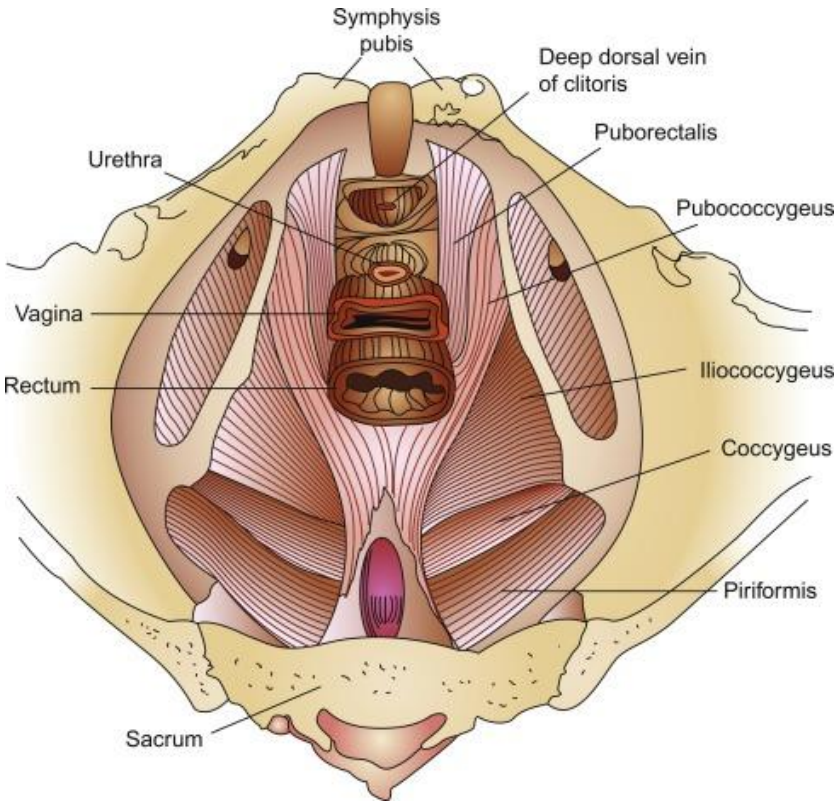

Fig 1.1 – Female pelvic floor showing the four main muscles comprising the pelvic floor: puborectalis, pubococcygeus, iliococcygeus and coccygeus. Reproduced with permission from Elsevier.

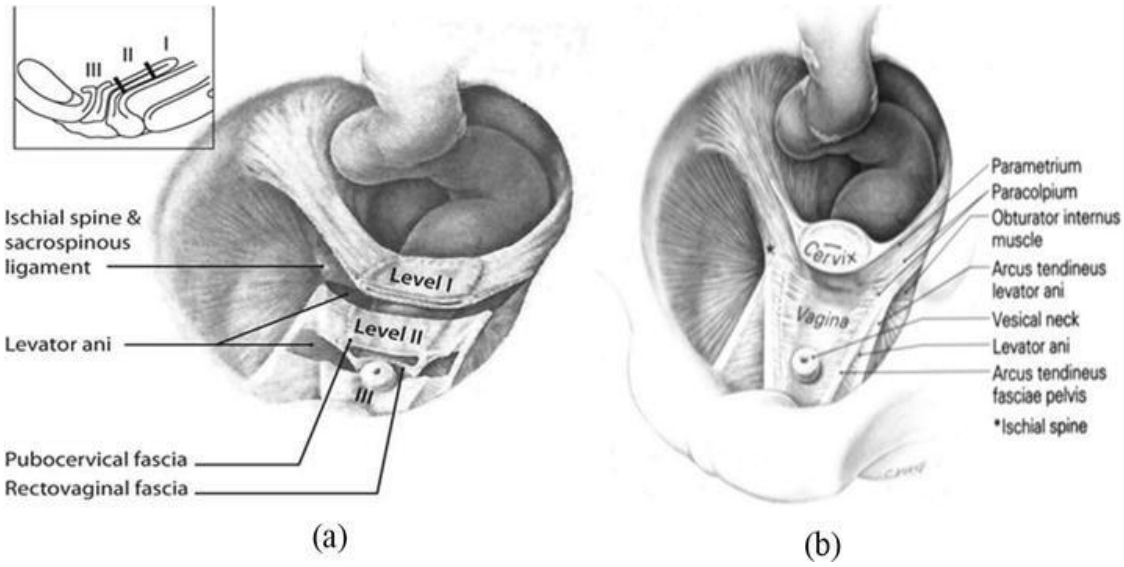

Fig 1.2 – DeLancey's three levels of support in the female pelvic floor. Reproduced with permission from Elsevier.

1.2– PELVIC ORGAN PROLAPSE (POP) AND STRESS URINARY INCONTINENCE (SUI):

1.2.1 – DEFINITION:

The International Continence Society (ICS) defines stress urinary incontinence (SUI) as "Complaint of involuntary loss of urine on effort or physical exertion including sporting activities, or on sneezing or coughing" (D'Ancona et al., 2019) .
Pelvic organ prolapse (POP) is defined as "the descent of one or more of the anterior vaginal wall, posterior vaginal wall, uterus (cervix) or vaginal vault (cuff scar after hysterectomy). The presence of any such sign should be correlated with relevant POP symptoms" (Haylen et al., 2011).

1.2.2 – EPIDEMIOLOGY:

A meta-analysis of 48 studies revealed that 16% of women aged 30 years or younger, and 29% of women aged between 30 and 60 years suffered from some form of urinary incontinence (Hampel et al., 1997). Of these women, 78% had SUI vs 51% suffering from

urge urinary incontinence and 27% had mixed urinary incontinence (Chapple and Mangera, 2017).

Similarly with POP, the prevalence increases with age. When defined as a sensation of a lump in the vagina, it's prevalence approximately ranges from 5% to 10% of the population (Cortes et al., 2017). Anterior vaginal wall prolapse is the most common followed by posterior and apical compartments (Hendrix et al., 2002).

1.2.3 – IMPACT:

SUI and POP have a significant impact on the physical and mental well-being of women. They also pose a great economic burden on the healthcare system. An estimated 135,000 women have surgery for urinary continence in the United States (Subak et al., 2001) at a cost of approximately $16.3 billion per annum (Wilson et al., 2001). Similarly in the UK, approximately £223 million is spent per annum to treat urinary incontinence (Turner et al., 2004).

1.2.4 – RISK FACTORS:

Common risk factors for SUI (Chapple and Mangera, 2017) are:

- age
- a high BMI
- female
- smoking
- pregnancy
- pelvic surgery
- vaginal delivery
- connective tissue disorders

For POP, the risk factors can be divided into predisposing factors and triggering factors (Cortes et al., 2017, Abrams et al., 2010).

Predisposing factors:

- neuropathic/muscular conditions
- congenital prolapse
- abnormal collagen
- obesity
- menopause

Triggering factors:

- pregnancy
- vaginal delivery
- obstetric injury
- chronic conditions leading to raised intra-abdominal pressure
- physical activities requiring heavy lifting

1.2.5 – PATHOPHYSIOLOGY:

SUI and POP are believed to result from weakening of the pelvic floor and/or weakness of the sphincter mechanism. This can be due to either anatomical or functional defects e.g., denervation injury during childbirth or other abdominal surgery. Female continence mechanisms are multifactorial and rely on a complex interplay between the nervous system, bladder, urethra and the pelvic floor. If we look at the anatomy, continence in males is reliant on two important sphincteric mechanisms: a proximal mechanism at the bladder neck and a distal mechanism at the prostatic apex (Chapple and Mangera, 2017). In females, the proximal bladder neck sphincter is absent in 40% of women and when present, it is significantly weaker than men (Chapple and Mangera, 2017). The distal urethral sphincter is supported by the pelvic floor. Women are therefore reliant on the integrity of the distal sphincter and the pelvic floor to maintain continence. There are various theories put forward over the years to describe the pathophysiologic mechanisms underlying SUI. These are described below:

1.2.5.1 – Alterations in urethra-vesical axis:

Originally described by Bonney in 1921 and popularised by the Swedish gynaecologist G.E.Enhorning in 1961, this theory states that the position of the urethra needs to be above the pelvic floor for equal transmission of pressures from bladder to urethra leading to a compensatory rise in urethral closure pressures (Daneshgari and Moore, 2007). This theory is based on Enhorning's studies on pressures of bladder and urethra in continent and incontinent women and prevailed till the late 70's (Daneshgari and Moore, 2007).

1.2.5.2 – Intrinsic Sphincter Deficiency:

In the late 70s and early 80s, Edward McGuire highlighted the importance of the intrinsic sphincter mechanism in achieving continence. This was evident from a study on sacral denervation in 3 paraplegic women showed the loss of anal and urethral skeletal muscle tone but the resting urethral smooth muscle tone remained normal and none of these patients developed SUI (Daneshgari and Moore, 2007). Based on his urodynamic evaluation and pressure studies of women with SUI, McGuire concluded that women with a Valsalva leak point pressure <60cm water have SUI due to intrinsic sphincter deficiency (ISD) and those >90cm water have SUI due to other conditions (Daneshgari and Moore, 2007). Valsalva leak point pressure is the "minimum total vesical pressure required to cause urinary incontinence in the absence of a detrusor muscle contraction" (Nitti and Combs, 1996).

1.2.5.3 – Hammock Theory:

The gynaecologist John DeLancey, in 1994, introduced the hammock theory whereby he described the urethra lying in a hammock-like sheet formed from the endopelvic fascia and anterior vaginal wall. When the laterally attached levator ani muscle contracts, it pulls the urethra against the vaginal wall and closes it (Chapple and Mangera, 2017).

1.2.5.4 – Integral Theory:

Proposed by Ulmsten and Petros in 1990, this theory states that a weakness in the anterior vaginal wall leads to a decrease in urethral closure pressures causing SUI (Petros and Ulmsten, 1993).

1.2.6– TREATMENT MODALITIES

Keeping the pathophysiology of both SUI and POP in mind, various surgical treatment modalities have been developed. Retropubic procedures like Marshall-Marchetti-Kanz and Burch colpocystourethropexy were the two commonest anti-incontinence procedures performed prior to 1970 (Stoffel et al., 2002). These were developed to reposition the urethra back above the pelvic floor based on Enhorning's theory on alteration of urethra-vesical axis. Bulking agents were developed to strengthen the intrinsic sphincter. Needle suspensions and pubovaginal slings were developed to strengthen the hammock-like support around the bladder neck as described in the hammock theory. The integral theory paved the way for the mid-urethral slings which led to the development of synthetic meshes placed tension free behind the urethra providing support to compress against (Petros, 2015).

The surgical treatments of POP are grouped as per the pathophysiology into anterior, apical and posterior compartment repairs. Anterior wall prolapse involves the vagina and bladder. The commonest procedures for anterior prolapse are anterior colporrhaphy and paravaginal repair. In a survey of gynaecologists in the UK, anterior colporrhaphy was the treatment of choice for anterior repair (Cortes et al., 2017). Biological or synthetic meshes have been used in this procedure to augment the repair. Apical prolapse involves the vagina and can be treated transabdominally with sacrocolpo- or sacrohysteropexy operations. They can also be treated transvaginally by running sutures from one uterosacral ligament to the other to provide increased apical support (Cortes et al., 2017). Posterior prolapse involves the rectum and is treated with posterior colporrhaphy. The goals of surgery are to achieve normal bladder, bowel and sexual function (Walters and Ridgeway, 2013).

1.3– BIOMATERIAL DEVELOPMENT AND USE IN THE PELVIC FLOOR

Traditionally, the surgical treatment of SUI and POP consists of tissue anchorage or plication to supportive structures using sutures. These techniques are collectively termed Native Tissue Repair (NTR). The repaired tissues, however, are weaker than the original tissues as there is a fibrotic reaction as the wound heals. This reaction leads to irregular and unorganized deposition of collagen fibres which decreases the strength of the repair especially along the lines of stress. Augmentation of this repair with biomaterials aims to overcome these issues by strengthening the wound (Downer et al., 2023). As defined by the National Institute of Health (NIH), a biomaterial is “any substance (other than a drug) or combination of substances, synthetic or natural in origin, which can be used for any period of time, as a whole or as part of a system which treats, augments, or replaces any tissue, organ, or function of the body” (Boretos and Eden, 1984).

1.3.1 Biological grafts:

Various biological grafts have been used in the pelvic floor and are listed in table 1.1. These are classified as autologous grafts (obtained from same individual), allogenous grafts (obtained from a donor of same species) or xenogenous grafts (obtained from donor of a different species). The first autologous graft was used in 1907 to treat SUI using the gracilis muscle (Rutman and Blaivas, 2009). Later, fascia from the rectus or the thigh muscles was preferred as fascia is avascular and thin. It is also easier to move from one part of the body to another compared to a flap which needs its blood supply to move with it. These procedures, however, are associated with significant donor site morbidity. Allogeneic grafts from cadaver fascia and xenogeneic grafts from porcine dermis, small intestinal submucosa (SIS) and bovine pericardium have been used to avoid donor site morbidity. These tissues are decellularized prior to implantation to avoid an immune reaction. The concern with allo- and xenogeneic grafts is inconsistency in tissue quality especially after decellularization. There is also a potential risk of viral or prion disease transmission.

Table 1.1 – Biological grafts used in pelvic floor surgery. Adapted with permission from Mr.Nadir Osman.

Biomaterial	Brand	Sterilization method	Modification	Elastin content	Matrix molecules
Cross-linked Porcine dermis	Pelvicol, PelviLace	Irradiated	Crosslinked with hexamethylene-di-isocyanate (HMDI)	High	Inactivated
Porcine small intestinal submucosa	Fortagen (cross-linked) Surgisis	Irradiated Ethylene oxide	Crosslinked with carbodiimide Nil	Low Low	Inactivated Growth factors, mucopolysaccharides & adhesive proteins
Cadaveric dermis	Tutoplast	Gamma-irradiated (low dose)	Freeze dried, solvent dehydration	High	Inactivated
Cadaveric fascia	Tutoplast	Gamma-irradiated (low dose)	Freeze dried, solvent dehydration	Moderate	Inactivated
Bovine pericardium	Veritas	Irradiated	Nil	Low	Assumed
Autologous fascia	-	-	Nil	Moderate	ECM intact

1.3.2 – Synthetic grafts:

Synthetic biomaterials have been used to repair the pelvic floor as far back as 1947 when a tantalum plate was implanted transvaginally to treat SUI in a series of patients (Goldberger and Davids, 1947). The idea was to let biomaterial-induced fibrosis strengthen the posterior part of the proximal urethra (Goldberger and Davids, 1947). In 1955, a mesh made from the same material was then used in a similar manner in 10 patients to prevent their bladder from prolapsing through weakened vaginal wall (Moore et al., 1955). This did not prove to be effective as 4 out of these 10 patients ended up with exposure of the mesh 6 to 18

months after surgery (Goldberger and Davids, 1947). This was not the first time tantalum was used in the body. Tantalum is a dense, malleable, biocompatible metal that was increasingly used during World War II for cranioplasties (Flanigan et al., 2014). Subsequently, it was used for ventral and inguinal hernia repairs and then for pelvic floor repair. At the time, the authors looked at fibrosis as a favourable end result as it would prevent biomaterial migration and strengthen the repaired tissues. We now know from studies of explanted meshes that this is not the case in the pelvic floor (Nolfi et al., 2016).

The first time a non-metallic mesh was used in the pelvic floor was by Moir in 1968 (Moir, 1968). The preferred procedure for SUI at the time was the eponymous Aldridge procedure where a narrow autologous rectus fascial sling was used under the bladder neck to support the urethra (Moir, 1968). Moir favoured a broader support fashioned from polyethylene gauze (Ethicon Mersilene ®). He attached this gauze from one side of the abdominal wall to the other, diving under the bladder neck and urethra like a "gauze-hammock" (Moir, 1968). No long-term follow-up complications were mentioned for this procedure. Wohlrab et al did a retrospective study of Mersilene suburethral slings placed in 772 women at a tertiary referral centre between 1996 and 2007 and found 8% of patients with mesh eroding into surrounding tissues with some cases presenting with bleeding and discharge 20 years after the original operation (Wohlrab et al., 2009).

In 1970, Morgan modified Moir's hammock operation by suspending the mesh from Cooper's ligaments instead of the rectus fascia. He also replaced the polyethylene mesh with a polypropylene one. Although no complications were reported in the initial cohort of 20 patients, Morgan et al. reported a 5% erosion rate in a 5 year follow up of 281 patients operated over a 16-year period (Morgan et al., 1985).

The landscape of surgery for SUI changed considerably when in 1995, Ulmsten and Petros described a new day-case procedure for SUI called the intravaginal slingoplasty. After using a local anaesthetic, they made a sagittal vaginal incision and dissected bluntly close to the urethra. They used a tunnelling device as an introducer to place the mesh like a U behind the mid-urethra. They used different mesh materials – polypropylene (Mersilene), polytetrafluoroethylene (Gore-tex), Teflon and Lyodura (Ulmsten and Petros, 1995).

This was swiftly followed in 1996 by Food and Drug Administration (FDA) clearance for the first synthetic sling material made from a bovine collagen coated polyester mesh called ProteGen (Heneghan et al., 2017). Even though this material was recalled 3 years later due to complications - erosion, pain, and infection (Kobashi et al., 1999) - it was used as a predicate device and was followed by a polypropylene-based transvaginal tape from Ethicon which was approved by the FDA in 1999 (FDA, 2024). Most of the mesh materials were first used during hernia operations and based on the results, found their way into the pelvic floor.

The most common biomaterial used in the pelvic floor mesh is polypropylene. Polypropylene is a thermoplastic polymer constructed from propylene monomers via chain-growth polymerization. It has heat resistance up to 168.3 C which allows sterilization for medical use without affecting its mechanical or chemical properties. Once melted, polypropylene monofilaments are formed using an industrial process called extrusion. Once a continuous monofilament of predetermined width and strength is extruded, it can be twisted or braided using a spin-finish applicator. Mesh is knitted using these monofilaments. Polypropylene was considered an inert material, however, it has been shown to degrade after implantation (Imel et al., 2015). Indeed, work done in our lab has demonstrated permanent mechanical deformation after 3 days of fatigue testing (Roman et al., 2019). This work was further refined in our lab by Farr et al combining mechanical distension and chemical oxidation with secondary electron hyperspectral imaging (SEHI) analysis to show mechanical (cracks/crazes) as well as oxidative changes (oxidised insoluble particles, polymer oxidation, changes in molecular structure) in polypropylene mesh (Farr et al., 2021).
Further evidence to support this will be seen in the review of explanted meshes later in this chapter.

1.3.3 – COMPLICATIONS AND CURRENT REGULATIONS:

In response to the increasing number of complications in women who had mesh surgery for POP and SUI, the International Uro-Gynaecological Association (IUGA) and International

Continence Society (ICS) jointly published terminology and classification of complications related to insertion of prosthesis (meshes, implants, tapes) and grafts in female pelvic floor surgery (Ward et al., 2008). The common complications and their definitions are as under (Stedman's, 2012):

- **Contraction:** "Shrinkage or reduction in size of biomaterial".
- **Prominence:** "Parts of biomaterial that protrude beyond the surface (e.g., due to wrinkling or folding with no epithelial separation)".
- **Exposure:** "A condition of displaying, revealing, exhibiting, or making accessible, e.g., vaginal mesh visualized through separated vaginal epithelium".
- **Extrusion:** "Passage gradually out of a body structure or tissue (e.g., a loop of tape protruding into the vaginal cavity".
- **Perforation:** "Abnormal opening into a hollow organ or viscus".
- **Dehiscence:** "A bursting open, splitting, or gaping along natural or sutured lines".
- **Sinus tract formation:** "(Localized) formation of a fistulous tract towards vagina or skin, where there is no visible implant material in the vaginal lumen or overlying skin".

As compared to SUI, complications are seen more in the group who had surgery for POP and in that cohort, transabdominal approach complications were fewer compared to the transvaginal approach (Mangir et al., 2019). In patients who underwent mesh surgery for SUI, the reported rate for serious complications is 4% (Ward et al., 2008). In the POP group, complication rate with the transabdominal approach is up to 10% on 7 year follow up (Nygaard et al., 2013). With the transvaginal route, a study reported a complication rate up to 42% at 7 years (Milani et al., 2018).

When women initially presented with these complications to their surgeons, they were dismissed (Cumberlege, 2020). With more and more women coming forward with complications, public concern grew which led to two public inquiries in the UK. The first was in Scotland in 2015 (Digital, 2018) and the second in England in 2017 (Government, 2017). This led to a decline in use of mesh for pelvic floor surgery in the UK. Baroness Julia

Cumberledge led the investigation into this matter and recently published her report in July 2020, titled “First Do No Harm” (Cumberlege, 2020). The clear themes emerging from the report were of patient’s voices being dismissed, failure of informed consent, patients wanting justice, patients not knowing who to complain to, failure of a database to capture complications and a focus on patient safety to prevent such a catastrophe from happening again (Cumberlege, 2020). As a result of their investigation, the report recommends mesh to be used as a last-line option and women should be fully informed about the risks, benefits and alternatives including doing nothing (Cumberlege, 2020). The National Institute for Health and Care Excellence (NICE) - in their most recently published guidance in 2019 - have not banned the use of mesh, a decision the Cumberledge report advises them to review (Cumberlege, 2020, NICE, 2020).

1.4 – WOUND HEALING:

To understand the pathophysiology behind fibrosis, it is important to talk about the mechanism of normal wound healing. Whenever the body is wounded, the healing of the wounded area undergoes three distinct phases of repair – the inflammatory phase leading to the proliferation phase and finally the remodelling or maturation phase (Eming, 2025). Figure 1.3 gives a brief overview of all three phases of wound healing.

With any wound, there is associated bleeding. The haemostatic coagulation pathway in the body is initiated by the initial trauma, which through a series of stepwise events, leads to vasoconstriction of surrounding vessels and formation of a coagulum or clot (Robbins, 2020). This clot, composed of collagen, fibrin, thrombin, and platelets, is biodynamic and acts as a scaffold attracting circulating leucocytes and fibroblasts. It does this by autocrine expression of transforming growth factor – beta (TGF-β) by leucocytes and fibroblasts which causes them to secrete pro-inflammatory cytokines like interleukin-1 (IL-1) and tumour necrosis factor-alpha (TNF-α) (Bevilacqua et al., 1985, Pohlman et al., 1986). The aim of increasing trans-endothelial migration of leukocytes to the wound site is to overwhelm any offending microbes or debris that are in the freshly injured wound (Robbins, 2020). This is followed by invasion of wound by macrophages within 48-96 hours. Resident macrophages can migrate to the wound site in response to chemokines or convert into tissue

macrophages from the circulating monocytes that migrate into the wound from the blood (Robbins, 2020, Guo and Dipietro, 2010). Their transition from one phenotype to another is crucial in wound healing. By production of proteolytic and lysosomal enzymes, nitric oxide and phagocytosis, the macrophages act in concert with neutrophils to kill any microbes and clear cell debris (Guo and Dipietro, 2010, Robbins, 2020). This is followed by secretion of matrix metalloproteinases (MMP) by monocytes, macrophages and fibroblasts to initiate remodelling of the damaged extracellular matrix (Robbins, 2020). The key cells in this inflammatory phase and a brief overview of the chain of events from tissue injury to repair are illustrated in figure 1.4.

Following on from this acute inflammatory phase, the wound enters the healing or proliferation phase. The fibroblasts take centre stage in this phase along with the epithelial and endothelial cells. In response to growth factors like epithelial growth factor (EGF) and transforming growth factor-beta (TGF-β) present at the wound site, the epithelial cells migrate from the wound edge and the fibroblasts start to produce collagen to build the provisional extracellular matrix (ECM) (Robbins, 2020, Guo and Dipietro, 2010). New vasculature is also formed at this point to increase blood flow to the wound and promote healing. Over the course of the proliferative stage, the fibroblasts are induced by TGF-β to transform into myofibroblasts to prepare for wound contraction (Robbins, 2020, Guo and Dipietro, 2010, Rolfe et al., 2011). At the end of this phase, the provisional matrix is chiefly composed of fibronectin and hyaluronic acid (Eming, 2025).

Once the provisional matrix is laid down, the wound healing enters the final stage – maturation or remodelling. The collagen fibres are haphazardly deposited by the fibroblasts in the ECM during the proliferation phase (Eming, 2025). The remodelling phase is characterised by reorganization of these fibres to make them more aligned which increases the strength of the wound. Depending on the depth and extent of the wound, this process can take anywhere from days to years and the reorganised tissue may regain up to 80% of its original strength within a year (Eming, 2025).

Up to this point in the normal wound healing process, there is no mention of fibrosis as there is normal deposition, degradation and remodelling of the ECM. Normal wound healing

occurs when all the cellular components (platelets, monocytes, macrophages, leucocytes, fibroblasts) act in concert with each other. Whenever there is a loss of communication between these components or wound healing is delayed, aberrant wound healing and fibrosis results.

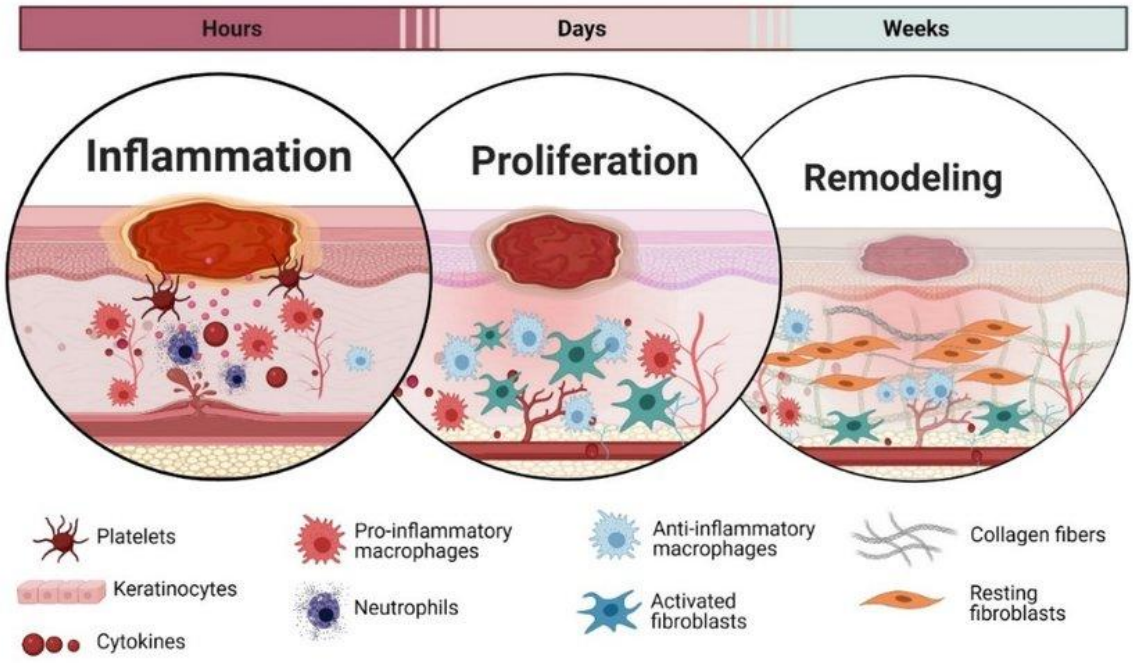

Fig 1.3 – Three different phases of wound healing shown with key cells involved in each phase. Reproduced from (Petkovic et al., 2021) under license from Creative Commons Attribution 4.0 International.

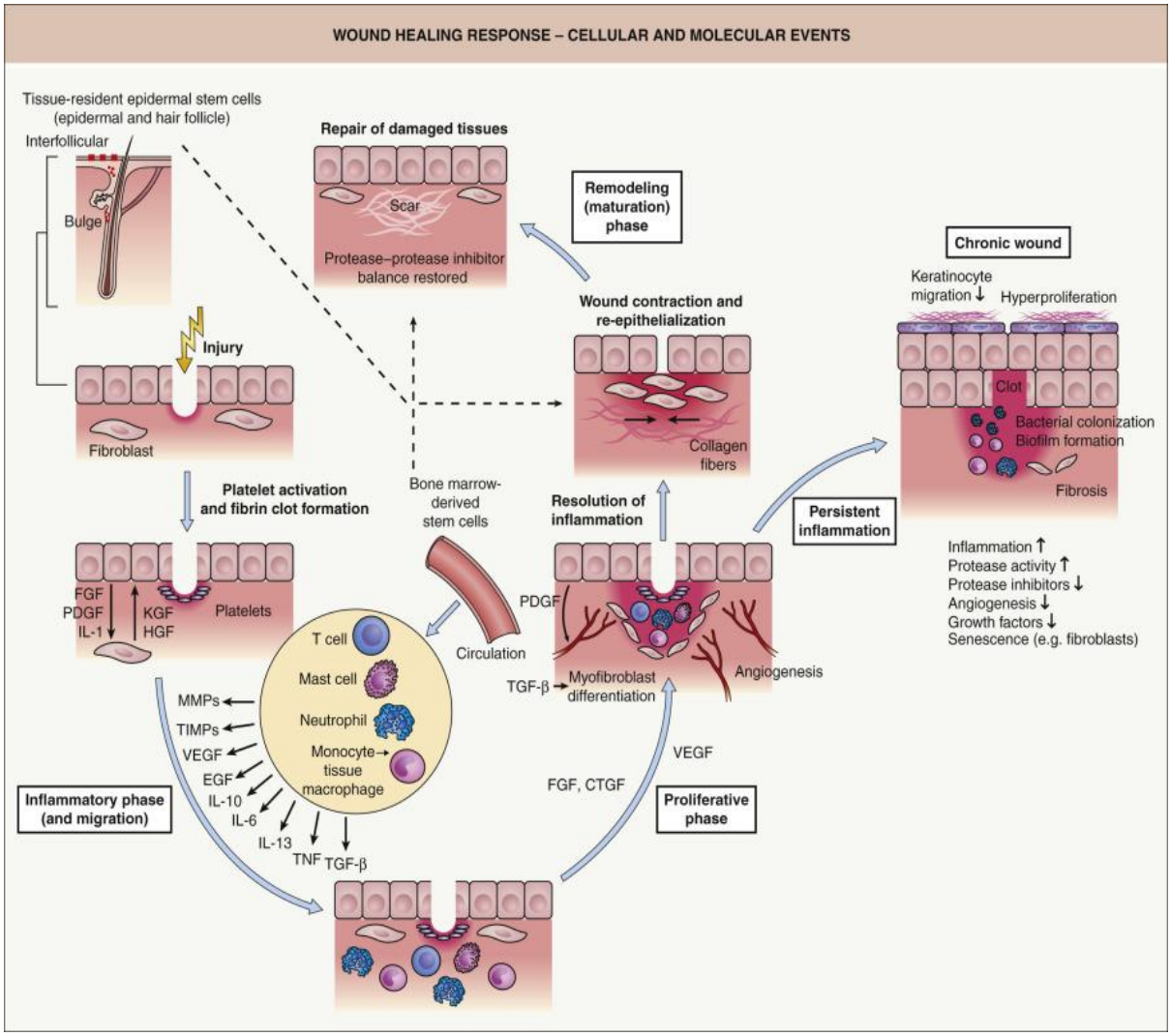

Fig 1.4 – Cellular and molecular events during different phases of wound healing. Following injury, haemostasis occurs due to interplay between leaked blood constituents and vasoactive factors. A bioactive fibrin clot is formed which facilitates an influx of different types of leukocytes, initiating the inflammatory phase. These leukocytes release growth factors and proinflammatory cytokines which attract more leucocytes, surrounding fibroblasts and endothelial cells to the wound. The proliferative phase is characterised by granulation tissue formation and angiogenesis, resolution of inflammation and deposition of collagen fibres. The granulation tissue and wound matrix transform into scar tissue during the remodelling phase. Stem cells within the tissue as well as circulating stem cells can assist in wound repair. If inflammation persists, this can lead to an aberrant wound healing response characterised by an increased protease activity, decreased angiogenesis, decreased growth factors and fibrosis. EGF, epidermal growth factor; HGF, hepatocyte growth factor; CTGF, connective tissue growth factor; FGF, fibroblast growth factor; KGF, keratinocyte growth factor; IL, interleukin; MMPs, matrix metalloproteinases; PDGF, platelet-derived growth factor; VEGF, vascular endothelial growth factor; TNF, tumor necrosis factor; TIMP,

tissue inhibitors of metalloproteinases. Reproduced from (Eming, 2025) with permission from Elsevier.

1.5– FIBROSIS:

Fibrosis can be defined as a pathological process caused in part by an increased ECM deposition to degradation ratio leading to loss of tissue architecture, scarring and depending on the location, loss of organ function(Robbins, 2020, Love and Jones, 2009, Rolfe et al., 2011) .

Fibrosis has been studied a lot more in organs than in biomaterial implantation. Although there is no standardised terminology, a consensus emerges from relevant studies of fibrosis. In most studies, when fibrosis occurs in organs, it is termed pathological fibrosis and if in response to implanted biomaterials, it is called biomaterial-induced fibrosis (Love and Jones, 2009, Davidson et al., 2020). As our focus is on biomaterials, we will focus more on the latter than the former but will briefly discuss the similarities and differences between the two here.

Compared to pathological fibrosis which usually occurs over months to years, biomaterial-induced fibrosis is usually complete in a couple of months with the formation of an acellular capsule around the biomaterial (Love and Jones, 2009, Anderson et al., 2008). The foreign body giant cell, formed by the fusion of macrophages, is only seen in biomaterial-induced fibrosis. If these are not present on the surface of the biomaterial, fibrosis will not occur at the biomaterial-blood interface (Love and Jones, 2009, Anderson et al., 2008).

From the literature, we can see how surgeons have previously regarded fibrosis as a good thing that increases wound strength and helps tether the biomaterial in place (Lee et al., 2006). We have since come to realise fibrosis to be a pathological process that weakens the surrounding tissue (Nolfi et al., 2016).

1.5.1 – Biomaterial-induced fibrosis:

When a biomaterial is implanted into the body, it is essentially a wound that initiates the healing pathway but with a foreign body within that wound. The foreign body response which leads to fibrosis has been studied and described beautifully by Anderson et al. in their classic paper on the subject (Anderson et al., 2008). Soon after implantation of the biomaterial, there is flooding of the surgical wound with blood. As discussed earlier, bioactive compounds in the blood lead to the formation of a clot which encourages platelet adhesion and aggregation. This biodynamic clot acts as a chemoattractant – through production of chemokines, cytokines and growth factors – towards white cells, especially neutrophils. Monocytes are recruited a few hours later and upon reaching the wound site, these differentiate into macrophages. The macrophages phagocytose cellular debris, bacteria, dead cells or any foreign bodies upto 10um in the wound (Sheikh et al., 2015). An overview of the foreign body response is illustrated in figure 1.5.

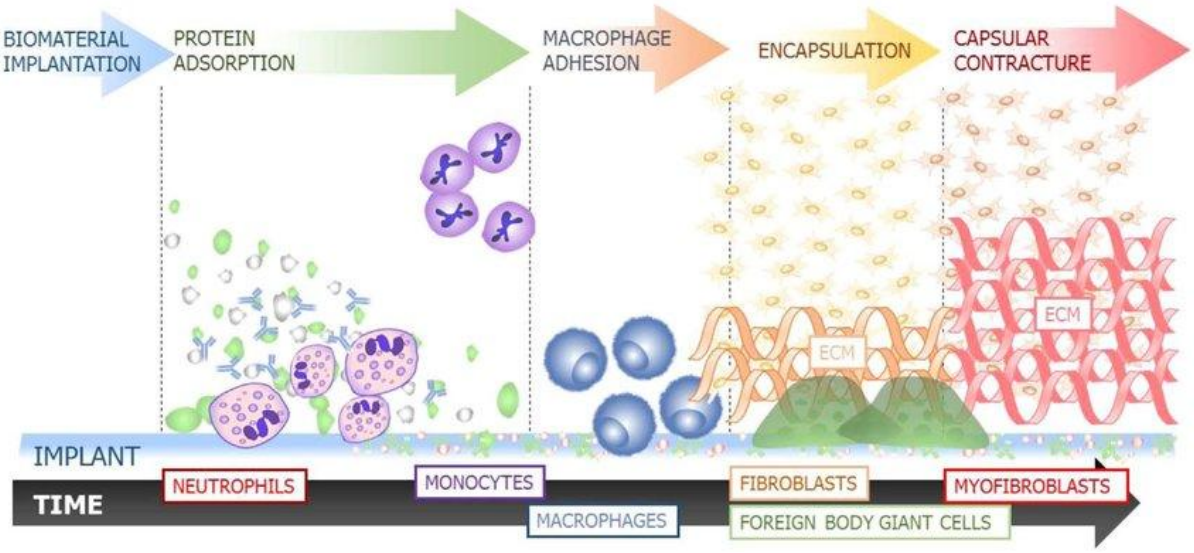

Figure 1.5 – An overview of the foreign body reaction in response to biomaterial implantation. Reproduced from (Barr et al., 2017) under Creative Commons Attribution 4.0 International license.

1.5.1.1 – Macrophage recruitment and adhesion:

The next step in the foreign body response is the recruitment of neutrophils, followed by monocytes and macrophages. Monocytes/macrophages are guided towards the biomaterial by secretion of chemokines at the implantation site by the initially adsorbed cells (Robbins, 2020, Anderson et al., 2008). The macrophages anchor themselves to the proteins adsorbed by the biomaterial using receptors called integrins (Anderson et al., 2008, Robbins, 2020, Love and Jones, 2009). Chemokines or cytokines are a group of proteins secreted by various cells that help them communicate with each other. These belong to four major families: XCL, CCL, CXCL and CX3CL (Esche et al., 2005). The biodynamic clot formed earlier releases cytokines like platelet-derived growth factor (PDGF), transforming growth factor (TGF-β), interleukin-1 (IL-1) and CXCL4 (also known as platelet factor 4 (PF4)), among other things to recruit more and more macrophages to the biomaterial site (Tang et al., 1998). Once at the site, these macrophages adhere to the biomaterial and continue secreting more cytokines like tumour necrosis factor (TNF-α), granulocyte-colony stimulating factor (G-CSF), granulocyte macrophage colony stimulating factor (GM-CSF) and IL-1 to continue the recruitment process (Broughton et al., 2006). Production of other important chemokines like CCL4, CCL7, CCL2, CCL13 and CCL22 have been demonstrated in in vitro cultures of biomaterial-adherent macrophages (Jones et al., 2007).

1.5.1.2 – Macrophage fusion and fibrous encapsulation:

Macrophages cannot phagocytose particles larger than 10 microns (Sheikh et al., 2015). As the implanted biomaterial is much larger in size, it resists phagocytosis. As a result, macrophages undergo a process termed frustrated phagocytosis whereby they fuse together to form multinucleated giant cells (Robbins, 2020, Anderson et al., 2008, Love and Jones, 2009). Although the exact molecular mechanisms of this process are not fully understood, two of the important cytokines that play a major role are interleukins 4 (IL-4) and 13 (IL-13) (Anderson et al., 2008). By upregulating mannose receptors on the surface of macrophages, these lead to macrophage fusion and foreign body giant cell formation (Kao et al., 1995, DeFife et al., 1997). Macrophages at this stage are not only influencing the

inflammatory response but also involved in remodelling of the extracellular matrix (Anderson et al., 2008). They secrete matrix metalloproteinases (MMP) and tissue inhibitors of metalloproteinases (TIMP) of which TIMP-1, TIMP-2 and MMP-9 can be detected in *in vitro* studies of biomaterial-adherent macrophages (Anderson et al., 2008). Metalloproteinases such as MMP-9 have also been detected in histopathological evaluation of explanted meshes (Nolfi et al., 2016). These giant cells are characteristic of the foreign body response to biomaterials. They can be continually replaced by newer giant cells and persist for the lifetime of the biomaterial, a fact confirmed by histological evaluation of explanted meshes from patients (Nolfi et al., 2016).

Giant cells form part of a collagenous fibrotic tissue or capsule around the biomaterial to wall it off from the surrounding environment (figure 6). This capsule, secreted by fibroblasts, can range from 50-200 µm in thickness. The formation of a fibrous capsule around the biomaterial walls it off from the surrounding environment to prevent further stimulation of the immune system (Robbins, 2020, Anderson et al., 2008, Love and Jones, 2009). This can also lead to deformation and failure of the biomaterial (Anderson et al., 2008).

1.5.1.3 – Macrophage phenotypes in wound healing and fibrosis:

Macrophages are important to both inflammatory and fibrotic pathways. Their function is determined by their mode of activation (Robbins, 2020, Anderson et al., 2008, Love and Jones, 2009, Witherel et al., 2019). There are two major pathways of macrophage activation: the classical pathway and the alternative pathway (Robbins, 2020). An overview of macrophage phenotypes and their polarising triggers is shown in figure 1.6. Classical activation of macrophages occurs chiefly by microbes and microbial products like endotoxins, or by foreign substances. These classically activated macrophages are described as M1 macrophages (Robbins, 2020, Witherel et al., 2019). The M1 macrophages develop in response to cytokines like interferon gamma (IFN-γ) and produce nitric oxide and lysosomal enzymes among other things, thereby enhancing their pro-inflammatory role in destroying the offending microbes and propagating the inflammatory response. The second pathway – alternative activation pathway – leads to production of macrophages called M2 macrophages in response to cytokines like IL-4 and IL-13 (Robbins, 2020). The M2

macrophages are primed to stop inflammation and promote wound healing (Robbins, 2020, Witherel et al., 2019).

The M1 macrophages are found in the wound immediately and up to 3 days after injury (Spiller et al., 2015, Arnold et al., 2007, Mirza et al., 2013). They stimulate acute inflammation by secretion of cytokines like TNF-α and IL-1β (Spiller et al., 2014). The M1 macrophages shift to the M2 phenotype between four to seven days post-injury (Spiller et al., 2015, Arnold et al., 2007, Mirza et al., 2013). The M2 macrophages, being pro-remodelling, secrete platelet derived growth factor-BB (PDGF-BB), CCL17 and CCL18 (Spiller et al., 2014, Tarique et al., 2015, Lewis et al., 2018, Belperio et al., 2004).

Although the classical activation pathway is hypothesised as occurring prior to the alternative pathway, in reality, the M1 and M2 macrophages are at the two extremes of the macrophage phenotype spectrum with dynamic switching occurring between the two ends of the spectrum as dictated by microenvironmental factors they find themselves in (Robbins, 2020, Anderson et al., 2008). There are studies describing various subtypes of macrophage (M2a, M2b, M2c, M2d and M2f), however it must be noted that controversy exists over the macrophage phenotype nomenclature (Martinez and Gordon, 2014, Murray et al., 2014, Ferrante et al., 2013, Fadok et al., 1998, Brecht et al., 2011).

Macrophages are very plastic and dynamic. They respond to their environment by expression of receptors and secreted factors. The environment can change over 20 microns in a tissue, which causes their phenotype to change in response to their microenvironment. Macrophages have also been described as displaying a hybrid M1/M2 phenotype especially at the implanted biomaterial surface (Yu et al., 2016, Spiller et al., 2015). In context of acute and chronic inflammation occurring at the biomaterial-body interface, a phenotype that is both pro-inflammatory and pro-remodelling can be envisioned, which has led to researchers looking at the ratio of M1 and M2 macrophages when designing *in vitro* models to study fibrosis.

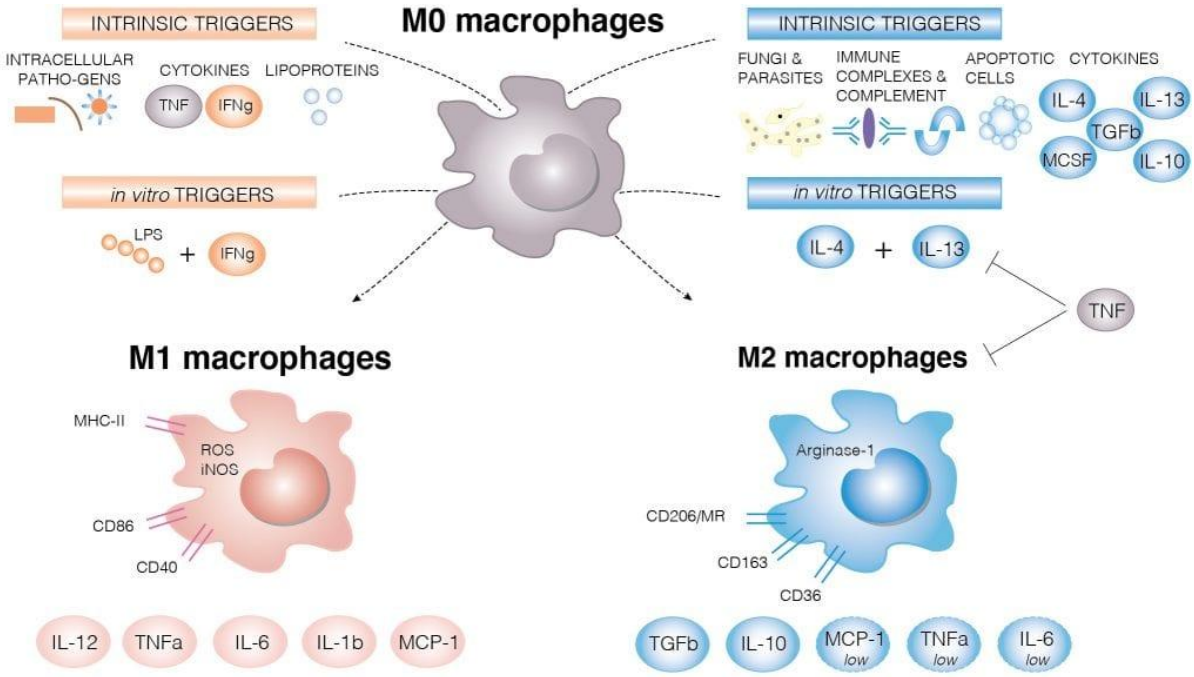

Fig 1.6 – An overview of macrophage phenotypes with triggers leading to M1 or M2 activation. Reproduced from (Atri et al., 2018) under Creative Commons Attribution 4.0 International license.

1.5.1.4 – Role of myofibroblasts:

Myofibroblasts (Fig 1.7) play a vital role not only in wound healing but also in aberrant wound healing and fibrosis (Love and Jones, 2009). Myofibroblasts develop from mesenchymal cells (Lama et al., 2007), epi- or endothelial cells (Thiery and Sleeman, 2006, Lee et al., 2006, Xu et al., 2009) and fibroblasts (Bucala R, 1994, Quan et al., 2006). They express alpha smooth muscle actin (α-SMA) and contribute to the ECM by producing collagen (Rolfe et al., 2011). As we saw in normal wound healing, their nature is transient, and their role is primarily in wound contraction and ECM deposition. During the proliferative phase of wound healing, the myofibroblasts contract to bring the wound edges together. Once tissue integrity is restored, they undergo apoptosis (Rolfe et al., 2011, Gabbiani, 1996). Persistence of myofibroblasts in chronic wounds leads to increased ECM deposition, contraction and fibrosis (Rolfe et al., 2011, Mutsaers et al., 1997). In fibrotic environments, the crosstalk between macrophages and fibroblasts is pivotal (Witherel et al., 2019). Due to the dynamic nature of macrophages and fibroblasts, it has proven challenging to study this in vivo. Most of the data we have available is from in vitro studies which, despite being

oversimplistic, provide crucial data to understand how these cells interact (Witherel et al., 2019). Macrophages and fibroblasts interact with each other using cytokines and in the context of wound healing, this can be for three main purposes: chemotaxis, collagen deposition and myofibroblast differentiation (Holt et al., 2010, Ploeger et al., 2013, Song et al., 2000). In normal wound healing, the macrophages would transition from M1 to M2 phenotype as discussed earlier. Holt et al showed that when fibroblasts and macrophages are stimulated by lipopolysachharide (LPS), both cell types significantly upregulate pro-inflammatory markers leading to foreign body giant cell formation. (Holt et al reference). In another study, primary murine cardiac fibroblasts were differentiated into myofibroblasts by treating them with TGF-β1. They were then co-cultured with monocytes for 72hrs at which point the monocytes differentiated into an anti-inflammatory phenotype characterised by increased IL-10 secretion (Humeres et al., 2016, Trinchieri, 1995). Ploeger et al utilised conditioned media from M1 and M2a phenotypes to test the effect on fibroblasts. They found that conditioned media from M1 macrophages increased secretion of pro-inflammatory cytokines (IL-6, MMP1, MMP2, MMP3, CCL2 and CCL7) whereas M2a macrophage-conditioned media did not have a significant effect on fibroblasts (Ploeger et al., 2013). But when the in vivo M1 to M2 transition was mimicked by culturing fibroblasts in conditioned media from M1 macrophages first and then changed to M2a conditioned media, genes encoding for proinflammatory cytokines (IL-6 and MMP-1) were downregulated and genes for collagen 1 production (COL1A1) were significantly upregulated (Ploeger et al., 2013). Zhu et al, however, found that M2a macrophage signalling promoted myofibroblast differentiation as shown by increased α-SMA secretion as well as increased expression of COL1A1 and TGF-β1 genes (Zhu et al., 2017). Studying the role of macrophage phenotype on ECM remodelling, Witherel et al utilised conditioned media from M1 and M2 phenotypes, as well as hybrid M1/M2 phenotypes generated by exposing monocytes to both M1 and M2-promoting cytokines (Witherel et al., 2021). *In vitro* conditioned media experiments revealed a higher gene expression of COL3A1, COL5A1 and fibronectin, perlecan and versican compared to control (fibroblasts cultured without conditioned media). They also found less aligned collagen in the matrix deposited by fibroblasts grown in conditioned media from the hybrid macrophage phenotypes (Witherel et al., 2021). The macrophage-fibroblast crosstalk and its effects are summarised in figure 1.8.

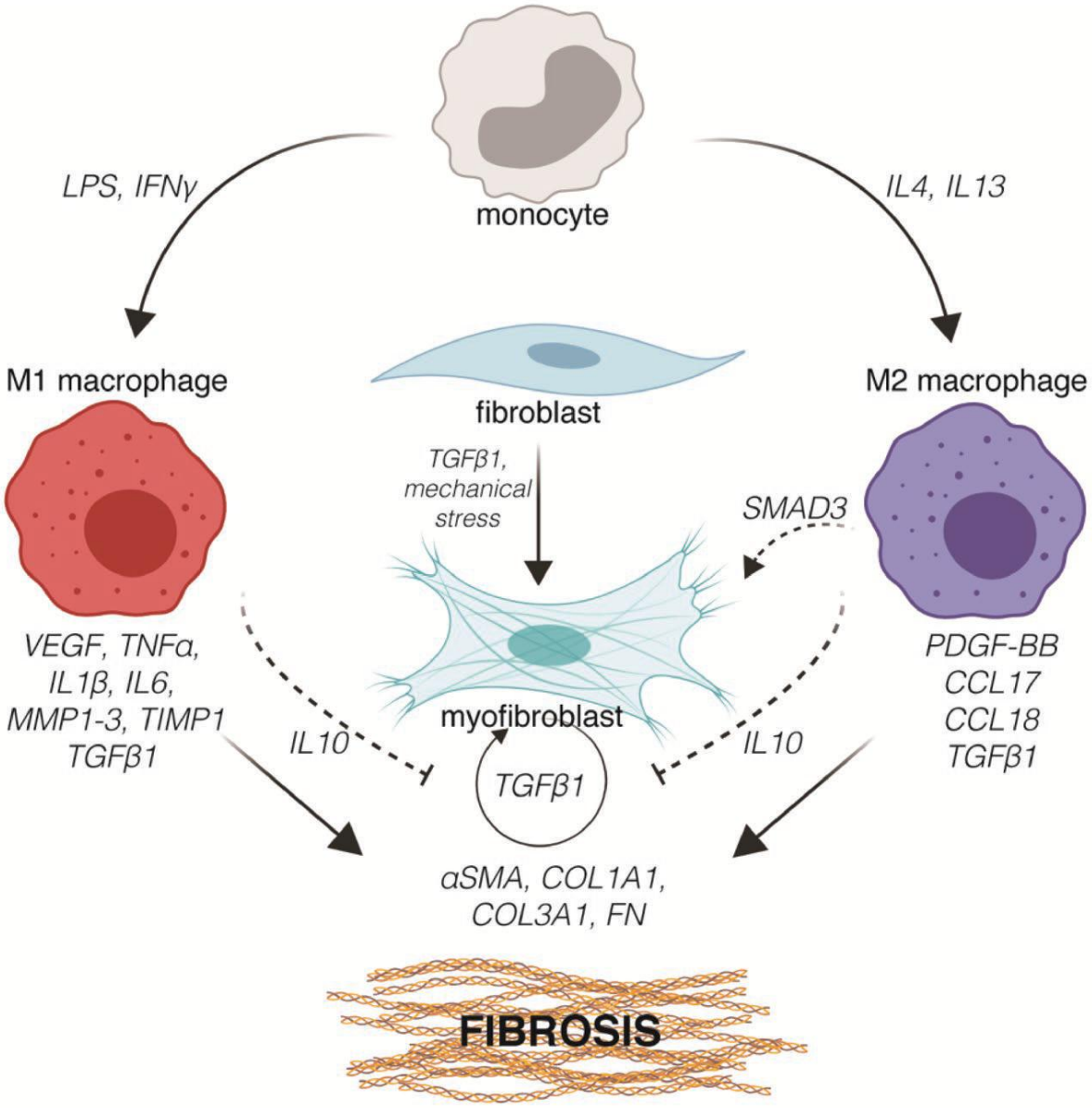

Fig 1.7 – Macrophage-fibroblast crosstalk in fibrosis. Image reproduced from (Witherel et al., 2019) with permission from Wiley.

1.6– IN VITRO MODELS OF FIBROSIS:

1.6.1 WHY IS AN IN-VITRO MODEL REQUIRED?

The current gold standard to test the body's response to biomaterials is implantation into animals (ISO, 2022) whereas *in vitro* tests are used to characterise the acute phase response to the biomaterials (ISO, 2017). The International Organisation of Standardisation (ISO) protocols in place for evaluation of biomaterials recommend appropriate animal models for immunological testing (Lock et al., 2019). There is a dearth of *in vitro* studies looking at fibrosis that correlate well with the *in vivo* environment. This is because fibrosis is a dynamic process involving a complex interplay between various systems and cells in the body, which can be difficult to replicate *in vitro*. It is difficult to simulate a complete immunological response *in vitro* as acquired immune responses develop over a prolonged period of time. However, the initial inflammatory response from the macrophages and fibroblasts can be studied *in vitro* to capture pro-fibrotic biomaterials prior to *in vivo* testing. This would not only help us understand the mechanisms underpinning biomaterial-induced fibrosis but also decrease the animal burden of research.

1.4.2 THE IDEAL MODEL:

The perfect in-vitro model to study fibrosis would have to replicate the entire in-vivo immune system response along with the ECM the biomaterial is placed in. Setting such a model would be technically extremely challenging, complex and expensive. Replicating certain key aspects of the immune response (macrophages) and parts of the ECM (fibroblasts) that play a big role in the fibrotic reaction, however, would be an achievable ideal. Such a system should have the following characteristics:

1) Simple to set up with potential to add complexity as needed.
2) Able to study the macrophage response to biomaterials as well as fibroblast response to the macrophage signalling.

3) Able to predict fibrotic tendency of a biomaterial by correlating well with *in vivo* data published in literature. This data would be obtained from the review of explanted

biomaterials to look at various factors like the thickness of the capsule surrounding the biomaterial, tissue integration, surface changes and deformation.

1.4.3 CURRENT IN-VITRO MODELS OF FIBROSIS:

There have been a few studies on in-vitro assessment of biomaterials. These have been detailed in Table 1.2. These vary in their complexity, choice of cells, chosen end points and readout parameters.

Table 1.2– *In vitro* models studying the inflammatory response to biomaterials.

Author	Biomaterials tested	Cells	Design
Grotenhuis et al (Grotenhuis et al., 2014)	Polypropylene, purified pepsinized porcine collagen, porcine acellular dermis matrix, polyethylene terephthalate	Human primary blood derived monocytes	2D mono-culture
Jannasch et al (Jannasch et al., 2017)	Glass, titanium, polytetrafluorethylene, silicone, polyethylene	Human primary macrophages	2D mono-culture
Zhou et al (Zhou et al., 2017)	Self-assembled monolayers with different surface properties	Human monocytic line THP-1, primary human dermal fibroblasts	2d co-culture (Transwell)
Parks et al (Parks et al., 2014)	PLGA	Human monocytes and fibroblasts	3d co-culture (hydrogel)

Jannasch et al (Jannasch et al., 2017) proposed an in-vitro testing platform to study the effect of various test conditions – human plasma treatment, IL-4 exposure, heat-inactivated plasma treatment and LPS stimulation - on predicting the fibrotic tendencies of biomaterials commonly implanted in the human body ranging from vascular prostheses and breast implants to joint replacement prostheses (Jannasch et al., 2017). They then conducted a literature review of pre-clinical and clinical studies of the same biomaterials after explantation. A comparison of in-vitro results with these in-vivo studies revealed the plasma treatment condition to be most predictive of the fibrotic potential of the tested biomaterials. It is the first human-based *in vitro* model that assesses the role of different test conditions in predicting the fibrotic tendency of various biomaterials when compared to *in vivo* assessments. They managed to combine a data set of five biomaterials, five test conditions, seven readout factors and ten donors into one novel simplified score that could be used to rank the materials.

Grotenhuis et al (Grotenhuis et al., 2014) conducted a simpler study by seeding primary blood derived monocytes on different biomaterials and looking at genetic markers specific for M1 and M2. They calculated an index of M1/M2 from the results obtained and those with a lower index were more fibrotic. One of the biomaterials studied is polypropylene which is of interest to us. Even though they use undifferentiated macrophages, their seeding strategy involves submerging all four biomaterials (12 in total for triplicate) in 25ml of media at a density of 750,000 macrophages per ml and rotated in a centrifuge for two hours. They have not used an undifferentiated macrophage cell-only control, choosing instead to use an LPS-stimulated group for M1 and IL-4 stimulated group for M2. For gene expression analysis, they have used only two genes each to define an M1 (TNF-α and IL-6) or M2 response (CD206 and CCL18). They quantified the proteins produced in the culture medium by ELISA. They labelled certain biomaterials as fibrotic based on the cytokine CCL18 seen in the conditioned media. For multifilament polypropylene, they found raised CCL18 in the conditioned media with increased differentiation to M2 phenotype.

Zhou et al developed a novel co-culture method to study the inflammatory properties of biomaterials (Zhou et al., 2017). They modified the classically used transwell assay by utilising a specially designed fence chamber to keep cells separate. Instead of using 3D

scaffolds, they immersed glass slides in different silane solutions (Chlorodimethyloctadecylsilane, 3-Aminopropyltriethoxysilane, Glycidoxypropyl trimethoxysilane and Triethoxysilylpropyl succinic anhydride) to generate self-assembled monolayers (SAM) with different terminal groups (-CH3, -NH2, -Oh and -COOH) to give them hydrophobic or hydrophilic properties. For co-culture, they used THP-1 monocytes and human dermal fibroblasts. The fence chambers were placed in a 24-well plate. After incubating for 24 hours, they removed the fence chambers and maintained an approximately 500 micron gap between the cells to allow for cellular cross-talk. They also established a human fibroblast control where instead of the THP-1 macrophages, they left RPMI medium without macrophages in the external chamber.
The main findings were an increase in pro-inflammatory cytokines in the hydrophobic SAMs compared to the hydrophilic ones. They also showed increased pro-fibrotic responses of fibroblasts as measured by increase in motility, outward migration and increased Fibronectin extra domain A (FN-EDA) and α-SMA expression when co-cultured with macrophages as opposed to monoculture. This co-culture model is a good template where the SAM layers can be replaced with various biomaterials to study their effect on fibrosis.

Parks et al (Parks et al., 2014) used a 3D collagen-based hydrogel to co-culture human foreskin fibroblasts with U937 monocyte cell line to study the response when challenged with poly(lactic -*co*-glycolic acid) (PLGA) particles. They utilised collagen for their hydrogel to mimic ECM in human tissue. They quantified the cytokines using ELISA and showed increased levels of inflammatory cytokines (IL1-b, IL-6, GM-CSF and TNF-a) on day 10 in response to PLGA. Interestingly, when compared to fibroblast monoculture, they found higher levels of IL-6 and GM-CSF in the co-culture suggesting a possible enhancement in the production of these cytokines as a result of activated monocyte – fibroblast cell signalling.

The challenge of fashioning an *in vitro* model of fibrosis is evident from the results of the above-mentioned studies. This is because fibrosis is a multifactorial and dynamic process that involves an immune system constantly reacting to the changing stimuli. Current studies have tried to replicate parts of the process and generated good results. Further studies are needed in this vital area to better delineate the mechanisms underlying biomaterial induced fibrosis and help devise a more accurate *in vitro* model that can predict the fibrotic potential

of biomaterials prior to *in vivo* implantation. To understand biomaterial-induced fibrosis better, a good starting point would be to examine meshes removed from symptomatic patients.

1.6.4 – LESSONS LEARNED FROM EXPLANTED MESH

Mesh is implanted to solve the issue of incontinence or prolapse for patients, however, sometimes it can cause side effects like erosion, pain etc (Rolfe et al., 2011, Davidson et al., 2020, Anderson et al., 2008). These patients undergo mesh removal with varying rates of success. In some centres, these explanted meshes have been studied grossly and histologically under the microscope and provide us with some interesting insights. These are summarised in Table 1.3 and discussed below.

One of the earliest studies of these meshes was done retrospectively by Iakovlev et al (Iakovlev et al., 2017) who looked at 63 polypropylene mesh explants removed in their hospital between 2010 and 2014. The majority of these were removed for pain and erosion. They reported all explanted specimens contained nerve ingrowth, surface cracking, edge curling as well as features consistent with chronic inflammation. Their study showed that polypropylene mesh can degrade and elicit a persistent inflammatory response which can lead to fibrosis.

Similarly, Wang et al (Wang et al., 2004) in their study of patients who had complications after polypropylene mesh implantation, found the mesh filaments to be surrounded by tissue macrophages with a pronounced foreign body reaction and fibrosis. Immunohistochemistry showed CD20+ B cells, CD4+ and CD8+ T-cells as well as CD68+ tissue macrophages. The control group (symptomatic women with voiding difficulty/prolapse but no erosion) showed most cells to be CD4+ with a mild mononuclear cell infiltration but without submucosal fibrosis. This study showed that in the patients with persistently defective vaginal healing, the vaginal epithelium had an intense inflammatory reaction to the polypropylene mesh with a strong foreign body reaction and fibrosis seen in the mesh fibres.

Fibrosis was the main finding, again, in a retrospective review conducted by Smith et al (Smith et al., 2013). They reviewed archival slides of meshes explanted between 2010 and 2012 from 102 patients due to pain, erosion, urinary retention and infection. The mesh

material was polypropylene in all but 2 cases – one PTFE and the other Mersilene. They reported majority of the meshes showing signs of fibrosis (70.1%) with 6.3% showing granulation tissue and 22.9% showing scar formation. Foreign body giant cell reaction was seen in 18.8% of the cases. Signs of inflammation and foreign body giant cells were present as well as seen in figure 1.8.

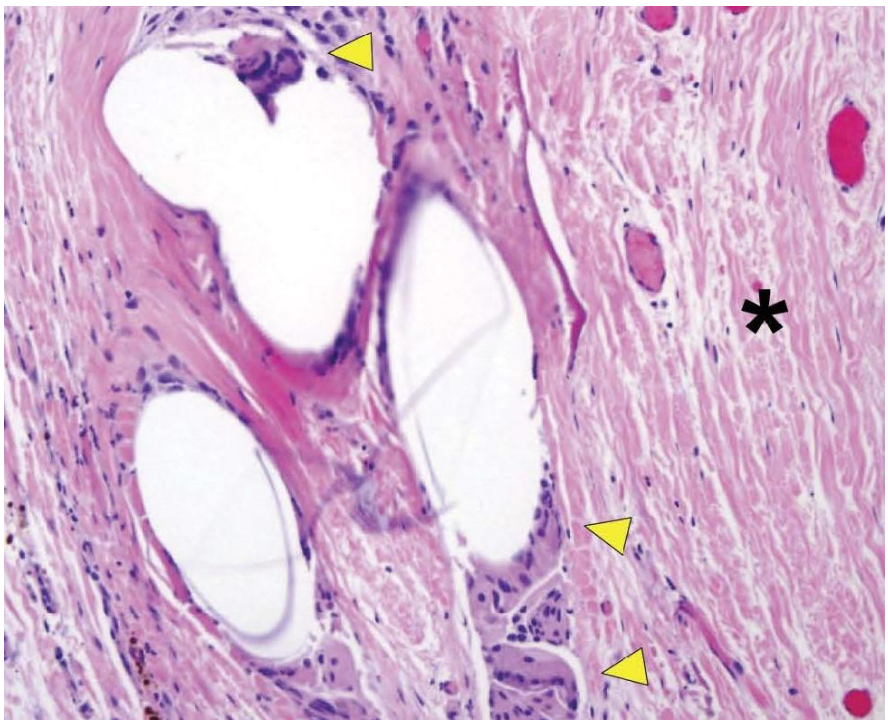

Fig 1.8 – Histological examination of explanted mesh showing foreign body giant cell reaction (arrows) and fibrosis (asterisk). Image reproduced with permission from Wolters Kluwer Health, Inc.

Nolfi et al (Nolfi et al., 2016) were the first ones to look at the macrophage response in the explanted meshes of patients with pain and mesh exposure. They compared this group to full thickness vaginal biopsy specimens from women who underwent surgery for prolapse repair. They looked at mesh-vaginal tissue complexes excised from 27 patients and the explantation was done between 4.5-93 months post-surgery. Biochemically, using Enzyme-linked Immunosorbent Assay (ELISA), they found raised pro-M1 and M2 cytokines and chemokines – IL-4, IL-10, TNF-α, IL-12p40p70, IL-12p70, CXCL10, CCL17 - in the mesh tissue compared to the non-mesh tissue.

Calculating the M2/M1 ratio from the cytokine and chemokine levels obtained using ELISA, they found a decreased value indicating a shift to a pro-inflammatory milieu. Although pro-

MMP2 was similar in mesh group as well as control, Pro- and active MMP9 were raised in the mesh group vs control. There was an increase in pro-MMP9 suggesting increased degradation which can lead to exposure. Within the mesh group, Pro-MMP9 was measured using the Fluorokine E human active mmp-9 kit and was 1.88-fold higher in the exposure group vs pain. There was no difference in cytokine or chemokine levels and for active and pro-MMP2 between the exposure and pain group. Immunofluorescence revealed pro-inflammatory M1 (CD86+ & CD68+) macrophages around the mesh fibres compared to few or almost none in the control group. Their results agreed with the other studies demonstrating an inflammatory response in the mesh-tissue complexes months to years after these were implanted in the patients.

In the pain group, an opposite effect was seen with an increase in the M2 macrophages which are associated more with tissue remodelling and fibrosis. There was also an increase in IL-10 which is increased in fibrotic responses. The macrophages were more concentrated around the mesh fibres.

Klosterhalfen et al conducted one of the biggest studies on explanted meshes. They reviewed 623 polypropylene meshes explanted from various parts of the body and showed that meshes with larger pores showed less calcification, bridging and inflammatory infiltrate (Klosterhalfen and Klinge, 2013). Similarly other clinical studies comparing lightweight and heavyweight polypropylene meshes found the lightweight meshes to be associated with reduced foreign body response and fibrosis (Orenstein et al., 2012). There were a few limitations with this study. They could not include mesh-tissue complexes from asymptomatic patients to compare the inflammatory response. The mesh removed from the patient was not marked so the part of the mesh examined did not correlate with the site of the complication. Nevertheless, it was an important study that showed a positive link between fibrosis and pain in patients who reacted to the polypropylene mesh.

Li et al (Li et al., 2017) retrospectively evaluated 266 mesh specimens explanted from 141 patients between July 2010 and June 2015. Two pathologists separately looked at the slides and were blinded from the patient's clinical histories and previous pathological reports. Clinically, the common indications for removal were exposure, pain, voiding dysfunction, infection and recurrent prolapse. The patients complaining of pain tended to be younger (<60 years) and those with erosion tended to be older (>60 years). Mild chronic

inflammation was found in 50.4% of the specimens and moderate inflammation in 33.8%. In the erosion group, the degree of inflammation correlated with distance to the eroded area. The inflammation was more marked nearer to the erosion. Tissue integration was seen in almost all specimens with mild fibrosis in 74.4% of specimens, moderate in 21.8% and none in 3.8%. Neo-vascularisation was seen in all specimens to various extents. Nerve fibres were seen in 67.7% of the specimens. 25.6% of these were within 1mm of the mesh filaments. Adipose tissue was identified in 18.4% cases microscopically. When correlated clinically, patients complaining of pelvic pain had greater chronic inflammation, however this did not reach statistical significance. Interestingly, patients with pelvic pain had a significant correlation with presence of adipose tissue (p=.025) although the mechanism behind this is not clearly understood.

A summary of studies of explanted meshes is shown in Table 1.3. Fibrosis is seen in all of the studies with some demonstrating an accompanying acute inflammatory component as well. Most studies use one or two immunohistochemistry or genetic expression markers to detect M1 or M2. Based on these studies we have generated a list of multiple M1(inflammatory) and M2(pro-fibrotic/anti-inflammatory) genetic expression markers (Table 1.4) which can be used to determine polarisation.

SUMMARY:

Fibrosis is a key feature in biomaterials explanted from the pelvic floor due to complications. This is supported by the gross and microscopic findings of fibrous encapsulation, foreign body giant cells, raised pro-fibrotic cytokines, mesh degradation and tissue erosion. Currently there is no simple *in vitro* model to assess the fibrotic potential of biomaterials used in the pelvic floor.

Table 1.3 – Summary of studies on mesh explants. Adapted from Thomas et al (Thomas et al., 2018).

Authors	Number of patients	Duration	Type of mesh	Implantation group	Location	Results
Nolfi et al (Nolfi et al., 2016)	27	4.5-93 months	Multiple	Exposure group vs pain group	Vagina	- Increase in proinflammatory cytokines in the excised mesh when compared with controls with no mesh exposure nor pain (n = 30) - Increase by 2.85 and 2.08 fold in the number of active MMP-9 and MMP-2 cells - Pro-MMP-9 were 88.4% higher in those explants removed for exposure when compared with pain
Smith et al (Smith et al., 2013)	102	2 years	PPL	N/A	Vaginal wall	- Fibrosis was present in 70.1% of the explanted mesh, along with FGGCs at 18.8%. Inflammation was only present in 10.4%.
Wang	24	1 week to 1 year	TVT/SPARC	N/A	Vagina	- All patients had either an acute or chronic inflammatory response of FBGCs, a foreign body reaction and fibrosis throughout follow-up

et al (Wang et al., 2004)						
Li et al (Li et al., 2017)	141	n/a	PPL	Pain vs exposure	Vagina	- Pain in younger age group, erosion in older age group. - Mild to mod fibrosis in all specimens - Chronic inflammation and increased adipose tissue in pain group

Table 1.4 – Most common genetic expression markers specific to M1 and M2 macrophages as identified from literature.

Protein/Gene	Symbol	Macrophage phenotype	Pro-inflammatory stimuli (LPS/IFN-g)	Anti-inflammatory stimuli (IL-4/IL-10)
Cluster of differentiation 80	CD 80	M1	Up	-
Cluster of differentiation 86	CD 86	M1	Up	-
Cluster of differentiation 163	CD 163	M2	-	Up
Cluster of differentiation 206	CD 206	M2	-	Up
Interleukin-1 beta	IL-1β	M1	Up	-
Tumor necrosis factor-alpha	TNF-α	M1	Up	--
Interleukin-6	IL-6	M1	Up	-
Transforming growth factor beta	TGF-β	M2	-	Up
Interleukin 10	IL-10	M2	-	Up
Chemokine Receptor 7	CCR7	M1	Up	-
Interleukin 13	IL-13	M2	-	Up

1.7 AIMS AND OBJECTIVES:

AIM:

Polypropylene mesh has been found to lead to sustained inflammation and fibrosis in some patients. Could this have been avoided with more critical in vitro testing prior to clinical implantation?

The aim of this research is to develop a useful *in vitro* model for immunological assessment of biomaterials used in the pelvic floor considering both biomechanical and oxidative stresses that such materials will encounter post implantation. In the current study, our focus will be on polypropylene as this is the material that has been used predominantly in the pelvic floor.

OBJECTIVES:

1. To culture freshly isolated macrophages and optimise a seeding strategy for them on polypropylene mesh such that RNA can be extracted from them post culture on the mesh.

2. To study the gene expression of macrophages in response to polypropylene mesh which has been subjected to mechanochemical stress. qPCR will be used for this purpose.

3. To assess the impact of macrophages seeded on polypropylene mesh on fibroblasts. This will be done by 2D culture in conditioned media collected from earlier experiments as described in 2. We will utilise qPCR to assess the genetic response and immunohistochemistry with epifluorescence microscopy to assess the morphological response to the macrophage conditioned media.

4. Use the results obtained from the experiments conducted in 2 and 3 and data obtained from the literature obtained on mesh explanted from the pelvic floor to propose a theoretical *in vitro* model that combines mechano-chemical stressing and immunological assessment of a biomaterial to predict it's fibrotic potential *in vivo*.

CHAPTER 2

MATERIALS AND METHODS

MATERIALS AND METHODS:

2.1. Preparation of polypropylene mesh scaffolds:

Strips of commercially available sterile polypropylene (PP) surgical mesh, (Prolene® Mesh, Ethicon), were cut into 1.5cm x 1.5cm strips using sterilised scissors within a cell culture cabinet along the longitudinal direction of the surgical mesh.

To mechanically and chemically stress the PP mesh, samples were clamped between the grips of an Ebers bioreactor (Ebers Medical Technology SL, Zaragoza, Spain). Samples were immersed in 3 % hydrogen peroxide solution (Sigma-Aldrich) and subjected to cyclic uniaxial distension at a frequency of 0.5 cycles per minute at 37 °C (to mimic the changes in abdominal pressure during normal breathing cycles) for 72 hours. These samples were then referred to as mechanochemically distressed samples throughout this thesis. Cells were not cultured on the mesh at any point during mechanochemical distension.

2.2 Monocyte isolation and culture

Primary blood derived monocytes were isolated from buffy coats from healthy blood donors obtained from NHS BT Manchester. Human monocytes were isolated from these leukocyte-enriched buffy coats. Blood was diluted 1:1 with HBSS without calcium and magnesium (Thermofisher Scientific, UK), layered on Ficoll-Paque Plus (Amersham Biosciences, UK) and centrifuged for 40 minutes at 400 x *g*. The mononuclear cell-rich layer was removed, washed twice with Hank's Balanced Salt Solution (HBSS) and resuspended in Iscove's Modified Dulbecco's Medium (IMDM) (Lonza, UK) supplemented with 2% human AB serum (Merck) and 5ml penicillin/streptomycin solution (Sigma-Aldrich). Mono-nuclear cells were seeded at a density of 8×10^7 into 10 cm^2 tissue culture plates and cultured for 2 hours after which nonadherent cells were removed by washing three times with HBSS and the culture medium replenished. To generate fully differentiated monocyte-derived macrophages

(MDM), adherent monocytes were cultured for 7 days in IMDM and media was changed on day 1, 3 and 7. These were then scraped off with a cell scraper (Thermofisher, UK) and seeded at a density of 1 x 10^6 cells in 150µl of IMDM media on non-stressed polypropylene mesh, mechano-chemically distressed polypropylene mesh or well plate for 7 days for subsequent experiments. Conditioned media from macrophages cultured on non-distressed and mechanochemically distressed polypropylene mesh was collected at Day 1, 3 and 7 and frozen for a few months for later experiments.

2.3 Fibroblast isolation and culture:

All procedures for isolation and culture of human dermal fibroblasts were undertaken in a sterile laminar flow culture hood reserved specifically for human cell lines. Human dermal fibroblasts (HDF) in a T75 flask (Nalgene, UK) at passage four were isolated from primary human tissues isolated under NHS ethics 15/YH/0177. Dulbecco's Modified Eagle Medium (DMEM) supplemented with 50mL FBS (Biowest Biosera UK), 5mL penicillin (100units/mL) and streptomycin (100ug/mL), and 2.5mL fungizone (630ng/mL) was used as tissue culturing media. After washing twice with 10ml PBS, 5mL Trypsin/EDTA was added to the T75 flask and incubated at 37C in a 5% CO2 atmosphere for five minutes. 15mL DMEM medium was added to the flask and the suspension was centrifuged at 1000rpm for 5 minutes. The pellet was isolated and resuspended. Cells were counted in a haemocytometer and 100,000 cells were added to two fresh T75 flasks for cell expansion.

HDF were seeded in a 12-well plate (Sarstedt) at 10,000 cells per well in complete DMEM supplemented with 50mL FBS, 5mL penicillin (100units/mL) and streptomycin (100ug/mL), and 2.5mL fungizone (630ng/mL) as tissue culturing media with cells incubated at 37^{o}C in a 5% CO2 atmosphere. As described earlier, conditioned media from macrophages contains IMDM. To assess the effect of IMDM on fibroblasts, HDF were also cultured in complete IMDM supplemented with 50mL FBS, 5mL penicillin (100units/mL) and streptomycin (100ug/mL), and 2.5mL fungizone (630ng/mL) as tissue culturing media with cells incubated at 37^{o}C in a 5% CO2 atmosphere. Both of these groups served as negative control.

For positive control, HDF were seeded in at a similar density in a 12-well plate in complete DMEM supplemented with 50mL FBS, 5mL penicillin (100units/mL) and streptomycin (100ug/mL), and 2.5mL fungizone (630ng/mL) with 5ng/ml TGF-β added. HDF were also cultured separately in complete IMDM supplemented with 50mL FBS, 5mL penicillin (100units/mL) and streptomycin (100ug/mL), and 2.5mL fungizone (630ng/mL) with 5ng/ml TGF-β added.

Conditioned media collected as described in section 2.2 was mixed 1:1 with DMEM. HDF were seeded at a density of 10,000 cells per well and cultured in conditioned media from macrophages cultured on non-distressed mesh and mechanochemically distressed mesh. To study the genetic expression, cells were cultured for 48 hrs. For immunohistochemical analysis, cells were cultured for 7 days.

2.4 Cell seeding optimisation:

To achieve sufficient RNA yield for subsequent analysis, the seeding protocol first needed to be optimised. Parameters including seeding volume, seeding density, utilising a steel ring to hold the biomaterial down, utility of a Cell protect buffer, elution of lysate separately or together, homogenisation of sample and comparing Trizol with lysate buffer in the Monarch kit. Concentration of RNA isolated was used to determine the optimum protocol. RNA extraction was performed as described in section 2.5.1.

2.4.1. Seeding volume:

Monocytes were isolated and cultured as described in section 2.2. After 7 days of culture cells were scraped off the tissue culture plastic using a cell scraper and seeded at a density of $1x10^6$ cells in 2ml, 1ml, 500µl and150µl on non-distressed polypropylene mesh for 4 hrs. This was followed by topping up with 1ml of media before being left overnight in an incubator at 37°C and 5% CO_2. LIVE/DEAD staining and imaging using a confocal microscope were performed (as described in section 2.7.1) after 3 days to assess cell attachment and viability.

2.4.2 Seeding density:

Monocytes were isolated and cultured as described in section 2.2. After 7 days of culture cells were scraped off the tissue culture plastic using a cell scraper. Cells were seeded in varying densities at $0.1x10^6$, 0.5×10^6, 1×10^6 and 3×10^6 cells in 150 µl of IMDM.

2.4.3 Stainless steel rings for anchoring:

As polypropylene floats, stainless steel rings custom-made by NHS Sheffield medical devices department with a 1cm inner diameter were utilised to keep polypropylene from floating.

Monocytes were isolated and cultured as described in section 2.2. Cells were seeded as described in section 2.2 at a seeding volume of 150µl and density of 0.1 x 10^6 cells per well. Three mesh samples were held in place with a stainless steel ring and three without.

2.4.4 Cell Protect buffer vs no Cell Protect buffer:

Monocytes were isolated and cultured as described in section 2.2. Macrophages were seeded as described in section 2.2. Cell protect buffer from the Monarch Total RNA miniprep kit was added on Day 3 to three of the samples prior to adding the lysis buffer and not for the other three. The three samples with the cell protect buffer were then incubated for 30 mins at 55C in 5% CO2. The remainder of the RNA extraction was carried out using the protocol described in section 2.5.1.

2.4.5 Elution of lysate separately vs together:

Monocytes were isolated and cultured as described in section 2.2. Macrophages were seeded as described in section 2.2. For three of the samples, after adding the lysis buffer, cell lysate from all three samples was collected and eluted through a single RNA purification column whereas the remaining three samples were eluted separately in three separate RNA purification columns.

2.4.6 Trizol vs Lysis buffer:

Monocytes were isolated and cultured as described in section 2.2. Macrophages were seeded as described in section 2.2. RNA extraction was carried out on day 3. For three of the samples, 0.2ml Chloroform was added to 1ml TRIzol per sample. After vigorous micropipetting, each sample was transferred to an RNase free Eppendorf and centrifuged at 12,000 x g for 15 mins at 4C. Clear aqueous phase at the top was aspirated carefully and transferred to an RNA purification column. The remaining steps of the procedure are described in section 2.4.4.1. For the other three samples, the protocol described in section 2.4.4.1 was followed from the start.

2.4.7 Homogenisation:

Monocytes were isolated and cultured as described in section 2.2. Macrophages were seeded as described in section 2.2. RNA extraction was carried out on day 3. Three of the samples were cut into 4 pieces and placed in a 2ml Eppendorf tube with 2mm metal beads. 300ul of lysis buffer was added to each tube. These were vortexed for 2 cycles of 30 seconds. The lysate was removed and pipetted into a gDNA spin column. The RNA extraction was carried out as described in section 2.51. For the remaining three samples, RNA extraction was carried out without vortexing as described in section 2.5.1.

2.5. Extraction and quantification of macrophage/fibroblast mRNA

2.5.1. RNA Extraction

RNA was extracted using the Monarch Total RNA Miniprep kit as per the manufacturer's instructions omitting the proteinase K step of the protocol. Lysis buffer was added at a volume of 300µl to each well to lyse the cells (macrophages and fibroblasts). The lysate was pipetted multiple times to ensure maximum cell lysis and then transferred to a gDNA removal column. Samples were centrifuged (Sanyo Hawk 15/05) at 16,000 x g for 30 seconds to remove gDNA. The flow through was saved and an equal volume of ethanol (>95%) was added to the sample and mixed thoroughly by pipetting. Each mixture was transferred to an RNA purification column fitted with a collection tube and centrifuged for 30 seconds at 16,000 x g. The flow-through was discarded. 500µl of RNA Wash buffer was added to each RNA purification column and centrifuged for 30 seconds at 16,000 x g. The flow-through was discarded. 5µl of DNAse I and 75µl of DNase I Reaction buffer were combined in an RNase-free microfuge tube and pipetted on top of each RNA purification column matrix. The samples were incubated for 15 minutes at room temperature. 500µl of RNA Priming Buffer was added to each RNA purification column and centrifuged for 30 seconds at 16,000 x g. Flow-through was discarded. 500µl of RNA Wash buffer was added to each RNA purification column and centrifuged for 30 seconds at 16,000 x g. Flow-through was discarded. 500µl of RNA Wash buffer was added again to each RNA purification column and centrifuged for two minutes at 16,000 x g. Each RNA purification column was transferred to a separate RNase-free microfuge tube. 60µl of nuclease-free water was

pipetted directly on top of each column matrix and centrifuged for 30 seconds at 16,000 x g. The eluted RNA was pipetted again on the column matrix and centrifuged again for 30 seconds at 16,000 x g for maximal RNA recovery. Spectrophotometric analysis of extracted RNA was carried out using Nanodrop 1000 (Thermo Fisher Scientific) to quantify RNA. RNA purity was assessed using the ratio of absorbance at 260nm to absorbance at 280nm. Samples with 260/280 of 2 or greater were deemed pure. RNA not being used for immediate downstream applications was stored in -80°C in RNase-free microfuge tubes.

2.5.2. Transcription into cDNA

mRNA extracted as described in Section 2.2.3.1 was transcribed into cDNA using a QuantiTect Reverse Transcription kit. For the gDNA elimination reaction, the mixture was prepared as per table 2.1 and stored on ice. The gDNA elimination reaction was carried out by incubating the samples in a Qiagen QIAquant 96 PCR machine for 2 minutes at 42C. The samples were then removed and placed on ice. The reverse-transcription master mix was prepared according to Table 2.2. 6µl of reverse-transcription master mix was added to each sample from the gDNA elimination reaction to achieve a total reaction volume of 20µl per sample. This was incubated in the QIAquant 96 PCR machine for 15 minutes at 42C to transcribe the cDNA and followed by incubation for 3 minutes at 95C to inactivate the QuantiTect reverse transcriptase.

Table 2.1 – Amount of different components for genomic DNA elimination reaction. All reactions are normalised to the sample containing least amount of RNA.

Component	Volume/reaction	Final concentration
gDNA Wipeout Buffer, 7x	2 µl	1x
Template RNA	Variable (upto 1µg)	
RNase-free water	Variable	
Total volume	14 µl	-

Table 2.2 – Amount of different components for reverse-transcription reaction.

Component	Volume/reaction	Final concentration
Quantiscript Reverse Transcriptase	**1** µl	
Quantiscript RT Buffer, 5x	**4** µl	**1x**
RT Primer Mix	**1** µl	

2.5.3. Quantification of cDNA

Taqman quantitative polymerase chain reaction was performed on the cDNA to quantify gene expression of macrophage markers using primers outlined in table 2.3. A standard reaction mixture was prepared using the components mentioned in table 2.4.

Table 2.3. A list of primers used for qPCR.

Primer	Assay ID	Supplier
CD86	Hs01567026_m1	**Applied Biosystems, UK**
CD80	Hs01045161_m1	**Applied Biosystems, UK**
CD206	Hs07288635_g1	**Applied Biosystems, UK**
TNF-α	Dr03126850_m1	**Applied Biosystems, UK**
IL-6	Hs00174131_m1	**Applied Biosystems, UK**
IL-10	Hs00961622_m1	**Applied Biosystems, UK**
IL-13	Hs00174379_m1	**Applied Biosystems, UK**
CCR7	Hs01013469_m1	**Applied Biosystems, UK**
IL1-β	Hs01555410_m1	**Applied Biosystems, UK**
TGF-β1	Hs00998133_m1	**Applied Biosystems, UK**
B2M	Hs00187842_m1	**Applied Biosystems, UK**

Table 2.4 – List of components used in a standard reaction mixture for qPCR.

Components	Volume
Lo-Rox Taqman master mix	5 µl
B2M housekeeping gene primer	0.5 µl

Gene expression marker primer of interest	0.5 µl
cDNA	1 µl
Nuclease-free water	3 µl
Total reaction volume	10 µl

Reaction mixtures were pipetted into a 96 well PCR plate and a qPCR reaction was carried out in a QiaQuant 96 PCR machine. Fluorescence was measured at 518nm (FAM) for genes of interest and 554nm (VIC) for housekeeping gene at each cycle. Ct values were obtained by recording cycles at which 0.04 fluorescence units were reached. A standard program for the qPCR thermocycler is detailed in table 2.5. Relative gene expression of the gene of interest compared to the housekeeping gene B2M is calculated using the $2^{-\Delta\Delta Ct}$ method where: ΔΔCt = ΔCt sample – ΔCt reference control (Livak and Schmittgen, 2001).

Table 2.5 – qPCR thermocycler standard settings for qPCR using TaqMan primers.

Step	Temperature (°C)	Time	
Initial denaturation	95	3 minutes	
Denaturation	95	10 seconds	Repeat
Annealing/Extension	60	30 seconds	X40
Hold	4	∞	

2.6. Immunostaining to assess a-SMA expression:

HDF were isolated and seeded as described in section 2.3. Cells were cultured for 7 days with conditioned media added at day 1 after seeding and changed on day 4. Cells were then fixed in 3.7% formaldehyde (Sigma Aldrich, UK) for 15 mins followed by three washes with Phosphate Buffered Solution (PBS). Following this, cells were incubated in 0.5% Triton X-100 (Sigma Aldrich, UK) in PBS for 20 mins and then washed thrice with PBS. 2.5% bovine serum albumin (BSA) (Sigma Aldrich, UK) in PBS was added as a blocking buffer for one hour. After one wash with PBS cells were incubated with the primary antibody (mouse anti-human α-SMA antibody – Abcam) diluted in 1% BSA, 1:1000) for 90 minutes. Following three more washes with PBS, cells were then incubated with the secondary antibody (anti-mouse TRITC conjugated antibody – Abcam) diluted in 1% BSA, 1:1000 for 30 minutes. Finally, following

three washes with PBS, 4',6-diamidino-2-phenylindole dihydrochloride (DAPI) (1:1000 in PBS) (Gibco Invitrogen, Paisley, UK) was added to the samples for 10 minutes.
Cells were imaged directly in the well plate using an Olympus IX73 inverted epifluorescence microscope. Images were saved at a 10x magnification and analysed in Image J software. α-SMA staining intensity was calculated by measuring the intensity in the red channel using Image J software using methodology documented on the ImageJ website (ImageJ, 2024). Three images from three different parts of each slide were used per condition (DMEM, IMDM, TGF-β, conditioned media from non-distressed mesh and mechanochemically distressed mesh). Each image was first split into different channels. The red channel image was selected and inverted to convert to grayscale. Threshold was set to when the red signal covers maximum stained areas. The image was then converted to binary. A rectangle was drawn over the entire image and analysed using mean, minimum and maximum gray value. This process was repeated for all other images. Values obtained were plotted and analysed using GraphPad Prism v10 for Mac (GraphPad Software, Inc., San Diego, CA).
Myofibroblast morphology in fibroblasts cultured in conditioned media was compared to positive control as well as image available in literature as shown in fig 2.1 (Gerarduzzi and Di Battista, 2017).

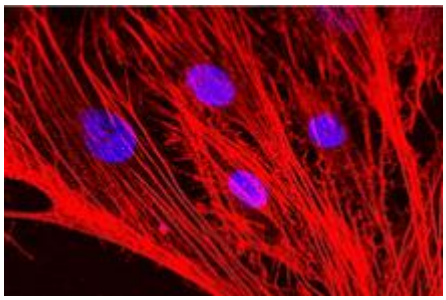

Fig 2.1: Fibroblasts treated with TGF-β showing myofibroblast morphology with α-SMA expression (Gerarduzzi and Di Battista, 2017). Image used with permission from Creative Commons using the license https://creativecommons.org/licenses/by/4.0/.

2.7. Imaging:

2.7.1 Live dead staining:

3 µl of Calcein AM was added to 12 µl of ethidium homodimer-1 in 6ml PBS. 1ml of solution was added to cells cultured on meshes in the well plate and gently moved to cover the sample entirely. Samples were incubated at 37C for 20 minutes and imaged using a confocal microscope (Zeiss LSM 700). Calcein has green fluorescence (479nm excitation and 517nm emission) indicating live cells. Dead cells are indicated by bright red fluorescence of ethidium homodimer-1 (528nm excitation and 617nm emission).

2.7.2 Microscopy:

Confocal microscopy of samples was conducted on a Zeiss LSM 700 using the 10x/1.4 dry objective. An argon 488nm laser was used for excitation of calcein and a Hene 543nm laser was used to excite ethidium homodimer-1. High magnification images were taken of each sample and each image was imported into ImageJ for further processing.

2.8. Statistical Analysis:

Statistical analysis was performed using GraphPad Prism v10 for Mac (GraphPad Software, Inc., San Diego, CA). Details of the statistical analysis performed is detailed in the figure legends.

CHAPTER 3

Development of optimal cell seeding strategy for macroporous biomaterials to extract sufficient RNA for downstream applications

3.1 INTRODUCTION:

Our primary aim was to set up an *in vitro* model to investigate the interaction between macrophages and biomaterials used in the pelvic floor. The biomaterial we chose to start with was polypropylene as it is most frequently used in the pelvic floor. To study how the macrophages interact with polypropylene, we needed to seed the macrophages on the mesh and leave them in contact long enough so they can adhere to it. As polypropylene mesh is macroporous, cell seeding presented a big challenge at the start of the project. Although there are protocols for seeding macrophages on biomaterials (Witherel et al., 2018), none of them tailor the seeding strategy to polypropylene. Also, there is no consensus on the optimal amount of cells to seed. In methods described in literature, macrophages are seeded from as little as 67 x 10^3 cells to 17.5 x 10^6 cells (Grotenhuis et al., 2014, Witherel et al., 2018, Boersema et al., 2016). As this is a key step in producing the model, we therefore performed a series of experiments to optimise the seeding strategy that results in maximal adherence of macrophages to the polypropylene mesh. To carry out PCR, we also needed a method to extract RNA from the cells that is sufficient for downstream applications. The kit we use to convert RNA to cDNA is optimised for use from 10pg to 1ug of RNA (QuantiTect, 2022). We performed experiments to optimise our RNA extraction method to get the maximum amount of RNA sufficient for qPCR analysis.

3.2 Results:

3.2.1 Seeding volume:

The amount of RNA extracted from cells seeded onto mesh in different volumes of media was compared. On visual inspection, cells seeded in a volume of 150µl stayed above the surface of the mesh as seen in figure 3.1. At all other volumes, the mesh was submerged in the media. LIVE/DEAD imaging showed there was a maximum attachment of cells in the 150µl media group with minimal attachment in the other groups as seen in fig 3.2. Cells attached maximally near the knots.

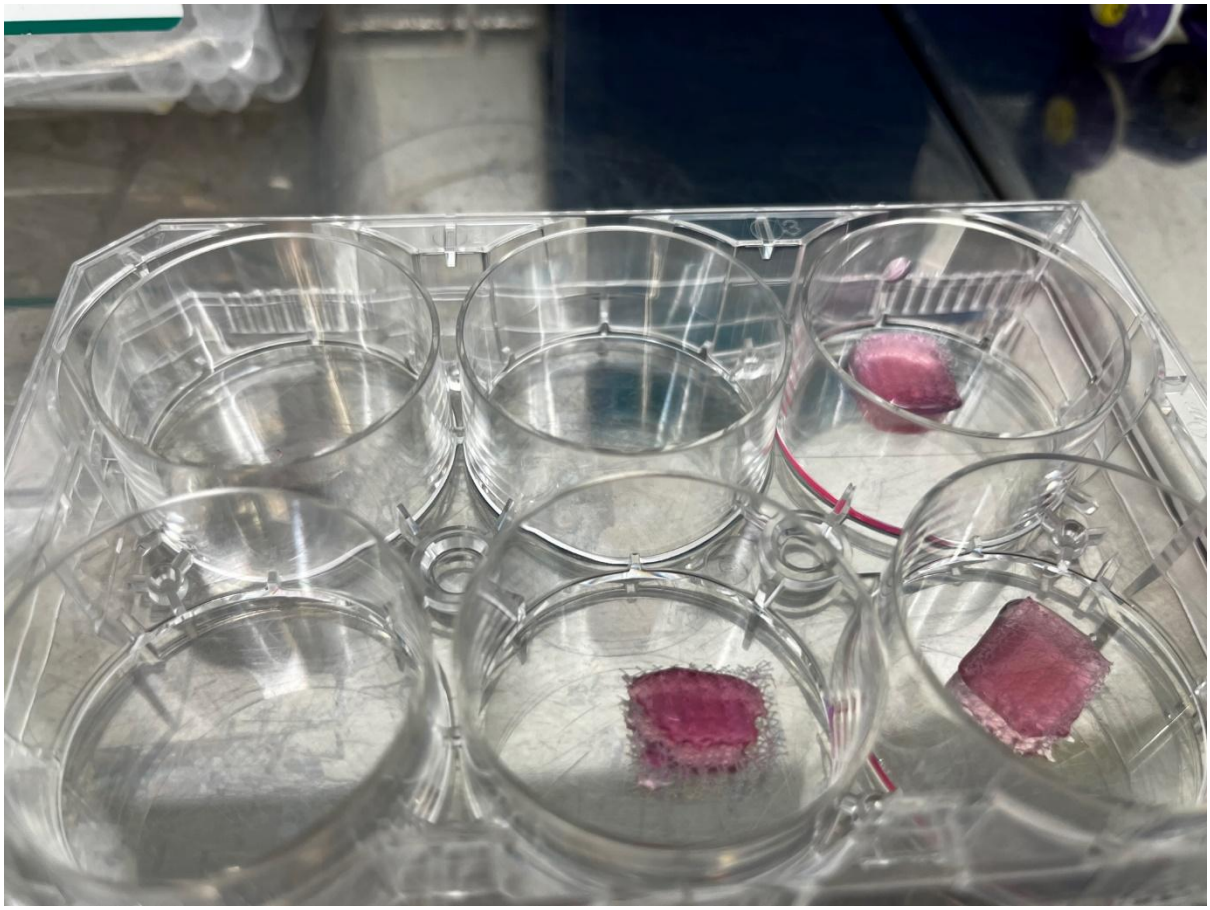

Fig 3.1 – Cells seeding at a volume of 150µl stay on the top surface of the mesh without seeping through to the bottom of the well plate.

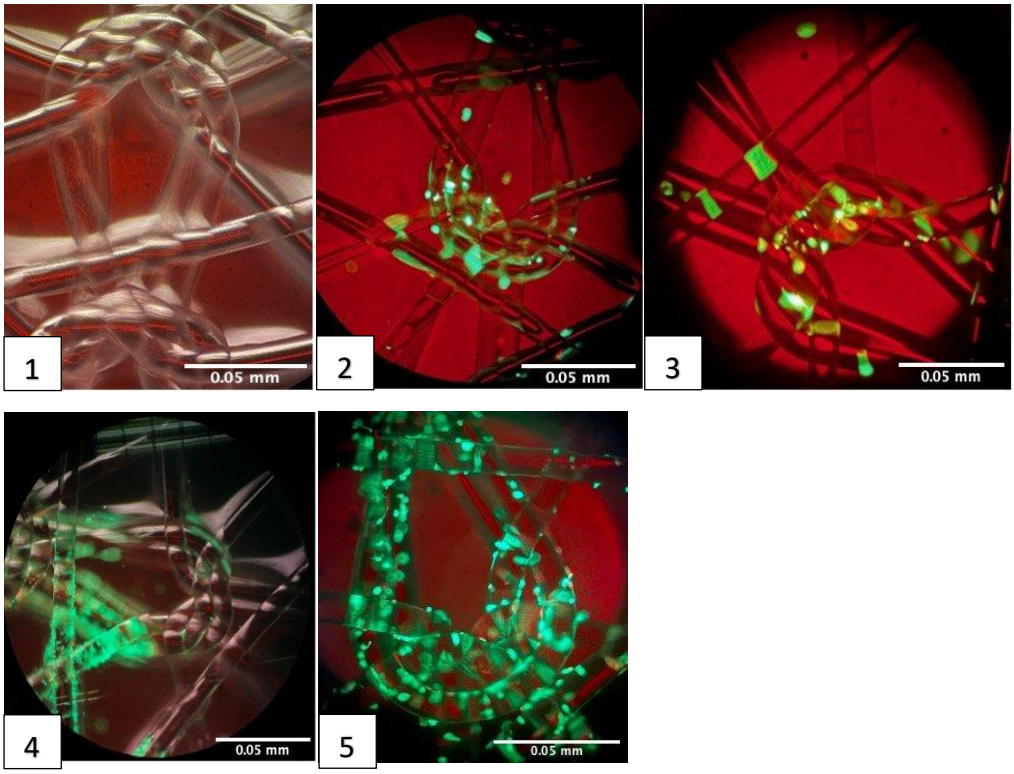

Fig 3.2 – Epifluorescence microscopy at 10x showing macrophage attachment to mesh. Green fluorescence implies cells are alive. (1) Control – mesh with no cells (2) 2ml seeding volume (3) 1ml seeding volume (4) 500µl seeding volume (5) 150µl seeding volume.

Negligible amounts of RNA were extracted from cells seeded in 2ml and 1ml (figure 3.3). The highest concentration of RNA was extracted from cells seeded in 150µl of media as seen in figure 3.3. From the RNA reverse transcription kit manual (QuantiTect, 2022), it was understood that we needed at least 0.2pg/µl of RNA for cDNA synthesis. Therefore, the amount of RNA obtained was sufficient to carry out qPCR. Based on our results, we chose 150µl as our seeding volume.

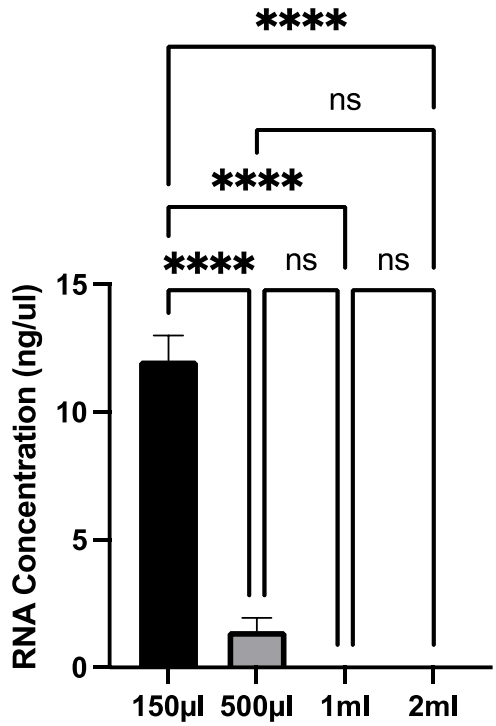

Fig 3.3 – Graph showing concentration of RNA extracted from different seeding volumes. Statistical analysis using One-way ordinary ANOVA with post-hoc analysis using Bonferroni correction. ** = significant with p-value <0.0001, ns = no significance.**

3.2.2 Seeding density:

RNA concentration was compared between samples with varying cell density.
The highest concentration of RNA was isolated from 1 x 10^6 cells with 13 ng/µl extracted on average (Figure 3.4). The minimum RNA concentration needed for downstream applications is 0.2pg/µl (QuantiTect, 2022) therefore, 1 x 10^6 cells in 150 µl was used as the seeding density.

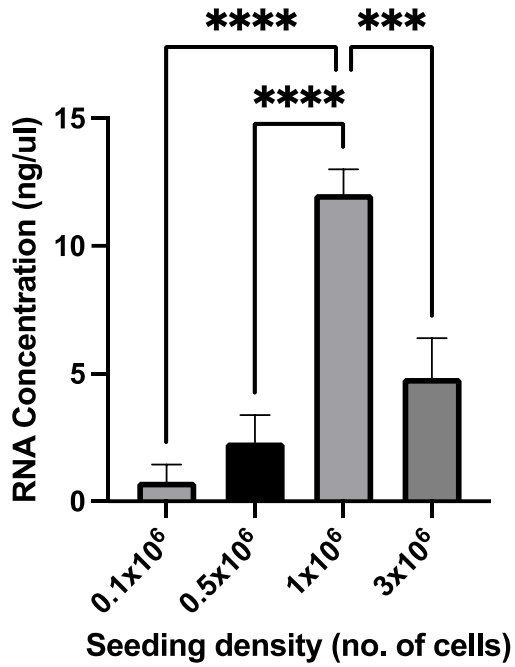

Fig 3.4 – Graph showing concentration of RNA extracted from different cell seeding densities. Statistical analysis using ordinary one-way ANOVA with post-hoc analysis using Bonferroni correction. * = significant, p-value <0.001, **** = significant with p-value <0.0001.**

3.2.3 Ring vs no ring:

Cells were seeded with a stainless steel to anchor the samples and to stop them from floating. There was no significant difference in the concentration of RNA extracted with or without the rings and both methods resulted in between the sufficient RNA for subsequent qPCR analysis. Based on these results, we decided not to use rings in our model.

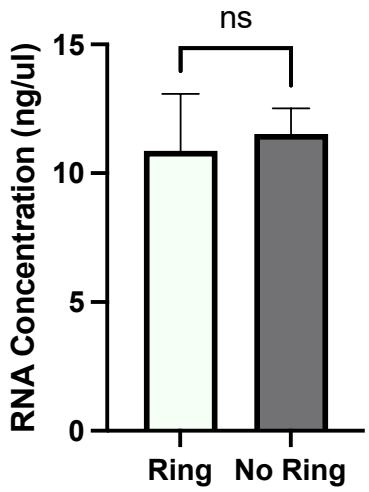

Fig 3.5 – Graph showing concentration of RNA extracted from group with stainless steel ring vs without. Statistical analysis using unpaired t-test. ns = not significant, p-value >0.05.

3.2.4 Cell Protect buffer vs no Cell Protect buffer:

Our RNA extraction kit contains an extra step to incubate the biomaterial with a Cell Protect buffer solution to maximise RNA recovery from white blood cells. This step requires incubation at 55 degrees Celsius for 30 minutes and adds to the RNA extraction time. We compared the RNA concentration between samples extracted with Cell Protect buffer and samples without. There was no significant difference in RNA concentration between the two groups. The RNA extracted was enough for qPCR. We therefore chose to omit the Cell Protect incubation step for our extraction protocol.

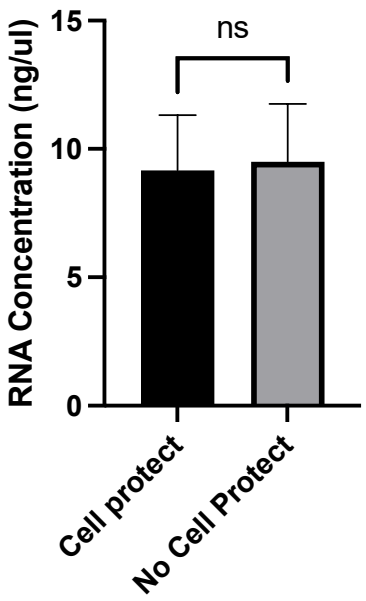

Fig 3.6 – Graph showing concentration of RNA extracted from group using Cell Protect buffer vs no Cell Protect buffer. Statistical analysis using unpaired t-test. Ns = not significant, p-value >0.05.

3.2.5 Elution of lysate separately vs together:

RNA concentration was compared between samples whose cell lysate was eluted separately during RNA extraction and those eluted together. There was slightly more RNA extracted from the group extracted separately compared to the group that was eluted together but this did not reach statistical significance. To keep our extraction method simple, we chose to elute our samples separately.

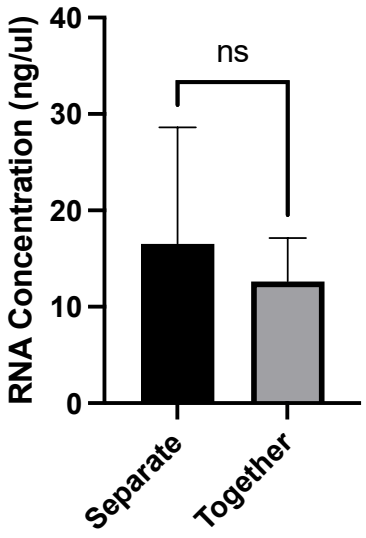

Fig 3.7 – Graph showing concentration of RNA extracted from group where cell lysate is eluted separately vs where cell lysate is eluted together. Statistical analysis using unpaired t-test. Ns = not significant, p-value >0.05.

3.2.6 Trizol vs Lysis buffer:

Most studies or protocols use Trizol to extract RNA (Grotenhuis et al., 2014, Witherel et al., 2018). As we had the Monarch Total RNA prep kit in our lab, we compared RNA extraction with this kit against extraction using Trizol. There was no difference in RNA concentration extracted from the group extracted with monarch kit lysis buffer. We therefore chose to extract RNA using the Monarch kit available in our lab.

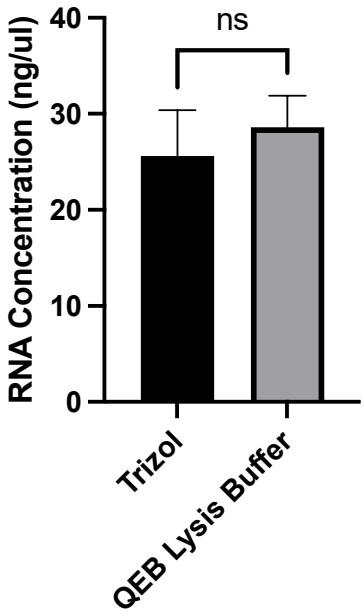

Fig 3.8 – Graph showing concentration of RNA extracted from group using Trizol vs group using QEB Lysis Buffer. Statistical analysis using unpaired t-test. ns = not significant, p-value >0.05.

3.2.7 Homogenisation:

RNA concentration was compared between samples homogenised with beads and those lysed directly in the well plate. There was no difference in the RNA concentration extracted from the group lysed directly in the well plate. For simplicity, we chose to lyse cells directly in the well plate without homogenization.

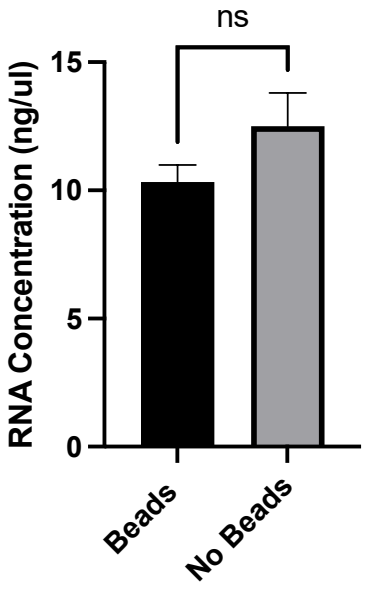

Fig 3.9 – Graph showing concentration of RNA extracted from group homogenised with beads prior vs group where cells are lysed in the well plate. Statistical analysis using unpaired t-test. ns = not significant, p-value >0.05.

3.3 DISCUSSION:

There is an increasing trend in the scientific world to design in-vitro models to assess the immune response to biomaterials (Lock et al., 2019). These have been discussed earlier in

section 1.4.3. There are various seeding strategies published in the literature (Grotenhuis et al., 2014, Zhou et al., 2017, Witherel et al., 2018). The challenge we faced at the start of this study was to adapt these strategies to polypropylene mesh which is macroporous. We therefore set up experiments to optimise cell seeding and then optimise subsequent RNA extraction.

Polypropylene is a thermoplastic polymer created from propylene (Maddah, 2016). It is considered inert and has a high coefficient of friction which makes it an ideal biomaterial for surgical purposes like making sutures that slip easily through tissue without causing much damage. When knitted into a mesh, they are constructed with large pores to promote tissue ingrowth and enough flexibility to be placed easily in the body to provide support (Klosterhalfen and Klinge, 2013) .Unfortunately these properties make it a difficult material for cell attachment. Its hydrophobic surface makes it difficult for macrophages to adhere to it in-vitro and its large pores (164 x 96μm) allow macrophages (30μm) to pass through them easily without attaching.

There is a dearth of published methods for seeding immune cells on biomaterials, especially for polypropylene. The studies that have published their seeding strategies either do not apply to polypropylene or need some modification of the biomaterials to promote cell adhesion. For example, Boersema et al wove polypropylene into a monofilament yarn with micro- and macro-pores to promote cell attachment (Boersema et al., 2016). This method is not suitable for our experiments as we did not wish to introduce bias by modifying the surface characteristics of the polypropylene mesh. Grotenhuis et al. in their study of macrophage response to biomaterials, incubated polypropylene (along with three other biomaterials) in a falcon tube with 700,000 monocytes per ml in 25mls of media for two hours (Grotenhuis et al., 2014). They do not mention whether all biomaterials were seeded in one falcon tube or separately and they do not mention the detailed configuration of the polypropylene material they used. Due to lack of detailed specifics, we did not test this technique. Witherel et al published a detailed general method of seeding macrophages on biomaterials but there is no mention of cell density or biomaterial porosity (Witherel et al., 2018). Following their generic method as a template, we initially seeded 500,000 macrophages in 2 mls of media with a stainless steel ring holding the polypropylene mesh

down. Cells were incubated on the mesh overnight and mesh was transferred to a separate 6 well plate the next day. There was minimal attachment of cells to the mesh as confirmed with live/dead staining and epifluorescent microscopy.

Our experience with macrophages mirrored that of our lab's previous work attempting to culture fibroblasts on polypropylene mesh. We therefore postulated that the cells failure to attach was due to decreased contact time with the mesh filaments and as the material is hydrophobic, we could increase contact time by seeding cells in enough media to keep them floating on the mesh surface for longer. As there is a big range (67,000 to 17.5 million) of cell seeding densities in literature (95,111,114), we chose a range of 0.1 x 10^6 cells to 3 x 10^6 cells to test. As a result of our experiments, we decided to proceed with an optimal cell seeding density of 1 x 10^6 cells in 150µl of media. Cells attached to the mesh were viable when viewed under a confocal microscope after live/dead staining.

Our ultimate aim was to obtain sufficient RNA for down stream analysis and multiple RNA extraction methods for macrophages have been widely published (Witherel et al., 2018). There are standardised kits available from different companies. Our lab uses the Monarch Total RNA prep kit from New England Biosciences, UK. There is no consensus on a particular kit the literature. Some advocate the use of TRIzol (Witherel et al., 2018, Blatt et al., 2020) for cell lysis whereas others use RNA extraction kits (Grotenhuis et al., 2014). We therefore tested TRIzol against the Monarch Total RNA prep kit and found no difference in the RNA extracted. We decided to utilise the Monarch Total RNA prep kit as it was readily available in our lab.

Biomaterials come in various configurations. Witherel et al advocate homogenisation of the biomaterials prior to extraction with either a probe homogeniser or bead-beaters(Witherel et al., 2018). As our polypropylene mesh is macroporous, we theorised that the cells are already exposed on the surface so we may not need to homogenise the mesh as the cell lysis buffer can reach them easily. Also, polypropylene mesh is tough and resistant to homogenisation. We did not find a difference in RNA extracted with or without homogenisation with a bead-beater. This agreed with our hypothesis that the exposed cells on the polypropylene mesh will lyse and release RNA without the need for homogenizing

the mesh. We therefore chose not to homogenize the polypropylene mesh for RNA extraction.

After running our optimisation experiments, we chose an optimal seeding density and volume of 1x 10^6 cells in 150µl of media on a mesh sized 1.5cm x 1.5cm, incubated at 37°C in 5% CO2 for 4 hours. Media was topped up to 2mls at this point and cells left to incubate overnight. On confocal microscopy after live/dead staining, cells were seen covering most of the mesh, especially around the knots. The simplest method for RNA extraction was to use the Monarch Total RNA prep kit for cell lysis without homogenising the polypropylene mesh and omitting the Cell Protect buffer step. This gave us a sufficient RNA yield for downstream applications which are discussed in the next chapter.

In summary, there is a lack of published methodology on seeding macrophages on macroporous biomaterials like polypropylene mesh. We conducted a series of experiments as guided by the literature to optimise the cell seeding and RNA extraction to obtain sufficient RNA for further experiments using qPCR. To our knowledge, this is the simplest cell seeding method to study undifferentiated primary blood monocyte derived macrophage response to unmodified “off the shelf” polypropylene mesh.

CHAPTER 4

Assessing the effect of mechanochemical distress on the surface changes and the biological response to polypropylene mesh

4.1 INTRODUCTION:

Polypropylene is a commonly used non-absorbable biomaterial in surgery. As a mesh, it has been used to reinforce the abdominal wall or pelvic floor (Mangir et al., 2019). Recently, especially in the context of pelvic floor repair, it has been the subject of debate and controversy due to a reported complication rate estimated to be anywhere between 5 and 42% after pelvic floor repair with polypropylene mesh (Abhari et al., 2021).

When implanted in the human body, the mesh is subjected to mechanical stress, the severity of which is dictated by the location of implantation. As it is a foreign body, it also triggers the body's inflammatory response (Anderson et al., 2008). Two of the key cells involved in this response are the macrophages and fibroblasts (Anderson et al., 2008, Setten et al., 2022). The macrophages recognise the biomaterial as a foreign body and try to destroy it by engulfing it. When they fail to engulf it, the macrophages undergo a process called frustrated phagocytosis. They fuse with each other to form foreign body giant cells and release reactive oxygen species (ROS) and degradative enzymes in an attempt to degrade the biomaterial (Anderson et al., 2008). The pH within phagosomes in the macrophages is highly acidic and has been shown to be below 5 (Westman and Grinstein, 2020). The concentration of ROS and degradative enzymes secreted in the microenvironment between the attached macrophage and biomaterial is high (Anderson et al., 2008). Depending on the chemistry of the biomaterial, they can undergo varying levels of degradation secondary to this oxidative stress. Although originally considered an inert biomaterial, polypropylene mesh has been shown to undergo changes in its chemical

composition when subjected to mechanical and oxidative stresses in-vivo and in-vitro. (Farr et al., 2021, Talley et al., 2017). The biological response to this chemical change is not well defined. When the macrophages cannot break a biomaterial down completely, they direct fibroblasts to secrete a capsule around the biomaterial to isolate it from further immunological interrogation and stop the inflammatory response (Anderson et al., 2008). This fibrous encapsulation of the biomaterial has been shown to cause biomaterial failure in different parts of the body (Anderson et al., 2008, Carnicer-Lombarte et al., 2021). Indeed, in studies of mesh explanted from the pelvic floor of symptomatic patients, some of the mesh fragments were found to be stiff and contracted due to this fibrotic reaction (Abhari et al., 2021, Knight et al., 2022, Seifalian et al., 2023).

Macrophages exist on a diverse phenotypic spectrum ranging from pro-inflammatory to pro-fibrotic depending on the environment (Witherel et al., 2019). In a normal regulated inflammatory response, the macrophages seamlessly transition between these phenotypes to coordinate the inflammatory response from start to finish. In a dysregulated response e.g. as seen in persistent inflammatory states, there is over-expression of certain pro-inflammatory and pro-fibrotic genes which can lead to fibrosis. When looking at meshes, macrophage response has been shown to vary with the type of biomaterial as well as the textile properties of the mesh e.g. it's porosity, hydrophobicity and flexibility (Sridharan et al., 2015). Zhu et al showed meshes with large pores to be less inflammatory with increased tissue ingrowth (Zhu et al., 2015). Li et al found the M1 phenotype to be predominant on rougher surfaces with increased pro-inflammatory cytokine secretion including IL1-β (Li et al., 2020). Miller lab has shown a difference in secretion of IL1-β and IL-10 when macrophages are grown on surfaces of different chemistry like polyethylene, polytetrafluoroethylene (PTFE) and polydimethylsiloxane, demonstrating the influence of varying surface chemistry on cytokine gene expression (Miller and Anderson, 1988, Miller et al., 1989).

To understand how the body responds to polypropylene meshes post implantation it is important to consider the material after mechano-chemical distress, rather than simply the pristine material. When it comes to designing better, more biocompatible, less fibrotic biomaterials for the human body in general and pelvic floor in specific, the mechanical and

oxidative stresses mentioned above must be factored in. Currently there is no standard test to assess these stresses with in-vitro tests mostly focussed on cytotoxicity and immunogenicity of a biomaterial in its pristine state or in animal models (Lock et al., 2019). In the previous chapter, we developed a method to allow macrophages to adhere to unmodified polypropylene mesh and extracted sufficient mRNA to assess expression of genes.

The aim of this chapter is to examine how macrophages respond to polypropylene meshes which have undergone mechanochemical distress compared to those which are pristine and in turn, how the factors secreted from macrophages cultured on these materials affect fibroblast phenotype. It is hoped that in the future this model could be further developed to be a useful predictive model to investigate novel biomaterials for use in the pelvic floor and beyond. To achieve this, we will:

1. Apply mechanical and oxidative stress to polypropylene mesh, culture macrophages on them and study the resulting physical changes using scanning electron microscopy (SEM) and atomic force microscopy (AFM).
2. Culture macrophages on non-distressed and mechanochemically distressed mesh and compare the response to both groups at the level of genetic expression.
3. Culture human dermal fibroblasts in conditioned media collected from macrophages cultured on non-distressed and mechanochemically distressed mesh groups and assess morphologic changes using immunostaining and light microscopy, as well as genetic changes using qPCR.

4.2 RESULTS

4.2.1 Does SEM/AFM reveal any surface changes on the mesh?

Before assessing the biological response of macrophages to polypropylene mesh, both non-distressed and distressed, it was important to assess whether macrophages cause any

changes to the surface of the mesh. To achieve this goal, polypropylene mesh was subjected to mechanochemical distress by my colleague Dr.Sabiniano Romano as described in section 2.1.1.1. Macrophages were cultured on non-distressed and distressed mesh as described in section 2.2.1.1. Surface analysis was performed by my colleague Dr.Nicholas Farr using Scanning Electron Microscopy (SEM) and Atomic Force Microscopy (AFM).

SEM and AFM were performed to analyse surface changes and topography. Low voltage SEM (1keV) imaging mode was selected to minimise the effect of sample charging. None of the samples underwent any coating prior to imaging to ensure results are not complicated by applied coatings. The SEM images obtained are shown in Fig 4.1. Fig4.1A & B are of control polypropylene mesh, C &D of mechanochemically stressed mesh without macrophages, E & F of non-mechanochemically stressed mesh with macrophages and G&H of mechanochemically stressed mesh with macrophages. Fig 4.1A& B show minimal surface markings that can be seen as a result of manufacturing stresses. When compared to Fig 4.1 A&B, stressed mesh (Fig 4.1 C&D) shows more grazing and cracks on it's surface which can be attributed to shearing and friction of the fibres after application of mechano-chemical stress. Small particles are also seen on the surface which are characteristic of mechanical debris secondary to wear. Figure 4.1 E & F (control PP + macrophages) and figure 4.1 G&H (mechanochemically stressed mesh + macrophages), both show cellular debris and residual extracellular matrix on their surface. The surface cracks and abrasions, although seen in both groups, are more pronounced in the mechanochemically stressed mesh and macrophages group (Figure 4.1 G&H).

To understand these changes in more detail, AFM was used and images are shown in Fig 4.2 E-H. Non-distressed (Fig 4.2E) mesh shows minor cracks and crazes whereas mechanochemically stressed mesh (Fig 4.2F) shows evidence of wear abrasion. Comparing the non-distressed mesh + macrophages image (Fig 4.2G) with mechanochemically distressed mesh + macrophages (Fig 4.2H), there are noticeably larger cracks and grooves along with ECM deposition as well as what appears to be wear debris (particles) in the stressed mesh with macrophages.

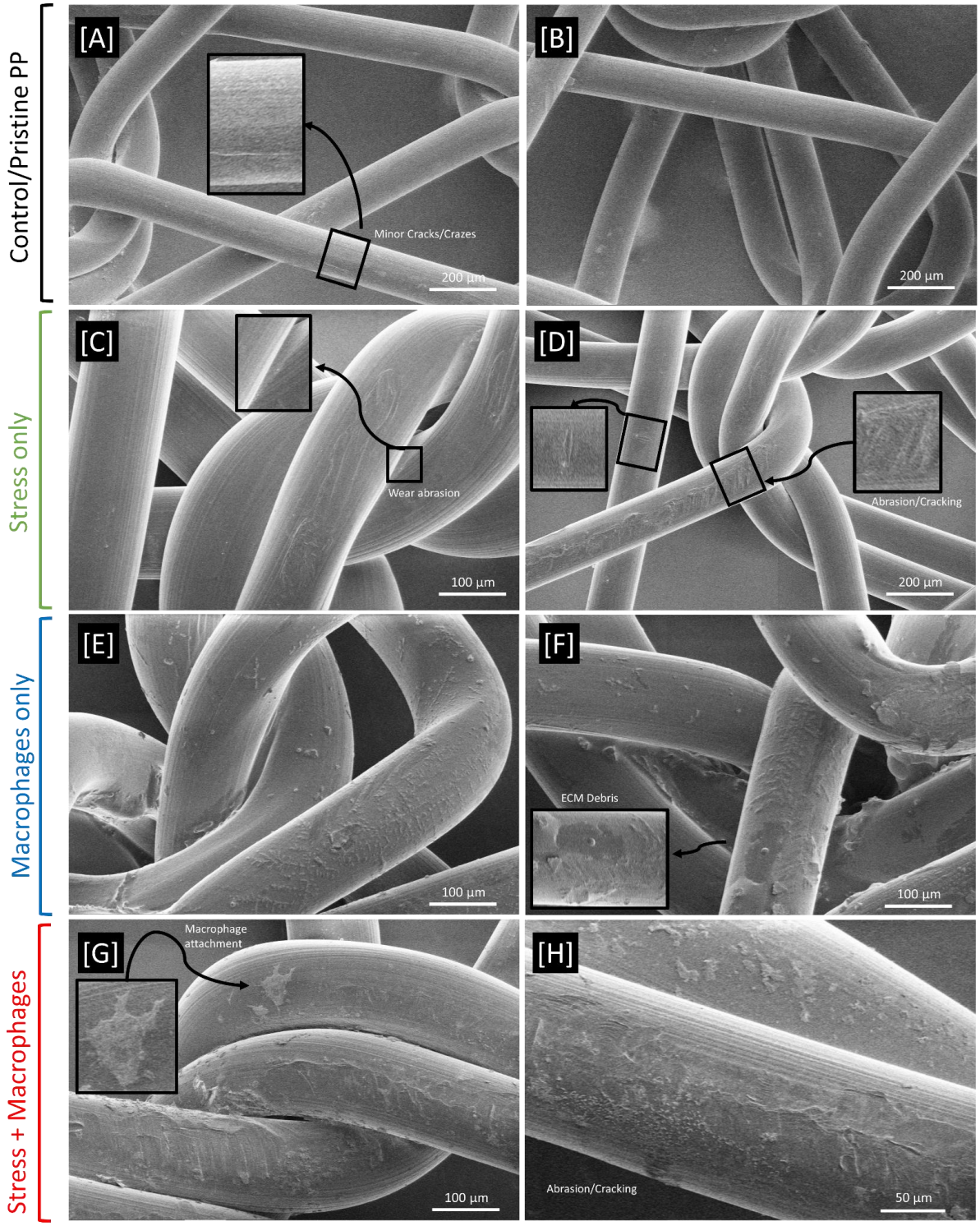

Fig 4.1. SEM images reproduced from (Farr et al., 2024) with permission from Elsevier. Fig A & B show images of pristine PP mesh (Control). C & D are images of mechano-chemically stressed PP

mesh without macrophages. E & F are images of control PP mesh with macrophages. G & H are images of mechano-chemically stressed PP mesh with macrophages.

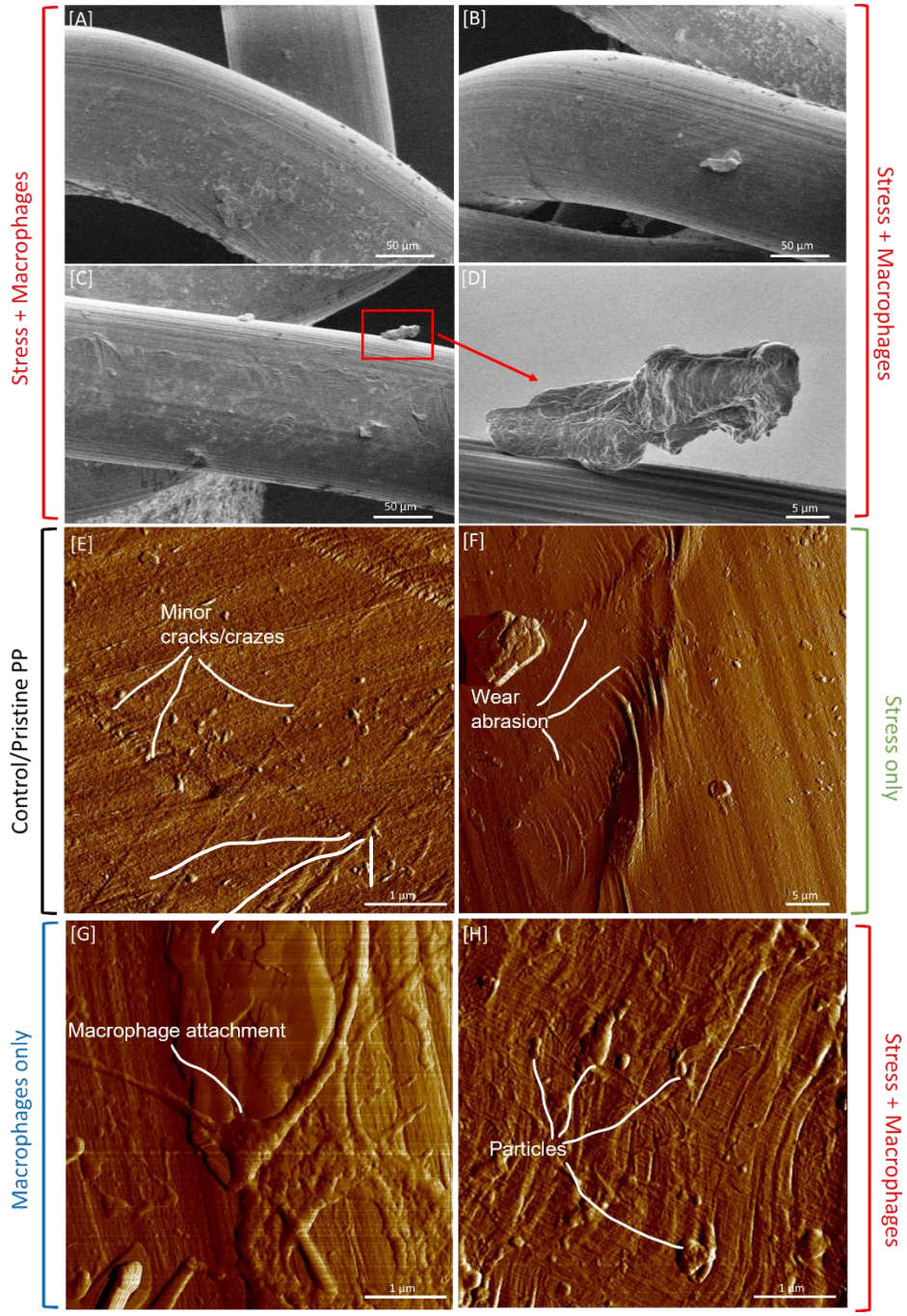

Fig 4.2– Images reproduced from (Farr et al., 2024) with permission from Elsevier. Fig 4.2 A-D show SEM images of mechano-chemically distressed PP mesh with macrophages. E-H show AFM images of control PP mesh (E), mechanochemically distressed PP mesh without macrophages (F), Control mesh with macrophages (G) and mechanochemically distressed mesh with macrophages (H).

4.2.2 Do macrophages respond differently to mechanochemically distressed mesh vs non distressed mesh?

Macrophages were cultured on tissue culture plastic as well as mechano-chemically distressed and non-distressed mesh as described in section 2.2. Macrophages cultured on tissue culture plastic were labelled as M-TCP control. RNA was extracted from each group as described in section 2.5.1. Using methods described in section 2.5, RT-qPCR was performed in three independent experiments with each experiment carried out in triplicate. Gene expression was normalised to the housekeeping gene B2M. Fold change values for each gene were calculated by averaging samples compared to M-TCP control and grouped column graphs generated as log2(Value/M-TCP) with standard deviation (SD).

Comparing the two mesh groups and looking at the proinflammatory genes first, there was a significant increase in expression of CD80, IL1-β and IL-6 in macrophages exposed to mechanochemically distressed mesh. Whereas macrophages grown on non-distressed mesh expressed more CCR7, macrophages cultured on both meshes expressed more TNF-α than the cell-only control. Among the pro-fibrotic genes, there was a significantly increased expression of TGF-β1, IL-10 and IL-13 in the mechanochemically distressed group and increased CD206 expression in the non-distressed mesh group. Both groups downregulated CD163 when compared to the cell-only controls. These results are shown as a graph in Fig 4.3.

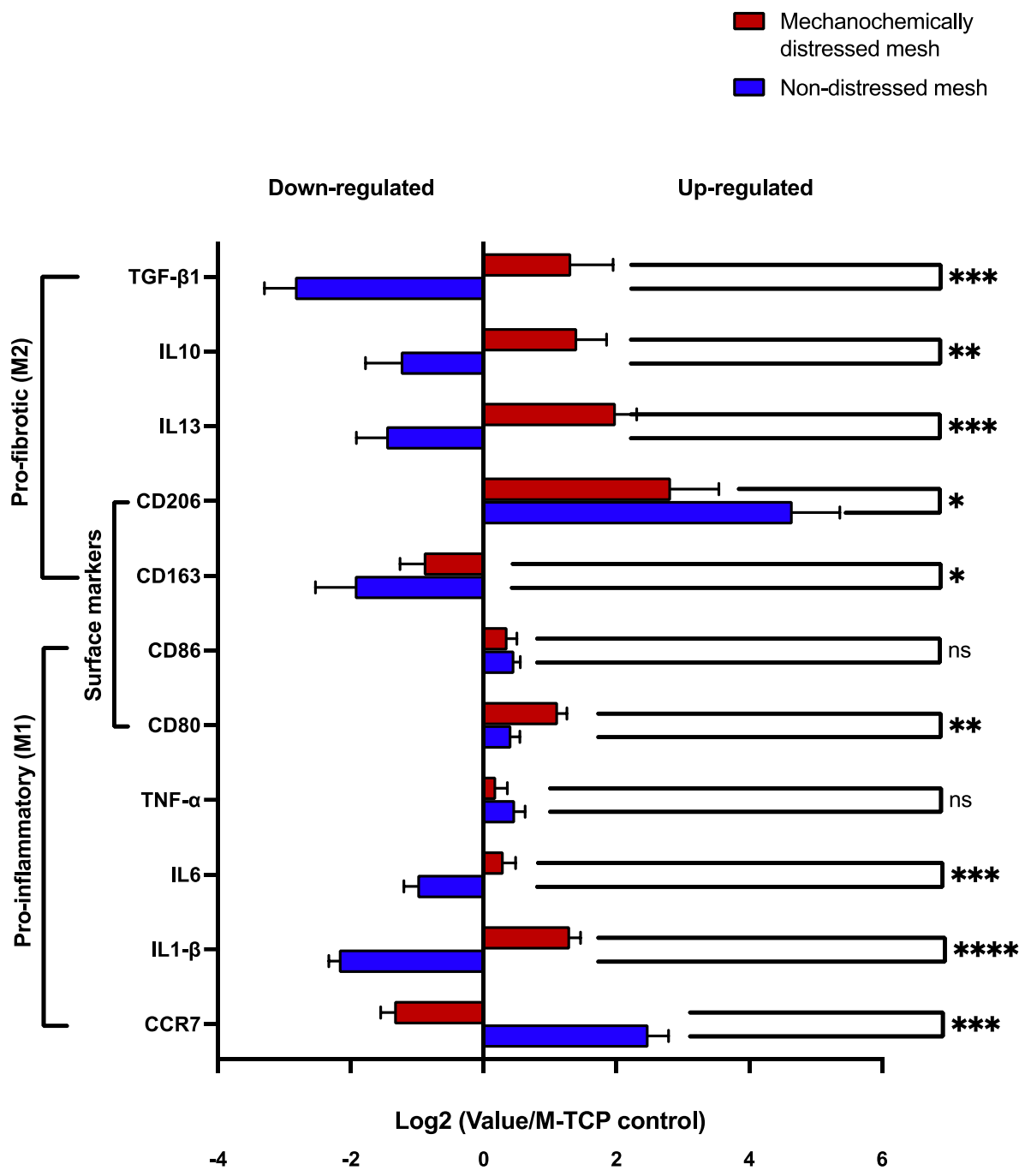

Fig 4.3: Expression of selected genes in macrophages exposed to control non-distressed mesh (blue bars) or mechanochemically distressed (red bars) PP surgical mesh. Fold changes of genes calculated as log2(value/M-TCP control). Data represent mean ± SD of three independent biological experiments, with each experiment carried out in triplicate(N=3,n = 3). Statistical analysis performed using an unpaired t-test on log-transformed data where *p<0.05, **p<0.01, ***p<0.001 and ****p<0.0001.

4.2.3 Fibroblast response to conditioned media from non-distressed and mechano-chemically distressed mesh:

To examine the effect of cytokines secreted by macrophages in response to stressed and non-stressed mesh, we collected conditioned media from each group and cultured fibroblasts in the conditioned media as described in section 2.2. As macrophages are cultured in IMDM and DMEM used for fibroblasts, we had an IMDM control to ensure that any changes seen were not due to IMDM. Fibroblasts treated with TGF-β were used as positive control. Gene expression was assessed using PCR 48 hours after cell culture with gene expression normalised to housekeeping gene GAPDH. Immunofluorescence was carried out on fibroblasts treated with TGF-β and conditioned media for 7 days as described in section 2.3. Untreated fibroblasts cultured in DMEM and IMDM were used as the negative control.

Firstly, comparing fibroblasts cultured in DMEM with those cultured in IMDM, there was no significant difference in genetic expression in both groups. This gave confidence that any changes seen in the conditioned media group were not due to IMDM. Expression of α-SMA was significantly higher in the TGF-β1 treated fibroblasts compared to DMEM or IMDM. Similarly, expression of COL1A1, COL5A1 and Fibronectin was significantly higher in the TGF-β1 treated fibroblasts ($p < 0.05$) (Fig 4.4). There was no significant difference in expression of COL3A1.

Looking at the fibroblasts cultured in conditioned media derived from macrophages cultured on non-distressed mesh and mechanochemically distressed mesh, there was no significant difference in the genetic expression of α-SMA, collagen type 1, 3 and 5 production and fibronectin when compared to DMEM and IMDM. Similarly, there was no significant difference when comparing the genetic expression of α-SMA, collagen type 1, 3 and 5 production and fibronectin in fibroblasts grown in conditioned media derived from macrophages cultured on non-distressed mesh and mechanochemically distressed mesh.

Fibroblasts grown in conditioned media derived from macrophages cultured on stressed mesh showed a slightly increased expression of α-SMA gene compared to negative control cells, but it did not achieve statistical significance ($p=0.107$).

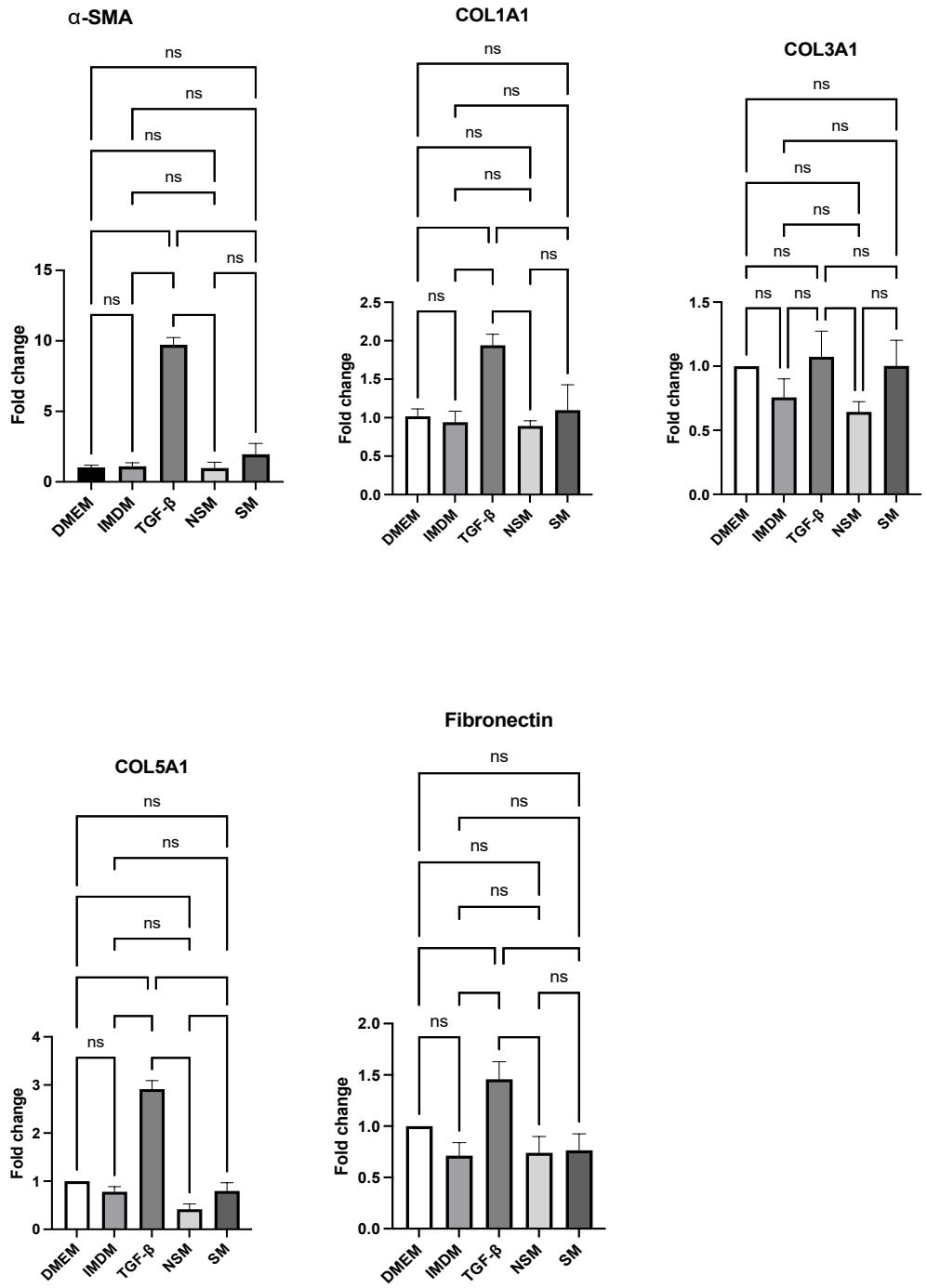

Fig 4.4: **Comparison of genetic expression of a-SMA, COL1A1, COL3A1, COL5A1 and Fibronectin in human dermal fibroblasts when cultured in DMEM and IMDM (negative control), TGF- β (positive control), conditioned media from non-stressed mesh group (NSM) and conditioned media from mechano-chemically stressed mesh group (SM). Data represent mean ± SD (n = 3 biological replicates). Statistical analysis using ordinary one way ANOVA with post-hoc analysis done using Bonferroni correction. Ns = not significant (p > 0.05), * = significant(p <0.05), ** = significant (p<0.01), *** = significant (p<0.001), **** = significant (p<0.0001).**

Cells were stained for α-SMA to look for evidence of myofibroblast differentiation. In the immunofluorescence images, intensity in the red channel (α-SMA) was calculated for all treated conditions as described in section 2.6 and graphed as shown in Fig 4.6. Statistical analysis showed no significant difference between the staining intensity of α-SMA from fibroblasts cultured in conditioned media from macrophages cultured on mechanochemically distressed and non-distressed mesh or the positive control (TGF-β). In the conditioned media groups α-SMA staining is present in both groups however the myofibroblast morphology is more pronounced in the cells cultured in the conditioned media derived from the macrophages cultured on mechanochemically distressed mesh. (Fig 4.5F & H) This myofibroblast morphology is less visible in the fibroblasts grown in conditioned media derived from macrophages cultured on non-distressed mesh. (Fig 4.5E & G)

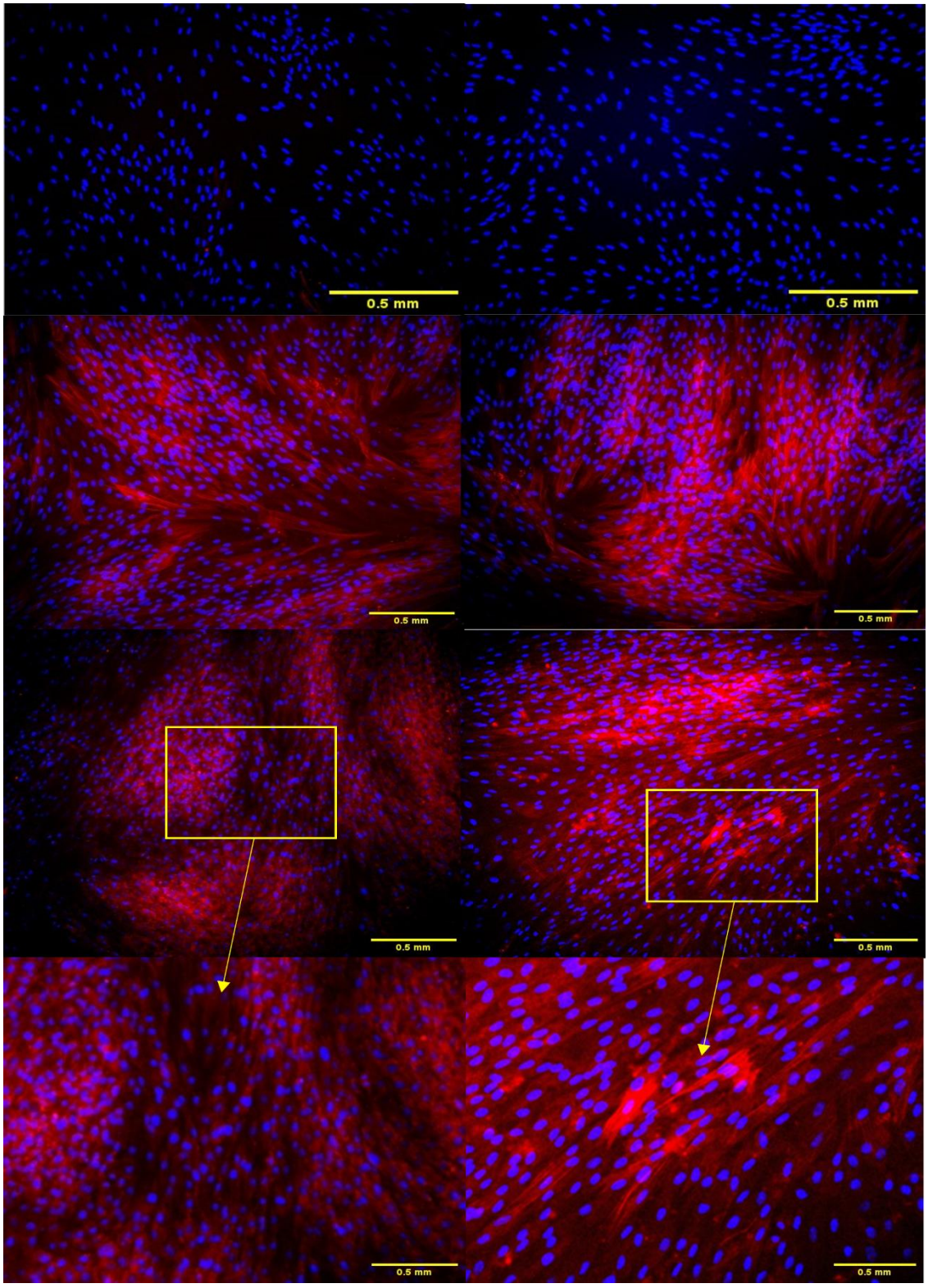

Fig 4.5 – Epifluorescence images at 10x magnification. Scale bar = 0.5mm. DAPI = blue, a-SMA = red. A – Fibroblasts in DMEM media (Negative Control), B – Fibroblasts in IMDM media (Negative control), C – Fibroblasts in DMEM media with TGF-β (Positive control), D – Fibroblasts in IMDM media with TGF-b (Positive control), E – Fibroblasts in conditioned media from non-stressed mesh + macrophages, F – Fibroblasts in conditioned media from stressed mesh + macrophages. G – Magnified view of E showing fibroblast morphology in detail. H – Magnified view of F showing fibroblast morphology in detail.

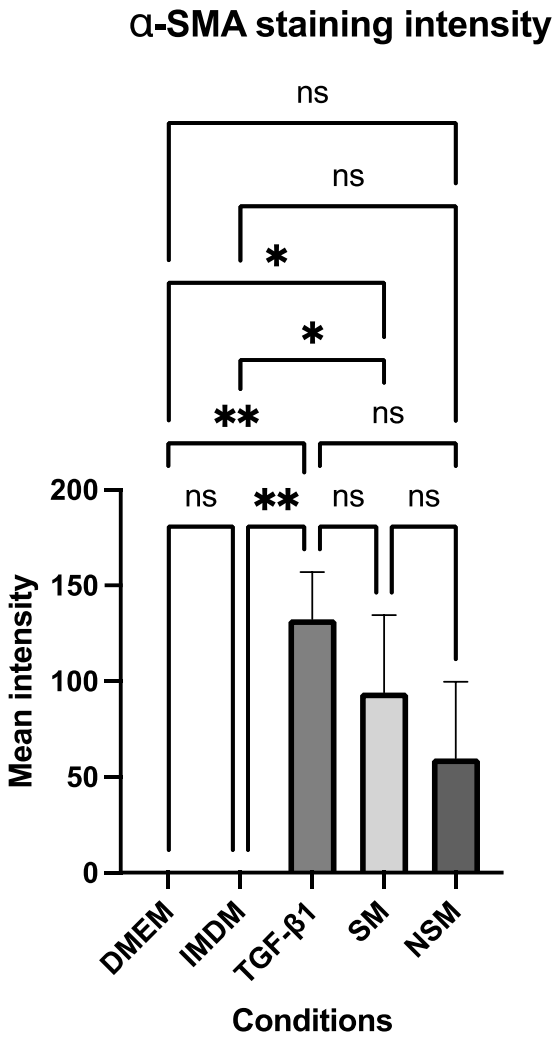

Fig 4.6: Analysis of staining intensity in the red channel as a measure of α-SMA production in fibroblasts cultured in DMEM & IMDM (negative control), TGF-β1 (positive control), conditioned media from non-stressed mesh group (NSM) and conditioned media from mechano-chemically stressed mesh group (SM). Statistical analysis using one-way ANOVA with post-hoc analysis using Bonferonni correction. ns = not significant ($p<0.05$), * = significant ($p>0.05$).

4.3 DISCUSSION:

Although polypropylene was thought to be inert, recent studies have shown it to degrade when subjected to mechanical and chemical stresses post implantation. (Iakovlev et al., 2017, Talley et al., 2017). Work done in our laboratory by Roman et al showed that polypropylene deforms irreversibly when subjected to repeated 25% mechanical distension for three days (Roman et al., 2019). More recently Farr et al utilised a novel spectroscopic characterisation technique called secondary electron hyperspectral imaging to demonstrate that when a chemical stress (oxidation by H2O2) is added on top of the mechanical distension, polypropylene shows surface oxidative changes in addition to the mechanical distortion which could lead to failure post-implantation (Farr et al., 2021). Neither of these studies were designed to look at the biological response to the PP mesh pre or post mechanical distension or oxidative treatment of the PP mesh. In order to develop an *in-vitro* test that attempts to replicate *in-vivo* conditions, we collaborated by adding the technique I developed in Chapter 3 to seed macrophages on polypropylene mesh before and after application of the mechano-chemical stresses by Dr Sabiniano Roman followed by SEM and AFM imaging of the meshes conducted by Dr Nicholas Farr.

Looking at the surface changes, there are cracks, crazes and wear abrasion in the mechanochemically distressed group which can be explained by friction between the fibres as well as the mechanical stress applied. Particles are also seen in areas of surface abrasion as mechanical wear debris.

qPCR was utilised to look at the macrophage response genetically. A mix of pro-inflammatory and anti-inflammatory/pro-fibrotic phenotype markers were chosen based on published literature (Witherel et al., 2019, Jannasch et al., 2017, Grotenhuis et al., 2014, Zhou et al., 2017, Nolfi et al., 2016). The markers selected were CD163, CD86, CD80, IL1-B, CCR7, TNF-α (pro-inflammatory) and CD206, TGF-β1, IL-10, IL-13 and IL-6 (anti-inflammatory/pro-fibrotic). Some or all of these markers were used in in-vitro studies (Witherel et al., 2019, Jannasch et al., 2017, Grotenhuis et al., 2014, Zhou et al., 2017) on fibrosis or studies of explanted meshes from the pelvic floor (Nolfi et al., 2016, Li et al., 2017). The timepoint of 7 days for culture was selected as it was the most common

timepoint from studies on biomaterial-induced fibrosis in literature. (Witherel et al., 2019, Jannasch et al., 2017, Grotenhuis et al., 2014, Zhou et al., 2017). There was a significant rise in the expression of almost all of the pro-inflammatory and profibrotic genes when the polypropylene mesh was subjected to mechanochemical distress. Of prime importance are the classic pro-inflammatory cytokine IL1-β and the pro-fibrotic cytokine TGF-β1, both of which were significantly raised in the mechanochemically distressed group.

The literature evidence behind the choice of pro-inflammatory cytokines is summarised beneath.

IL1-β is a potent pro-inflammatory cytokine whose role in fibrosis has been studied mostly in organ-based fibrosis. Although a pro-inflammatory cytokine, it's levels peak at day 1 post-injury and decline rapidly over the next 3-7 days (Artlett, 2013). When it is persistently elevated, it can promote a fibrotic response. This dichotomous role of IL-1β has been highlighted in various studies. (Luo et al., 2009, Chaudhuri et al., 2007). Kolb et al demonstrated its pro-fibrotic effect by using adenoviral gene transfer to induce overexpression of IL1-β in rat lungs leading to a severe acute inflammatory response with severe progressive lung fibrosis. (Kolb et al., 2001). Similar results on IL1-β administration were demonstrated by Gasse et al and Wilson et al(Gasse et al., 2007, Wilson et al., 2010). Further highlighting the role played by IL1- β in fibrosis, Guo et al demonstrated the protective effect of neutralising IL1- β on silica-induced pulmonary fibrosis (Guo et al., 2013). In biomaterial-induced fibrosis, it's role has been studied in the context of inflammasome activation in macrophages. (Witherel et al., 2019) Cells contain certain proteins called NOD-like receptor (NLR) proteins which act as sensors within cells to various patterns which can be due to pathogens – pathogen associated molecular patterns (PAMP) or cell damage associated molecular patterns (DAMP) (Vasconcelos et al., 2022). When activated in response to pathogens, they assemble to form multi-protein complexes called inflammasomes. When activated, inflammasomes activate a protease enzyme called caspase 1 which converts IL1-β and IL-18 into it's active form. This inflammasome activation is carried out via a pathway called NOD-like receptor family Pyrin domain containing 3 (NLRP3) pathway (Vasconcelos et al., 2019). When persistently stimulated, it can cause prolonged release of IL-13 and cause chronic inflammation. NLRP3 activation does require a priming step. One such step for the macrophages is release of ROS in response to phagocytosis of

biomaterial components. This has been shown to be the case in wear debris resulting from joint replacements (Vasconcelos et al., 2019). Macrophages cannot phagocytose materials more than 10 micron in size. In the absence of infection, the discovery of wear debris (particles) on SEM of mechanochemically distressed mesh as shown in figure 4.2C (<10 microns) therefore could be one of the reasons there is a significant rise of IL1-β in the mechanochemically distressed mesh as compared to control mesh. This observation is further strengthened by the study done by Vasconcelos et al which demonstrated impaired activation of NLRP3 inflammasome pathway in macrophages by large scale 3D chitoscan scaffolds as compared to nanoscale chitosan which is a powerful NLRP3 inflammasome activator in macrophages (Vasconcelos). Further highlighting the pro-fibrotic role of the inflammasome and IL1- β is the study done by Barone et al. The authors implanted electronic medical devices coated with an NLRP3 inhibitor (MCC950) in a nerve injury animal model and showed a reduction in IL-1 β with normal tissue repair as compared to dexamethasone which blocked the foreign body response with poor tissue repair (Barone et al., 2022).

Similarly, IL-6 is another pro-inflammatory cytokine released by the macrophages in the early stages of inflammation. Although it plays a key role in regulation of acute inflammation, especially the transition from the inflammatory to the remodelling stage (Garbers et al., 2018, Braun et al., 2016), it has been shown to exhibit a pro-fibrotic effect through the TGF-β pathway via trans signalling (O'Reilly et al., 2014). IL-6 plays a major role in fibrotic diseases like systemic sclerosis, cardiac and renal fibrosis (O'Reilly et al., 2014) Further highlighting the pro-fibrotic role of IL-6, Ma et al demonstrated a reduction in angiotensin II induced cardiac fibrosis in IL-6 knockout mice (Ma et al., 2012). To strengthen their argument further, they co-cultured fibroblasts and macrophages which led to elevated production of IL-6, α-SMA, and collagen 1 by fibroblasts. Treatment of the co-culture with IL-6 neutralising antibody led to significant reductions in TGF-β1 expression leading Ma et al to conclude that IL-6 can drive cardiac fibrosis via the TGF-β pathway(Ma et al., 2012).

Amongst the pro-fibrotic cytokines, TGF-β1 is the most important regulator of fibrosis. (Meng et al., 2016). TGF-β is a pro-fibrotic cytokine belonging to the TGF superfamily. It has three known isoforms in humans – TGF-β 1,2 and 3 with TGF-β1 being the most abundant

isoform. (Flanders et al., 1998, Wakefield and Hill, 2013). TGF-β serves two important functions in the context of inflammation. It promotes wound healing and suppresses the inflammatory process. An increase in the amount of TGF-β, however, can lead to fibrosis. This has been demonstrated in multiple studies looking at the role of raised TGF-β in various organ based fibrotic diseases (Meng et al., 2016, Connor et al., 1989, Murakami et al., 1997, Jones et al., 2008). During inflammation, once TGF-β is secreted by the macrophages, it acts via the canonical pathway involving the SMAD proteins. SMAD proteins are a class of intracellular signalling proteins. TGF-β1 attaches to the TGF-β receptor which phosphorylates the SMAD 2 and SMAD 3 proteins. SMAD 4 attaches to the phosphorylated SMAD2/3 complex and translocates it into the cell nucleus where it attaches to DNA and transcribes factors which once they exit the cell, carry out their effects. One such factor is α-SMA which transforms fibroblasts to myofibroblasts, a key effector cell in fibrosis (Kendall and Feghali-Bostwick, 2014). Myofibroblasts can then further activate latent TGF-β in surrounding tissues to activate them, thereby continuing the fibrotic reaction. (Wipff et al., 2007). Suppression of TGF-β by either TGF-β1 knockdown or locally administered TGF-β1 inhibitors has shown reduction in this fibrotic reaction around implants in various studies. (DiEgidio et al., 2014, Mazaheri et al., 2003, Park et al., 2015). Similarly, Noscovica et al demonstrated a decrease in fibrotic encapsulation of silicone implants in mice when TGF-β activation is inhibited (Noskovicova et al., 2021). Similarly, SMAD-3 knockout mice do not demonstrate much lung fibrosis after exposure to bleomycin, a potent inducer of lung fibrosis via the TGF-β pathway (Gu et al., 2007).

Conversely, when TGF-β1 was overexpressed in mice by using adenovectors, Sime et al demonstrated an increase in lung fibrosis (Sime et al., 1997). IL-13, another key pro-fibrotic cytokine, expresses its profibrotic effects by activation and stimulation of TGF-β1 (Lee et al., 2001). Its fibrotic effect has been demonstrated by increased lung fibrosis in mice with transgenic overexpression of IL-13 (Zhu et al., 1999). Kaviratne et al demonstrated a complete abrogation of schistosomiasis-induced liver fibrosis in IL-13 knockout mice (Kaviratne et al., 2004). IL-13 in combination with TNF-α has also been shown to increase TGF-β1 production by macrophages (Fichtner-Feigl et al., 2006).

Another cytokine exhibiting a pleiotropic effect is IL-10. Although an anti-inflammatory cytokine at normal concentrations, it can exhibit pro-fibrotic properties when over-expressed (Steen et al., 2020). Lee et al demonstrated this effect by showing increased TGF-β expression in the lungs of IL-10 transgenic mice (Lee et al., 2002). Interestingly, raised levels of IL-10 have also been seen in in-vivo studies as well as immunostaining of mesh explanted from symptomatic patients. Brown et al implanted and left three polypropylene meshes of varying weight and porosities for 12 weeks in Rhesus macaques (Brown et al., 2015). On explantation and histological evaluation, they found significantly raised IL-10 levels and a pro-fibrotic response in the lighter, more porous meshes. Nolfi et al looked at meshes explanted from patients complaining of pain and/or exposure upto 36 months post implantation and demonstrated an increased level of IL-10 in patients complaining of pain (Nolfi et al., 2016).

When we look at biomaterial-induced fibrosis *in vivo*, the mechanochemical stresses take place over years which makes replicating these changes *in vitro* challenging. This is why we utilised methodology refined in our lab (Farr et al., 2021) to simulate a mechanochemically degraded mesh using ISO standards for accelerated degradation (ISO, 2010). The timepoints selected for mRNA extraction from macrophages reflect macrophage response to a new mesh seven days after implantation as compared to one that is years down the line from implantation, having been mechanically and chemically stressed.

To understand the effects of increased pro-inflammatory and pro-fibrotic genetic expression of macrophages on fibroblasts, they were cultured in conditioned media obtained from the earlier experiments. The genetic markers were selected from those commonly used in literature (Witherel et al., 2021) as well as based on work done previously in our lab by Dr Samuel Higginbotham on fibrosis (Higginbotham et al., 2024). A time point of 48 hours was chosen as previously, when cultured for longer than 48 hours, there was a decline in a-SMA expression. For immunohistochemistry analysis, there was no detection of staining in TGF-β treated fibroblasts which is why a 7 day timepoint was selected. As fibroblasts are cultured in DMEM whereas macrophages are cultured in IMDM, both these media were used in negative and positive controls to rule out any confounding factors. The results showed a significant rise in α-SMA gene expression in positive controls but a weak response in the fibroblasts cultured in conditioned media derived from the stressed mesh group. The

timepoints could also be optimised further but this could not be done due to time and budget constraints.

The results, when taken separately, show upregulation of certain proinflammatory/profibrotic genes and downregulation of others. When taken together, they present a compelling argument of a persistent inflammatory and fibrotic response as the implanted biomaterial ages within the body. Inflammation starts with secretion of pro-inflammatory cytokines (IL1-β, TNF-α, IL-6 etc) and subsides after 48-72 hours to give way to reparative cytokines (TGF-β, IL-10, IL-13) which stimulate tissue remodelling via ECM production (Guo and Dipietro, 2010). Persistence or dysregulation of this response leads to fibrosis. When we correlate this with the clinical picture, the pathophysiology fits. Patients implanted with mesh present years later with either erosion or pain. This could suggest a mesh that continues to elicit an inflammatory response due to repeat mechanochemical stresses which progress to a fibrotic response. There are certain limitations to this model which are discussed in detail in the next chapter.

CHAPTER 5

General Discussion

5.1 **DISCUSSION**

SUI and POP are highly prevalent health problems that have a significant impact on the patient's quality of life and the finances of the health care system (Rodriguez-Mias et al., 2015). As the population ages, this burden is set to increase. Surgical treatment of these conditions initially favoured native tissue repair before polypropylene mesh was first used to treat SUI in 1970 and then widely adopted in the 1990's (Mangir et al., 2019). The initial promising results were then overshadowed by reports of life-changing complications like erosion and pain in women who had these implants (Dyer, 2016). This led to manufacturers of these meshes facing multiple lawsuits in the US and Europe (Iakovlev et al., 2017). Although polypropylene is considered inert when implanted in the human body, there is a growing body of evidence to the contrary (Anderson et al., 2008). In the context of the pelvic floor, it is subjected to increased pressure which can cause cracks as demonstrated by microscopic analysis of explanted meshes reported by Iakovlev et al (Iakovlev et al., 2017) and in our lab by Farr et al (Farr et al., 2021). Further studies of explanted meshes from the pelvic floor showed features consistent with fibrosis and chronic inflammation (Nolfi et al., 2016, Clave et al., 2010).

Fibrosis has been extensively studied in organs, but biomaterial-induced fibrosis is a relatively new field of inquiry. The classic work of Anderson et al led the way in explaining the pathogenesis behind this phenomenon but the understanding of the mechanobiology of biomaterial induced fibrosis is constantly evolving (Anderson et al., 2008). As discussed earlier, fibrosis is a multifactorial process and involves a complex interplay between biomaterial and the environment it is implanted in. Ultimately whether a biomaterial integrates well into the tissue it is implanted in is determined by the result of its interrogation by the host immune system. Biomaterials that continue to stimulate the

immune system can lead to chronic inflammation and ultimately, fibrosis. This interaction is determined by the material properties of the biomaterial.

Any testing method for biomaterials prior to implantation should, therefore, incorporate both mechanical and biological testing. Currently, the in vitro biological testing of biomaterials is very limited and only tests for cytotoxicity as per ISO standard 10993-5 (6,7) with increased reliance on animal testing for biocompatibility (Lock et al., 2019). Moreover, the correlation between in vitro testing and in vivo outcomes is poor as shown in a recently conducted European multicentre analysis on in vitro analysis and in vivo outcomes for bone regeneration (Hulsart-Billstrom et al., 2016). The ISO standard 10993-2 specifies requirements for the welfare of animals when conducting in vivo testing of biomaterials and focusses on the three R's: reduction in the overall use of animals, refinement of current testing methods and replacement of animal testing with other validated scientific methods to reduce the animal burden of testing (Lock et al., 2019). We developed a novel simple fatigue test in our lab that applied cyclical uniaxial loads to biomaterials used in the pelvic floor(Roman et al., 2019). Farr et al refined this further and applied mechanical as well as oxidative stress combined with SEHI to identify materials that may not be suitable for implantation (Farr et al., 2021).There remains a gap in in-vitro biological testing of biomaterials. To address this gap, we aimed to develop a useful in vitro model that incorporates not only mechanical and oxidative stresses that the biomaterial is subjected to in the pelvic floor but also biological cells to assess their response as the material is stressed.

The initial challenge at the beginning of the study was to devise a method to seed non-polarised macrophages on macroporous polypropylene mesh which would allow sufficient RNA extraction for further analysis. There have been various methods described in literature. Each of these methods has limitations which we believe would have introduced bias eg. Boersema et al (Boersema et al., 2016) modified the surface properties of the biomaterial to aid attachment which would not allow us to test the macrophage response to unaltered polypropylene mesh. It would also bias our study as biomaterial surface changes have been shown to alter macrophage phenotype (Li et al., 2020). Zhou et al used THP-1 cell lines which would not be representative of how primary human macrophages respond to the biomaterial (Zhou et al., 2017). Grotenhuis et al and Jannasch et al polarised

macrophages prior to seeding which is not representative of how undifferentiated macrophages respond to the mesh in the body at the time of implantation (Grotenhuis et al., 2014, Jannasch et al., 2017). It would alter the study as polarised macrophages would produce pro-inflammatory or pro-fibrotic cytokines prior to seeding on biomaterials which would misrepresent the effect of biomaterial on macrophage phenotype. The method developed here overcomes the challenges seen in previous studies and reviewed in chapter 3 and allows for the seeding of undifferentiated primary human monocyte-derived macrophages on pristine and stressed polypropylene mesh. The optimised seeding method utilising a seeding density of 1 x 10^6 macrophages in 150µl of culture media is novel and resulted in sufficient mRNA extraction for downstream qPCR analysis.

Polypropylene mesh has been shown to undergo mechanical and oxidative degradation *in vitro* (Roman et al., 2019) as well as *in vivo* (Iakovlev et al., 2017, Talley et al., 2017, Imel et al., 2015). It has also been shown that this mechanical and oxidative degradation got worse the longer the mesh stayed in the pelvic floor (Imel et al., 2015). In their study of inflammatory response in explanted meshes, Wang et al suggest a prolonged inflammatory reaction with increased number of the M2 macrophages in severely degraded meshes (Wang et al., 2023). The next challenge, therefore, was to simulate these conditions in vitro. This was done by combining the newly developed seeding method with the novel techniques developed in the lab earlier (Farr et al., 2021). We chose pro-inflammatory (CD163, CD86, CD80, IL1-B, CCR7, TNF-α) and pro-fibrotic markers (CD206, TGF-β1, IL-10, IL-13 and IL-6) from studies done in vivo, in vitro or from immunohistochemical analysis of explanted vaginal meshes. This was to correlate our in vitro findings with in vivo results available in literature. The most striking findings were an increased proinflammatory and profibrotic response of macrophages to mesh that had been mechanochemically distressed as compared to non-distressed mesh. IL1-β, a potent pro-inflammatory marker and TGF-β, a potent pro-fibrotic marker were both significantly raised, along with IL-10, IL-6 and IL-13. This correlated well with the findings of Nolfi et al who found raised IL-10 proteins in meshes explanted from patients due to increased pain. Brown et al similarly found increased IL-10 in Restorelle mesh explanted from Rhesus monkeys 12 weeks after implantation (Brown et al., 2015). IL-10 is produced by the M2 macrophage which Wang et al found to be the predominant phenotype in moderate to severely degraded explanted

meshes (Wang et al., 2023). Although Jannasch et al did not use polypropylene, interestingly, they found very low levels of IL1-β secretion by the macrophages cultured on various biomaterials. This correlates with low expression of IL1-β in macrophages cultured on non-distressed mesh. This highlights the importance of stressing the biomaterials as once polypropylene was mechanochemically distressed in our experiments, IL1-β expression was significantly increased. An overview of the significant results is shown in figure 5.4.

Surface analysis revealed cracks and crazes in the mechanochemically distressed mesh. They also revealed wear debris particles which were not seen on the non-distressed mesh. The discovery of wear debris on SEM can also help explain the persistent rise of IL1-β. As discussed earlier, inflammasomes play an important role as a sensor of foreign objects in the immune pathway. One of the mechanisms by which they get activated is via phagocytosis of foreign objects (debris, pathogens etc). The particles seen on SEM in the mechano-chemically stressed group are less than 10 microns as shown in figure 4.2(D).
The genetic response of macrophages differed when the mesh was new vs when it was mechanochemically distressed. Based on these findings, we can hypothesise why mesh fibrosis occurs clinically. When the mesh is implanted in the human body, the macrophages cannot phagocytose it, so they attempt to isolate it from the surrounding environment by forming giant cells and cause the fibroblasts to secrete a fibrous capsule around it. As the mesh gets stressed in the pelvis over time both mechanically and due to enzymatic and oxidative degradation, it stimulates an inflammatory response not only by virtue of changed physico-chemical characteristics but also by wear debris which gets phagocytosed by macrophages and activates the inflammasomes which cause further inflammation. The role of inflammasomes in biomaterial induced fibrosis was highlighted by Barone et al who showed improved tissue repair with a reduction in IL1-β by coating implants with MCC950 which inhibits the inflammasome pathway (Barone et al., 2022).
This cycle of immune cells changing properties of implanted mesh which in turn changes the immune response continues until implant failure occurs secondary to fibrosis, as shown in figure 5.1. This may get amplified in presence of any infection (Wang et al., 2023).

We also looked at fibroblasts to assess if they change to myofibroblasts in response to the cytokines secreted from macrophages in conditioned media saved from earlier experiments.

As discussed earlier in Chapter 1, myofibroblasts appear in the last stages of normal wound healing and their contraction of surrounding tissue assists in bringing the opposite ends of the wound together. They also deposit extracellular matrix during wound healing. In fibrosis, excessive ECM deposition and contraction from myofibroblasts can lead to scarring and cause pain. TGF-β, a potent pro-fibrotic cytokine can cause fibrosis and the canonical pathway which can lead to this is illustrated in Fig 5.2.

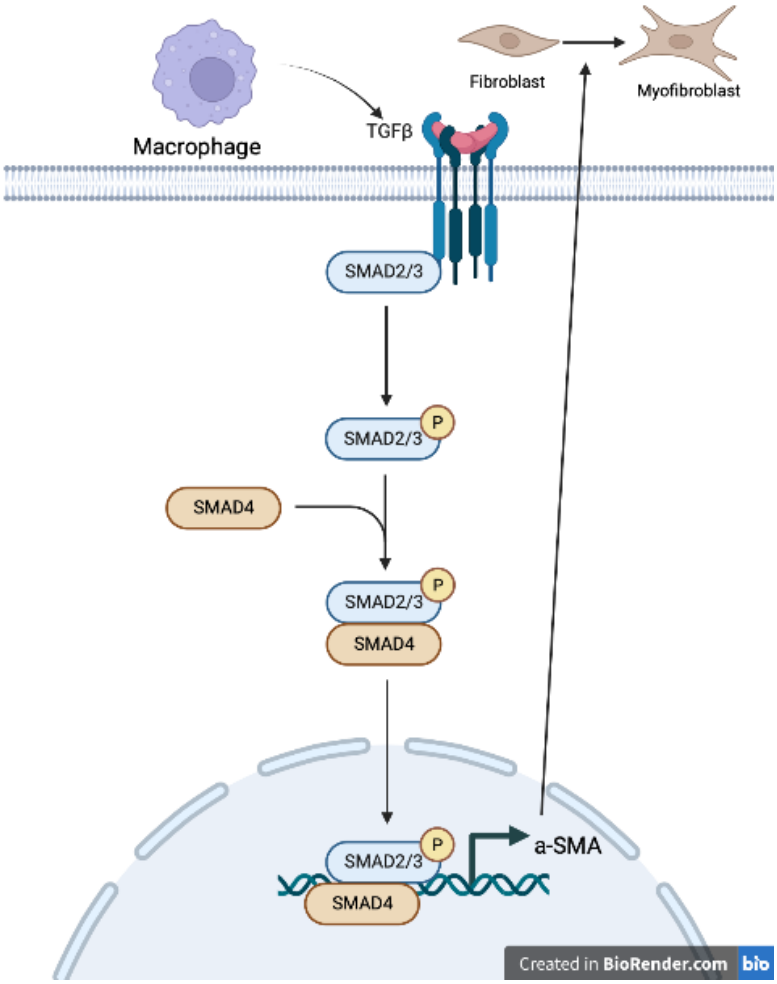

Fig 5.1: Schematic depicting the canonical TGF-b pathway. Macrophages produce TGF-b in response to pro-fibrotic biomaterials. This leads to the phosphorylation of the SMAD2/3 protein which, combined with SMAD4, causes production of a-SMA protein. This is released into the microenvironment and causes activation of fibroblasts to myofibroblasts.

Fibroblasts cultured in conditioned media from the stressed and non-stressed mesh did not show a significant pro-fibrotic response when compared to exposure to the positive control

of TGF-β. On immunohistochemical analysis, myofibroblast morphology was seen in some of the fibroblasts cultured in conditioned media from macrophages seeded on stressed mesh which could represent an early response. A possible reason for this could be that this was a short-term exposure experiment with one-way signalling from macrophage to fibroblast. Fibroblasts *in vivo* would engage in a two-way crosstalk with the macrophages and also respond to the biomaterial as well as the environment.

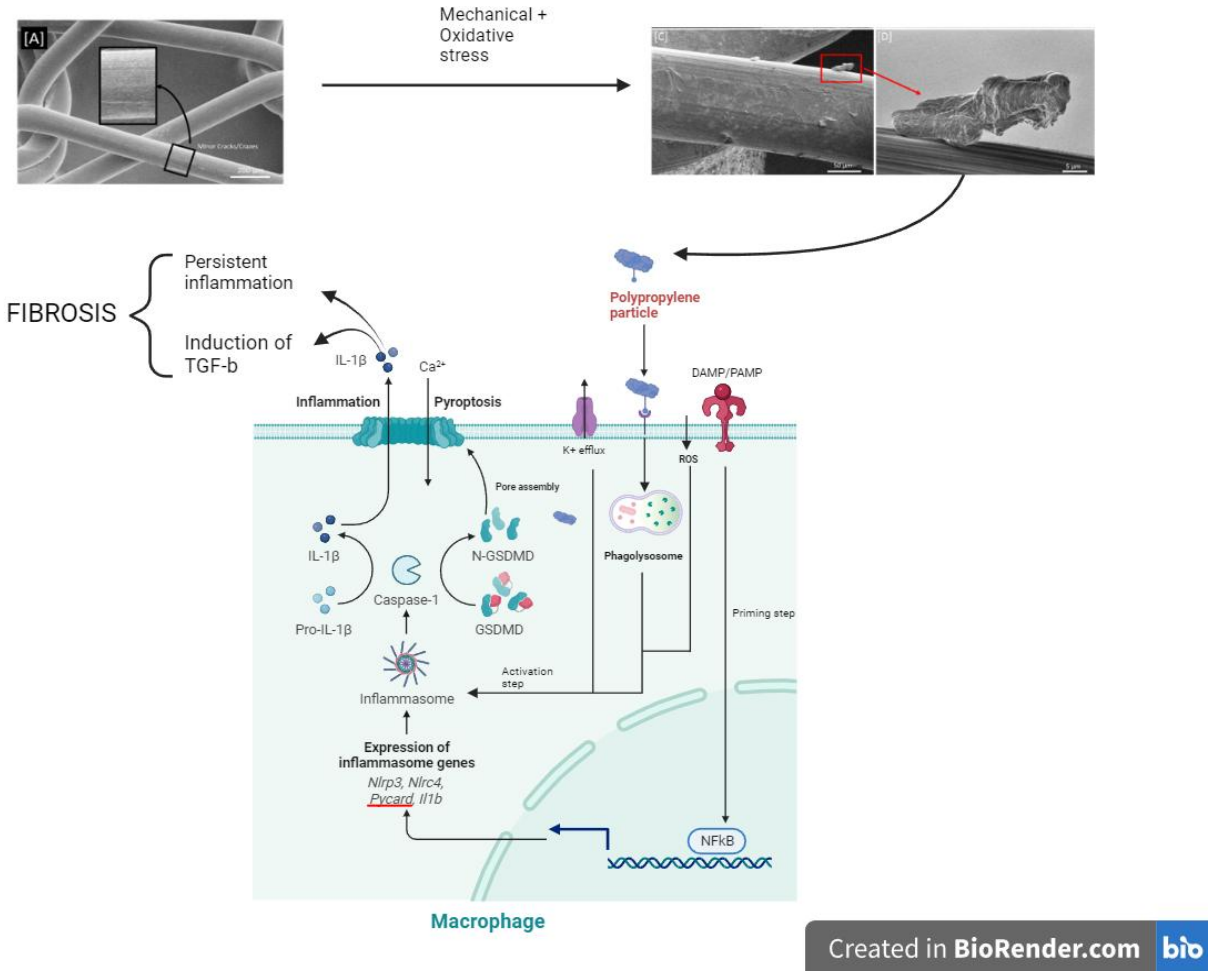

Fig 5.2: A schematic showing the inflammasome activation pathway. The priming step is by recognition of DAMP/PAMP which results in the expression of inflammasome genes leading to formation of an inflammasome. Particles produced on the surface of PP mesh as a result of mechano-oxidative stress are phagocytosed by the macrophage, which along with reactive oxygen species sensed by the macrophage, activates the inflammasome which leads to cleavage of Pro IL1-β into it's active form. This is released into the microenvironment between macrophage and the biomaterial leading to prolonged inflammation and induction of the TGF-β pathway, ultimately leading to fibrosis.

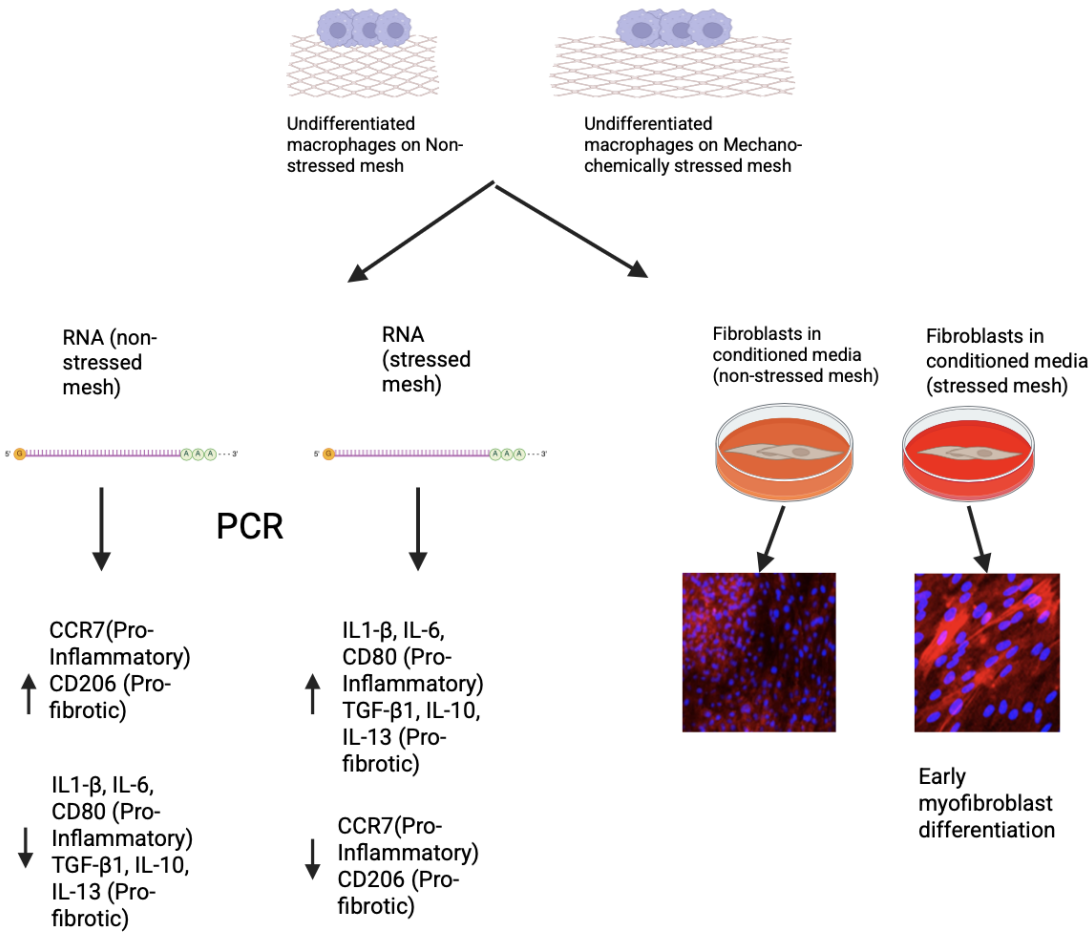

Fig 5.3 – A summary of significant results. On the left, data is depicted from genetic expression analysis of RNA from macrophages cultured on non-stressed and stressed mesh. On the right, data is depicted from epifluorescence microscopy of fibroblasts cultured in conditioned medium collected from macrophages cultured on non-stressed and stressed mesh.

5.2 LIMITATIONS:

- While initially we planned to develop an *in vitro* model and test it on a range of different biomaterials, of necessity, we focussed on polypropylene as this was the most commonly used biomaterial in the pelvic floor with extensive reports of

adverse responses to it hence the most relevant material to focus on in developing our new testing methods.

- Another limitation was in the fibroblast experiments where conditioned media was used instead of a co-culture model. This meant looking only at one way talk (Macrophages > Fibroblasts) as opposed to a two way crosstalk (Macrophages ⇌ Fibroblasts) that could be observed when macrophages and fibroblasts are co-cultured.
- Another limitation was that genetic expression was studied in using common markers described in literature, rather than full RNA sequencing.
- Specific protein quantification of the conditioned media was not done using ELISA - this would have made the data more complete.
- Of necessity we selected a few fixed timepoints as indicated from the commonly used ones in the literature. It would be useful to study different timepoints to see how the macrophage and fibroblast responses changes as time progresses.

5.3 FUTURE WORK:

With more time, I would further optimise the macrophage and fibroblast experiments. Instead of just using genetic markers described in literature, utilising full RNA sequencing could reveal novel macrophage responses not previously described in literature. It would be useful to establish a co-culture model to assess two-way crosstalk between macrophages and fibroblasts. This would allow us to assess any change in the response of macrophages and fibroblasts because of crosstalk between the two. It would also be useful to use different time points to see how this response changes over time. There are various ways in which a co-culture model can be established. One of them would be to seed macrophages on one side of the biomaterial and seed fibroblasts on tissue culture plastic. The mesh can be suspended in media in the well with cultured fibroblasts. (Fig 5.4A) This would allow separate extraction of RNA from macrophages on the mesh and fibroblasts in the well plate. Proteins can be quantified in the conditioned media collected at different time points using ELISA assays. Another method would be to utilise hydrogels which would contain the biomaterial in the middle with macrophages on one side and fibroblasts on the other. (Fig

5.4B) This would allow contact between macrophages and fibroblasts as they grow on the mesh as would happen in vivo.

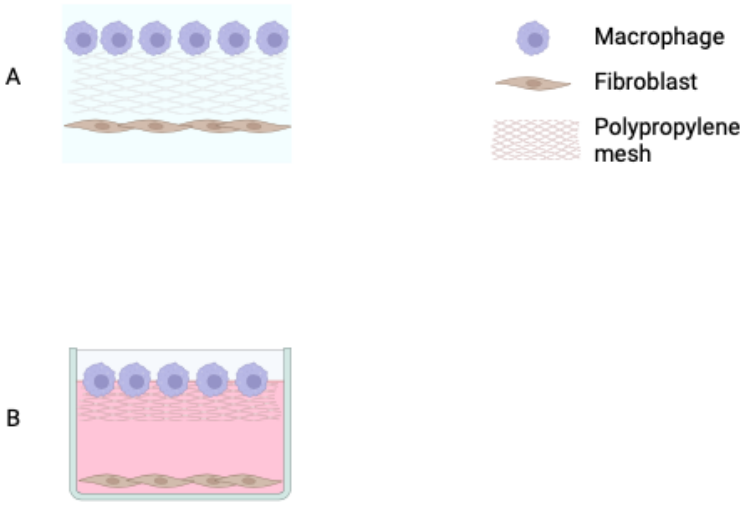

Fig 5.4– Schematic depicting different co-culture models of macrophages and fibroblasts on biomaterials. (A) shows mesh encased in a hydrogel with macrophages on top end and fibroblasts on the bottom end. (B) shows macrophages cultured on mesh suspended in culture media in a well with fibroblasts seeded at the bottom.

In particular I would assess other biomaterials in development like polyurethane which has so far outperformed PP in its response to repeated distension and oxidative stress comparing the macrophage response to polypropylene versus the response to polyurethane to further validate our model.

To explore the effect of inflammasomes and test our theory, a similar methodology could be used as described by Barone et al by coating the biomaterial with an inflammasome inhibitor like MC9550 to see if there is a decrease in IL1-β in the stressed biomaterial group.

This would generate data that can add to our understanding of biomaterial induced fibrosis and help improve biocompatibility of biomaterials.

Another interesting avenue of study would be to assess the contribution of the diabetic tissue microenvironment to the response to a biomaterial. Diabetes leads to hyperglycaemia and macrophages have been shown to have a prolonged pro-inflammatory response in diabetes (Al Sadoun, 2022) . This could be done by introducing a hyperglycaemic environment into the model to assess whether it changes the macrophage and fibroblast response to the biomaterials. Another way to do this would be to use macrophages derived from monocytes from the buffy coat of diabetic blood donors.

5.4 CONCLUSIONS

In conclusion, a novel *in vitro* model has been developed that allows immunological evaluation of a biomaterial before and after application of mechanical and oxidative stresses similar to what the biomaterial would experience *in vivo*. Polypropylene mesh, when tested in this model, exhibits a strong pro-inflammatory and pro-fibrotic response after it is mechanically and chemically stressed. These are strong red flags against its clinical use. This model can now be used to examine other potentially safer biomaterials in development.

REFERENCES:

ABHARI, R. E., IZETT-KAY, M. L., MORRIS, H. L., CARTWRIGHT, R. & SNELLING, S. J. B. 2021. Host-biomaterial interactions in mesh complications after pelvic floor reconstructive surgery. *Nat Rev Urol,* 18**,** 725-738.

ABRAMS, P., ANDERSSON, K. E., BIRDER, L., BRUBAKER, L., CARDOZO, L., CHAPPLE, C., COTTENDEN, A., DAVILA, W., DE RIDDER, D., DMOCHOWSKI, R., DRAKE, M., DUBEAU, C., FRY, C., HANNO, P., SMITH, J. H., HERSCHORN, S., HOSKER, G., KELLEHER, C., KOELBL, H., KHOURY, S., MADOFF, R., MILSOM, I., MOORE, K., NEWMAN, D., NITTI, V., NORTON, C., NYGAARD, I., PAYNE, C., SMITH, A., STASKIN, D., TEKGUL, S., THUROFF, J., TUBARO, A., VODUSEK, D., WEIN, A., WYNDAELE, J. J., MEMBERS OF, C. & FOURTH INTERNATIONAL CONSULTATION ON, I. 2010. Fourth International Consultation on Incontinence Recommendations of the International Scientific Committee: Evaluation and treatment of urinary incontinence, pelvic organ prolapse, and fecal incontinence. *Neurourol Urodyn,* 29**,** 213-40.

AL SADOUN, H. 2022. Macrophage Phenotypes in Normal and Diabetic Wound Healing and Therapeutic Interventions. *Cells,* 11.

ANDERSON, J. M., RODRIGUEZ, A. & CHANG, D. T. 2008. Foreign body reaction to biomaterials. *Semin Immunol,* 20**,** 86-100.

ARNOLD, L., HENRY, A., PORON, F., BABA-AMER, Y., VAN ROOIJEN, N., PLONQUET, A., GHERARDI, R. K. & CHAZAUD, B. 2007. Inflammatory monocytes recruited after skeletal muscle injury switch into antiinflammatory macrophages to support myogenesis. *J Exp Med,* 204**,** 1057-69.

ARTLETT, C. M. 2013. Inflammasomes in wound healing and fibrosis. *J Pathol,* 229**,** 157-67.

ASHTON-MILLER, J. A. & DELANCEY, J. O. 2007. Functional anatomy of the female pelvic floor. *Ann N Y Acad Sci,* 1101**,** 266-96.

ATRI, C., GUERFALI, F. Z. & LAOUINI, D. 2018. Role of Human Macrophage Polarization in Inflammation during Infectious Diseases. *Int J Mol Sci,* 19.

BARONE, D. G., CARNICER-LOMBARTE, A., TOURLOMOUSIS, P., HAMILTON, R. S., PRATER, M., RUTZ, A. L., DIMOV, I. B., MALLIARAS, G. G., LACOUR, S. P., ROBERTSON, A. A. B., FRANZE, K., FAWCETT, J. W. & BRYANT, C. E. 2022. Prevention of the foreign body response to implantable medical devices by inflammasome inhibition. *Proc Natl Acad Sci U S A,* 119**,** e2115857119.

BARR, S., HILL, E. W. & BAYAT, A. 2017. Functional biocompatibility testing of silicone breast implants and a novel classification system based on surface roughness. *J Mech Behav Biomed Mater,* 75**,** 75-81.

BELPERIO, J. A., DY, M., MURRAY, L., BURDICK, M. D., XUE, Y. Y., STRIETER, R. M. & KEANE, M. P. 2004. The role of the Th2 CC chemokine ligand CCL17 in pulmonary fibrosis. *J Immunol,* 173**,** 4692-8.

BEVILACQUA, M. P., POBER, J. S., WHEELER, M. E., COTRAN, R. S. & GIMBRONE, M. A., JR. 1985. Interleukin 1 acts on cultured human vascular endothelium to increase the adhesion of polymorphonuclear leukocytes, monocytes, and related leukocyte cell lines. *J Clin Invest,* 76**,** 2003-11.

BLATT, S. E., LURIER, E. B., RISSER, G. E. & SPILLER, K. L. 2020. Characterizing the Macrophage Response to Immunomodulatory Biomaterials Through Gene Set Analyses. *Tissue Eng Part C Methods,* 26**,** 156-169.

BOERSEMA, G. S. A., UTOMO, L., BAYON, Y., KOPS, N., VAN DER HARST, E., LANGE, J. F. & BASTIAANSEN-JENNISKENS, Y. M. 2016. Monocyte subsets in blood correlate with obesity related response of macrophages to biomaterials in vitro. *Biomaterials,* 109**,** 32-39.

BORETOS, J. W. & EDEN, M. 1984. *Contemporary Biomaterials: Material and Host Response, Clinical Application, New Technology and Legal Aspects.,* Park Ridge, NJ, Noyes Publications.

BRAUN, G. S., NAGAYAMA, Y., MARUTA, Y., HEYMANN, F., VAN ROEYEN, C. R., KLINKHAMMER, B. M., BOOR, P., VILLA, L., SALANT, D. J., RAFFETSEDER, U., ROSE-JOHN, S., OSTENDORF, T. & FLOEGE, J. 2016. IL-6 Trans-Signaling Drives Murine Crescentic GN. *J Am Soc Nephrol,* 27**,** 132-42.

BRECHT, K., WEIGERT, A., HU, J., POPP, R., FISSLTHALER, B., KORFF, T., FLEMING, I., GEISSLINGER, G. & BRUNE, B. 2011. Macrophages programmed by apoptotic cells promote angiogenesis via prostaglandin E2. *FASEB J,* 25**,** 2408-17.

BROUGHTON, G., 2ND, JANIS, J. E. & ATTINGER, C. E. 2006. The basic science of wound healing. *Plast Reconstr Surg,* 117**,** 12S-34S.

BROWN, B. N., MANI, D., NOLFI, A. L., LIANG, R., ABRAMOWITCH, S. D. & MOALLI, P. A. 2015. Characterization of the host inflammatory response following implantation of prolapse mesh in rhesus macaque. *Am J Obstet Gynecol,* 213**,** 668 e1-10.

BUCALA R, S. L., CHESNEY J, HOGAN M, CERAMI A 1994. Circulating fibrocytes define a new leukocyte subpopulation that mediates tissue repair. *Molecular Medicine*.

CARNICER-LOMBARTE, A., CHEN, S. T., MALLIARAS, G. G. & BARONE, D. G. 2021. Foreign Body Reaction to Implanted Biomaterials and Its Impact in Nerve Neuroprosthetics. *Front Bioeng Biotechnol,* 9**,** 622524.

CHAPPLE, C. R. & MANGERA, A. 2017. Stress Urinary Incontinence. *In:* HAMDY, F. C. & EARDLEY, I. (eds.) *Oxford Textbook of Urological Surgery.* Oxford: Oxford University Press.

CHAUDHURI, V., ZHOU, L. & KARASEK, M. 2007. Inflammatory cytokines induce the transformation of human dermal microvascular endothelial cells into myofibroblasts: a potential role in skin fibrogenesis. *J Cutan Pathol,* 34**,** 146-53.

CLAVE, A., YAHI, H., HAMMOU, J. C., MONTANARI, S., GOUNON, P. & CLAVE, H. 2010. Polypropylene as a reinforcement in pelvic surgery is not inert: comparative analysis of 100 explants. *Int Urogynecol J,* 21**,** 261-70.

CONNOR, T. B., JR., ROBERTS, A. B., SPORN, M. B., DANIELPOUR, D., DART, L. L., MICHELS, R. G., DE BUSTROS, S., ENGER, C., KATO, H., LANSING, M. & ET AL. 1989. Correlation of fibrosis and transforming growth factor-beta type 2 levels in the eye. *J Clin Invest,* 83**,** 1661-6.

CORTES, E., BELAL, M., SAHAI, A. & MORLEY, R. 2017. Pelvic Organ Prolapse. *In:* HAMDY, F. C. & EARDLEY, I. (eds.) *Oxford Textbook of Urological Surgery.* Oxford: Oxford University Press.

CUMBERLEGE, J. 2020. *First do no harm: the report of the Independent Medicines and Medical Devices Safety Review.* [Online]. Available: https://www.gov.uk/government/publications/independent-medicines-and-medical-devices-safety-review-report [Accessed September 2021].

D'ANCONA, C., HAYLEN, B., OELKE, M., ABRANCHES-MONTEIRO, L., ARNOLD, E., GOLDMAN, H., HAMID, R., HOMMA, Y., MARCELISSEN, T., RADEMAKERS, K., SCHIZAS, A., SINGLA, A., SOTO, I., TSE, V., DE WACHTER, S., HERSCHORN, S., STANDARDISATION STEERING COMMITTEE, I. C. S., THE, I. C. S. W. G. O. T. F. M. L. U. T., PELVIC FLOOR, S. & DYSFUNCTION 2019. The International Continence Society (ICS) report on the terminology for adult male lower urinary tract and pelvic floor symptoms and dysfunction. *Neurourol Urodyn,* 38**,** 433-477.

DANESHGARI, F. & MOORE, C. 2007. Pathophysiology of Stress Incontinence in Women. *In:* CHAPPLE, C. R., ZIMMERN, P. E., BRUBAKER, L., SMITH, A. R. B., BO, K. (ed.) *Multidisciplinary Management of Female Pelvic Floor Disorders.* 1 ed. Philadelphia: Churchill Livingstone Elsevier.

DAVIDSON, M. D., BURDICK, J. A. & WELLS, R. G. 2020. Engineered Biomaterial Platforms to Study Fibrosis. *Adv Healthc Mater,* 9**,** e1901682.

DEFIFE, K. M., JENNEY, C. R., MCNALLY, A. K., COLTON, E. & ANDERSON, J. M. 1997. Interleukin-13 induces human monocyte/macrophage fusion and macrophage mannose receptor expression. *J Immunol,* 158**,** 3385-90.

DIEGIDIO, P., FRIEDMAN, H. I., GOURDIE, R. G., RILEY, A. E., YOST, M. J. & GOODWIN, R. L. 2014. Biomedical implant capsule formation: lessons learned and the road ahead. *Ann Plast Surg,* 73**,** 451-60.

DIGITAL, N. 2018. *Retrospective review of surgery for urogynaecological prolapse and stress urinary incontinence using tape or mesh: Hospital Episode Statistics (HES), Experimental Statistics, April 2008 – March 2017.* [Online]. Available: https://files.digital.nhs.uk/D2/99117D/Retrospective_Review_of_Surgery...-_exe.pdf [Accessed 25/6 2024].

DOWNER, M., BERRY, C. E., PARKER, J. B., KAMENI, L. & GRIFFIN, M. 2023. Current Biomaterials for Wound Healing. *Bioengineering (Basel),* 10.

DRAKE, R., VOGL, A., MITCHELL, A., TIBBITTS, R., RICHARDSON, P. AND HORN, A. 2020. *Gray's Anatomy for Students*, Elsevier.

DYER, O. 2016. Johnson and Johnson faces lawsuit over vaginal mesh devices. *BMJ,* 353**,** i3045.

EMING, S. A. 2025. Biology of Wound Healing. *In:* BOLOGNIA, J., SCHAFFER, J. AND CERRONI, L. (ed.) *Dermatology.* 5 ed. Philadelphia: Elsevier.

ESCHE, C., STELLATO, C. & BECK, L. A. 2005. Chemokines: key players in innate and adaptive immunity. *J Invest Dermatol,* 125**,** 615-28.

FADOK, V. A., BRATTON, D. L., KONOWAL, A., FREED, P. W., WESTCOTT, J. Y. & HENSON, P. M. 1998. Macrophages that have ingested apoptotic cells in vitro inhibit proinflammatory cytokine production through autocrine/paracrine mechanisms involving TGF-beta, PGE2, and PAF. *J Clin Invest,* 101**,** 890-8.

FARR, N. T. H., ROMAN, S., SCHAFER, J., QUADE, A., LESTER, D., HEARNDEN, V., MACNEIL, S. & RODENBURG, C. 2021. A novel characterisation approach to reveal the mechano-chemical effects of oxidation and dynamic distension on polypropylene surgical mesh. *RSC Adv,* 11**,** 34710-34723.

FARR, N. T. H., WORKMAN, V. L., SAAD, S., ROMAN, S., HEARNDEN, V., CHAPPLE, C. R., MURDOCH, C., RODENBURG, C. & MACNEIL, S. 2024. Uncovering the relationship between macrophages and polypropylene surgical mesh. *Biomater Adv,* 159**,** 213800.

FDA, U. 2024. *510(k) premarket notification.* [Online]. Available: https://www.accessdata.fda.gov/scripts/cdrh/cfdocs/cfPMN/pmn.cfm?ID=K974098 [Accessed 24/06 2024].

FERRANTE, C. J., PINHAL-ENFIELD, G., ELSON, G., CRONSTEIN, B. N., HASKO, G., OUTRAM, S. & LEIBOVICH, S. J. 2013. The adenosine-dependent angiogenic switch of macrophages to an M2-like phenotype is independent of interleukin-4 receptor alpha (IL-4Ralpha) signaling. *Inflammation,* 36**,** 921-31.

FICHTNER-FEIGL, S., STROBER, W., KAWAKAMI, K., PURI, R. K. & KITANI, A. 2006. IL-13 signaling through the IL-13alpha2 receptor is involved in induction of TGF-beta1 production and fibrosis. *Nat Med,* 12**,** 99-106.

FLANDERS, K. C., REN, R. F. & LIPPA, C. F. 1998. Transforming growth factor-betas in neurodegenerative disease. *Prog Neurobiol,* 54**,** 71-85.

FLANIGAN, P., KSHETTRY, V. R. & BENZEL, E. C. 2014. World War II, tantalum, and the evolution of modern cranioplasty technique. *Neurosurg Focus,* 36**,** E22.

GABBIANI, G. 1996. The Cellular Derivation and the Life Span of the Myofibroblast. *Pathology - Research and Practice,* 192**,** 708-711.

GARBERS, C., HEINK, S., KORN, T. & ROSE-JOHN, S. 2018. Interleukin-6: designing specific therapeutics for a complex cytokine. *Nat Rev Drug Discov,* 17**,** 395-412.

GASSE, P., MARY, C., GUENON, I., NOULIN, N., CHARRON, S., SCHNYDER-CANDRIAN, S., SCHNYDER, B., AKIRA, S., QUESNIAUX, V. F., LAGENTE, V., RYFFEL, B. & COUILLIN, I. 2007. IL-1R1/MyD88 signaling and the inflammasome are essential in pulmonary inflammation and fibrosis in mice. *J Clin Invest,* 117**,** 3786-99.

GERARDUZZI, C. & DI BATTISTA, J. A. 2017. Myofibroblast repair mechanisms post-inflammatory response: a fibrotic perspective. *Inflamm Res,* 66**,** 451-465.

GOLDBERGER, M. A. & DAVIDS, A. M. 1947. The Treatment of Urinary Stress Incontinence by The Implantation of a Tantalum Plate. *American Journal of Obstetrics and Gynecology,* 54**,** 829-837.

GOVERNMENT, S. 2017. *Scottish Independent Review of the use, safety and efficacy of transvaginal mesh implants in the treatment of stress urinary incontinence and pelvic organ prolapse in women.* [Online]. Available: https://www.gov.scot/publications/scottish-independent-review-use-safety-efficacy-transvaginal-mesh-implants-treatment-9781786528711/ [Accessed 25/06 2024].

GROTENHUIS, N., VD TOOM, H. F., KOPS, N., BAYON, Y., DEERENBERG, E. B., MULDER, I. M., VAN OSCH, G. J., LANGE, J. F. & BASTIAANSEN-JENNISKENS, Y. M. 2014. In vitro model to study the biomaterial-dependent reaction of macrophages in an inflammatory environment. *Br J Surg,* 101**,** 983-92.

GU, L., ZHU, Y. J., YANG, X., GUO, Z. J., XU, W. B. & TIAN, X. L. 2007. Effect of TGF-beta/Smad signaling pathway on lung myofibroblast differentiation. *Acta Pharmacol Sin,* 28**,** 382-91.

GUO, J., GU, N., CHEN, J., SHI, T., ZHOU, Y., RONG, Y., ZHOU, T., YANG, W., CUI, X. & CHEN, W. 2013. Neutralization of interleukin-1 beta attenuates silica-induced lung inflammation and fibrosis in C57BL/6 mice. *Arch Toxicol,* 87**,** 1963-1973.

GUO, S. & DIPIETRO, L. A. 2010. Factors affecting wound healing. *J Dent Res,* 89**,** 219-29.

HAMPEL, C., WIENHOLD, D., BENKEN, N., EGGERSMANN, C. & THUROFF, J. W. 1997. Definition of overactive bladder and epidemiology of urinary incontinence. *Urology,* 50**,** 4-14; discussion 15-7.

HAYLEN, B. T., FREEMAN, R. M., SWIFT, S. E., COSSON, M., DAVILA, G. W., DEPREST, J., DWYER, P. L., FATTON, B., KOCJANCIC, E., LEE, J., MAHER, C., PETRI, E., RIZK, D. E., SAND, P. K., SCHAER, G. N., WEBB, R., INTERNATIONAL UROGYNECOLOGICAL, A., INTERNATIONAL CONTINENCE, S. & JOINT, I. I. C. S. W. G. O. C. T. 2011. An International Urogynecological Association (IUGA)/International Continence Society (ICS) joint terminology and classification of the complications related directly to the insertion of prostheses (meshes, implants, tapes) and grafts in female pelvic floor surgery. *Neurourol Urodyn,* 30**,** 2-12.

HENDRIX, S. L., CLARK, A., NYGAARD, I., ARAGAKI, A., BARNABEI, V. & MCTIERNAN, A. 2002. Pelvic organ prolapse in the Women's Health Initiative: gravity and gravidity. *Am J Obstet Gynecol,* 186**,** 1160-6.

HENEGHAN, C. J., GOLDACRE, B., ONAKPOYA, I., ARONSON, J. K., JEFFERSON, T., PLUDDEMANN, A. & MAHTANI, K. R. 2017. Trials of transvaginal mesh devices for pelvic organ prolapse: a systematic database review of the US FDA approval process. *BMJ Open,* 7**,** e017125.

HIGGINBOTHAM, S., WORKMAN, V. L., GIBLIN, A. V., GREEN, N. H., LAMBERT, D. W. & HEARNDEN, V. 2024. Inhibition and reversal of a TGF-beta1 induced myofibroblast phenotype by adipose tissue-derived paracrine factors. *Stem Cell Res Ther,* 15**,** 166.

HOLT, D. J., CHAMBERLAIN, L. M. & GRAINGER, D. W. 2010. Cell-cell signaling in co-cultures of macrophages and fibroblasts. *Biomaterials,* 31**,** 9382-94.

HULSART-BILLSTROM, G., DAWSON, J. I., HOFMANN, S., MULLER, R., STODDART, M. J., ALINI, M., REDL, H., EL HAJ, A., BROWN, R., SALIH, V., HILBORN, J., LARSSON, S. & OREFFO, R. O. 2016. A surprisingly poor correlation between in vitro and in vivo testing of biomaterials for bone regeneration: results of a multicentre analysis. *Eur Cell Mater,* 31**,** 312-22.

HUMERES, C., VIVAR, R., BOZA, P., MUNOZ, C., BOLIVAR, S., ANFOSSI, R., OSORIO, J. M., OLIVARES-SILVA, F., GARCIA, L. & DIAZ-ARAYA, G. 2016. Cardiac fibroblast cytokine profiles induced by proinflammatory or profibrotic stimuli promote monocyte recruitment and modulate macrophage M1/M2 balance in vitro. *J Mol Cell Cardiol*.

IAKOVLEV, V. V., GUELCHER, S. A. & BENDAVID, R. 2017. Degradation of polypropylene in vivo: A microscopic analysis of meshes explanted from patients. *J Biomed Mater Res B Appl Biomater,* 105**,** 237-248.

IMAGEJ. 2024. *Image Intensity Processing* [Online]. Available: https://imagej.net/imaging/image-intensity-processing [Accessed 30/06 2024].

IMEL, A., MALMGREN, T., DADMUN, M., GIDO, S. & MAYS, J. 2015. In vivo oxidative degradation of polypropylene pelvic mesh. *Biomaterials,* 73**,** 131-41.

ISO. 2010. *ISO 10993-13:2010* [Online]. Available: https://www.iso.org/obp/ui#iso:std:iso:10993:-13:ed-2:v1:en [Accessed 26/6 2024].

ISO. 2017. *ISO 10993-4:2017* [Online]. Available: https://www.iso.org/standard/63448.html [Accessed 26/6 2024].

ISO. 2022. *ISO 10993-6:2016* [Online]. Available: https://www.iso.org/standard/61089.html [Accessed 25/6 2024].

JANNASCH, M., GAETZNER, S., WEIGEL, T., WALLES, H., SCHMITZ, T. & HANSMANN, J. 2017. A comparative multi-parametric in vitro model identifies the power of test conditions to predict the fibrotic tendency of a biomaterial. *Sci Rep,* 7**,** 1689.

JONES, J. A., BARBOUR, J. R., STROUD, R. E., BOUGES, S., STEPHENS, S. L., SPINALE, F. G. & IKONOMIDIS, J. S. 2008. Altered transforming growth factor-beta signaling in a murine model of thoracic aortic aneurysm. *J Vasc Res,* 45**,** 457-68.

JONES, J. A., CHANG, D. T., MEYERSON, H., COLTON, E., KWON, I. K., MATSUDA, T. & ANDERSON, J. M. 2007. Proteomic analysis and quantification of cytokines and chemokines from biomaterial surface-adherent macrophages and foreign body giant cells. *J Biomed Mater Res A,* 83**,** 585-96.

KAO, W. J., MCNALLY, A. K., HILTNER, A. & ANDERSON, J. M. 1995. Role for interleukin-4 in foreign-body giant cell formation on a poly(etherurethane urea) in vivo. *J Biomed Mater Res,* 29**,** 1267-75.

KAVIRATNE, M., HESSE, M., LEUSINK, M., CHEEVER, A. W., DAVIES, S. J., MCKERROW, J. H., WAKEFIELD, L. M., LETTERIO, J. J. & WYNN, T. A. 2004. IL-13 activates a mechanism of tissue fibrosis that is completely TGF-beta independent. *J Immunol,* 173**,** 4020-9.

KENDALL, R. T. & FEGHALI-BOSTWICK, C. A. 2014. Fibroblasts in fibrosis: novel roles and mediators. *Front Pharmacol,* 5**,** 123.

KLOSTERHALFEN, B. & KLINGE, U. 2013. Retrieval study at 623 human mesh explants made of polypropylene--impact of mesh class and indication for mesh removal on tissue reaction. *J Biomed Mater Res B Appl Biomater,* 101**,** 1393-9.

KNIGHT, K. M., KING, G. E., PALCSEY, S. L., SUDA, A., LIANG, R. & MOALLI, P. A. 2022. Mesh deformation: A mechanism underlying polypropylene prolapse mesh complications in vivo. *Acta Biomater,* 148**,** 323-335.

KOBASHI, K. C., DMOCHOWSKI, R., MEE, S. L., MOSTWIN, J., NITTI, V. W., ZIMMERN, P. E. & LEACH, G. E. 1999. Erosion of Woven Polyester Pubovaginal Sling. *Journal of Urology,* 162**,** 2070-2072.

KOELBL, H., STRASSEGGER, H., RISS, P. A. & GRUBER, H. 1989. Morphologic and functional aspects of pelvic floor muscles in patients with pelvic relaxation and genuine stress incontinence. *Obstet Gynecol,* 74**,** 789-95.

KOLB, M., MARGETTS, P. J., ANTHONY, D. C., PITOSSI, F. & GAULDIE, J. 2001. Transient expression of IL-1beta induces acute lung injury and chronic repair leading to pulmonary fibrosis. *J Clin Invest,* 107**,** 1529-36.

LAMA, V. N., SMITH, L., BADRI, L., FLINT, A., ANDREI, A. C., MURRAY, S., WANG, Z., LIAO, H., TOEWS, G. B., KREBSBACH, P. H., PETERS-GOLDEN, M., PINSKY, D. J., MARTINEZ, F. J. & THANNICKAL, V. J. 2007. Evidence for tissue-resident mesenchymal stem cells in human adult lung from studies of transplanted allografts. *J Clin Invest,* 117**,** 989-96.

LEE, C. G., HOMER, R. J., COHN, L., LINK, H., JUNG, S., CRAFT, J. E., GRAHAM, B. S., JOHNSON, T. R. & ELIAS, J. A. 2002. Transgenic overexpression of interleukin (IL)-10 in the lung causes mucus metaplasia, tissue inflammation, and airway remodeling via IL-13-dependent and -independent pathways. *J Biol Chem,* 277**,** 35466-74.

LEE, C. G., HOMER, R. J., ZHU, Z., LANONE, S., WANG, X., KOTELIANSKY, V., SHIPLEY, J. M., GOTWALS, P., NOBLE, P., CHEN, Q., SENIOR, R. M. & ELIAS, J. A. 2001. Interleukin-13 induces tissue fibrosis by selectively stimulating and activating transforming growth factor beta(1). *J Exp Med,* 194**,** 809-21.

LEE, J. M., DEDHAR, S., KALLURI, R. & THOMPSON, E. W. 2006. The epithelial-mesenchymal transition: new insights in signaling, development, and disease. *J Cell Biol,* 172**,** 973-81.

LEWIS, C., ZHU, M., LIEU, M., MOODLEY, S., WANG, Y., MCCONAGHY, T., LARNER, B., WIDDOP, R., SOBEY, C., DRUMMOND, G. & KEMP-HARPER, B. 2018. CCL18 as a

Mediator of the Pro-Fibrotic Actions of M2 Macrophages in the Vessel Wall during Hypertension. *The FASEB Journal,* 31.
LI, J., ZHANG, Y. J., LV, Z. Y., LIU, K., MENG, C. X., ZOU, B., LI, K. Y., LIU, F. Z. & ZHANG, B. 2020. The observed difference of macrophage phenotype on different surface roughness of mineralized collagen. *Regen Biomater,* 7**,** 203-211.
LI, L., WANG, X., PARK, J. Y., CHEN, H., WANG, Y. & ZHENG, W. 2017. Pathological findings in explanted vaginal mesh. *Hum Pathol,* 69**,** 46-54.
LIVAK, K. J. & SCHMITTGEN, T. D. 2001. Analysis of relative gene expression data using real-time quantitative PCR and the 2(-Delta Delta C(T)) Method. *Methods,* 25**,** 402-8.
LOCK, A., CORNISH, J. & MUSSON, D. S. 2019. The Role of In Vitro Immune Response Assessment for Biomaterials. *J Funct Biomater,* 10.
LOVE, R. J. & JONES, K. S. 2009. Biomaterials, fibrosis, and the use of drug delivery systems in future antifibrotic strategies. *Crit Rev Biomed Eng,* 37**,** 259-81.
LUO, D. D., FIELDING, C., PHILLIPS, A. & FRASER, D. 2009. Interleukin-1 beta regulates proximal tubular cell transforming growth factor beta-1 signalling. *Nephrol Dial Transplant,* 24**,** 2655-65.
MA, F., LI, Y., JIA, L., HAN, Y., CHENG, J., LI, H., QI, Y. & DU, J. 2012. Macrophage-stimulated cardiac fibroblast production of IL-6 is essential for TGF beta/Smad activation and cardiac fibrosis induced by angiotensin II. *PLoS One,* 7**,** e35144.
MADDAH, H. A. 2016. Polypropylene as a Promising Plastic: A Review. *American Journal of Polymer Science.,* 6**,** 1-11.
MANGIR, N., ALDEMIR DIKICI, B., CHAPPLE, C. R. & MACNEIL, S. 2019. Landmarks in vaginal mesh development: polypropylene mesh for treatment of SUI and POP. *Nat Rev Urol,* 16**,** 675-689.
MARTINEZ, F. O. & GORDON, S. 2014. The M1 and M2 paradigm of macrophage activation: time for reassessment. *F1000Prime Rep,* 6**,** 13.
MAZAHERI, M. K., SCHULTZ, G. S., BLALOCK, T. D., CAFFEE, H. H. & CHIN, G. A. 2003. Role of connective tissue growth factor in breast implant elastomer capsular formation. *Ann Plast Surg,* 50**,** 263-8; discussion 268.
MENG, X. M., NIKOLIC-PATERSON, D. J. & LAN, H. Y. 2016. TGF-beta: the master regulator of fibrosis. *Nat Rev Nephrol,* 12**,** 325-38.
MILANI, A. L., DAMOISEAUX, A., INTHOUT, J., KLUIVERS, K. B. & WITHAGEN, M. I. J. 2018. Long-term outcome of vaginal mesh or native tissue in recurrent prolapse: a randomized controlled trial. *Int Urogynecol J,* 29**,** 847-858.
MILLER, K. M. & ANDERSON, J. M. 1988. Human monocyte/macrophage activation and interleukin 1 generation by biomedical polymers. *J Biomed Mater Res,* 22**,** 713-31.
MILLER, K. M., HUSKEY, R. A., BIGBY, L. F. & ANDERSON, J. M. 1989. Characterization of biomedical polymer-adherent macrophages: interleukin 1 generation and scanning electron microscopy studies. *Biomaterials,* 10**,** 187-96.
MIRZA, R. E., FANG, M. M., ENNIS, W. J. & KOH, T. J. 2013. Blocking interleukin-1beta induces a healing-associated wound macrophage phenotype and improves healing in type 2 diabetes. *Diabetes,* 62**,** 2579-87.
MOIR, J. C. 1968. The gauze-hammock operation. (A modified Aldridge sling procedure). *J Obstet Gynaecol Br Commonw,* 75**,** 1-9.
MOORE, J., ARMSTRONG, J. T. & WILLIS, S. H. 1955. The use of tantalum mesh in cystocele with critical report of ten cases. *Am J Obstet Gynecol,* 69**,** 1127-35.

MORGAN, J. E., FARROW, G. A. & STEWART, F. E. 1985. The Marlex sling operation for the treatment of recurrent stress urinary incontinence: A 16-year review. *American Journal of Obstetrics and Gynecology,* 151**,** 224-226.

MURAKAMI, K., TAKEMURA, T., HINO, S. & YOSHIOKA, K. 1997. Urinary transforming growth factor-beta in patients with glomerular diseases. *Pediatr Nephrol,* 11**,** 334-6.

MURRAY, P. J., ALLEN, J. E., BISWAS, S. K., FISHER, E. A., GILROY, D. W., GOERDT, S., GORDON, S., HAMILTON, J. A., IVASHKIV, L. B., LAWRENCE, T., LOCATI, M., MANTOVANI, A., MARTINEZ, F. O., MEGE, J. L., MOSSER, D. M., NATOLI, G., SAEIJ, J. P., SCHULTZE, J. L., SHIREY, K. A., SICA, A., SUTTLES, J., UDALOVA, I., VAN GINDERACHTER, J. A., VOGEL, S. N. & WYNN, T. A. 2014. Macrophage activation and polarization: nomenclature and experimental guidelines. *Immunity,* 41**,** 14-20.

MUTSAERS, S. E., BISHOP, J. E., MCGROUTHER, G. & LAURENT, G. J. 1997. Mechanisms of tissue repair: from wound healing to fibrosis. *The International Journal of Biochemistry & Cell Biology,* 29**,** 5-17.

NICE. 2020. *Recommendations | Urinary Incontinence And Pelvic Organ Prolapse In Women: Management | Guidance | NICE.* [Online]. Available: https://www.nice.org.uk/guidance/ng123/chapter/Recommendations#surgery-for-women-with-both-stress-urinary-incontinence-and-pelvic-organ-prolapse [Accessed 25/06 2024].

NITTI, V. W. & COMBS, A. J. 1996. Correlation of Valsalva leak point pressure with subjective degree of stress urinary incontinence in women. *J Urol,* 155**,** 281-5.

NOLFI, A. L., BROWN, B. N., LIANG, R., PALCSEY, S. L., BONIDIE, M. J., ABRAMOWITCH, S. D. & MOALLI, P. A. 2016. Host response to synthetic mesh in women with mesh complications. *Am J Obstet Gynecol,* 215**,** 206 e1-8.

NOSKOVICOVA, N., SCHUSTER, R., VAN PUTTEN, S., EZZO, M., KOEHLER, A., BOO, S., COELHO, N. M., GRIGGS, D., RUMINSKI, P., MCCULLOCH, C. A. & HINZ, B. 2021. Suppression of the fibrotic encapsulation of silicone implants by inhibiting the mechanical activation of pro-fibrotic TGF-beta. *Nat Biomed Eng,* 5**,** 1437-1456.

NYGAARD, I., BRUBAKER, L., ZYCZYNSKI, H. M., CUNDIFF, G., RICHTER, H., GANTZ, M., FINE, P., MENEFEE, S., RIDGEWAY, B., VISCO, A., WARREN, L. K., ZHANG, M. & MEIKLE, S. 2013. Long-term outcomes following abdominal sacrocolpopexy for pelvic organ prolapse. *JAMA,* 309**,** 2016-24.

O'REILLY, S., CIECHOMSKA, M., CANT, R. & VAN LAAR, J. M. 2014. Interleukin-6 (IL-6) trans signaling drives a STAT3-dependent pathway that leads to hyperactive transforming growth factor-beta (TGF-beta) signaling promoting SMAD3 activation and fibrosis via Gremlin protein. *J Biol Chem,* 289**,** 9952-60.

ORENSTEIN, S. B., SABERSKI, E. R., KREUTZER, D. L. & NOVITSKY, Y. W. 2012. Comparative analysis of histopathologic effects of synthetic meshes based on material, weight, and pore size in mice. *J Surg Res,* 176**,** 423-9.

PARK, S., PARK, M., KIM, B. H., LEE, J. E., PARK, H. J., LEE, S. H., PARK, C. G., KIM, M. H., KIM, R., KIM, E. H., HEO, C. Y. & CHOY, Y. B. 2015. Acute suppression of TGF-ss with local, sustained release of tranilast against the formation of fibrous capsules around silicone implants. *J Control Release,* 200**,** 125-37.

PARKS, A. C., SUNG, K. & WU, B. M. 2014. A three-dimensional in vitro model to quantify inflammatory response to biomaterials. *Acta Biomater,* 10**,** 4742-4749.

PARKS, A. G., PORTER, N. H. & MELZAK, J. 1962. Experimental study of the reflex mechanism controlling the muscle of the pelvic floor. *Dis Colon Rectum,* 5**,** 407-14.

PETKOVIC, M., MOURITZEN, M. V., MOJSOSKA, B. & JENSSEN, H. 2021. Immunomodulatory Properties of Host Defence Peptides in Skin Wound Healing. *Biomolecules,* 11.

PETROS, P. 2015. Creating a gold standard surgical device: scientific discoveries leading to TVT and beyond: Ulf Ulmsten Memorial Lecture 2014. *Int Urogynecol J,* 26**,** 471-6.

PETROS, P. E. & ULMSTEN, U. I. 1993. An integral theory and its method for the diagnosis and management of female urinary incontinence. *Scand J Urol Nephrol Suppl,* 153**,** 1-93.

PLOEGER, D. T., HOSPER, N. A., SCHIPPER, M., KOERTS, J. A., DE ROND, S. & BANK, R. A. 2013. Cell plasticity in wound healing: paracrine factors of M1/ M2 polarized macrophages influence the phenotypical state of dermal fibroblasts. *Cell Commun Signal,* 11**,** 29.

POHLMAN, T. H., STANNESS, K. A., BEATTY, P. G., OCHS, H. D. & HARLAN, J. M. 1986. An endothelial cell surface factor(s) induced in vitro by lipopolysaccharide, interleukin 1, and tumor necrosis factor-alpha increases neutrophil adherence by a CDw18-dependent mechanism. *J Immunol,* 136**,** 4548-53.

QUAN, T. E., COWPER, S. E. & BUCALA, R. 2006. The role of circulating fibrocytes in fibrosis. *Curr Rheumatol Rep,* 8**,** 145-50.

QUANTITECT. 2022. *QuantiTect Reverse Transcription Handbook* [Online]. Available: https://www.qiagen.com/us/resources/download.aspx?id=f0de5533-3dd1-4835-8820-1f5c088dd800&lang=en [Accessed 08/08 2022].

ROBBINS, S., COTRAN, R., KUMAR, V., ABBAS, A., ASTER, J. AND PERKINS, J. 2020. *Robbins & Cotran Pathologic Basis Of Disease.,* Philadelphia, Elsevier.

RODRIGUEZ-MIAS, N. L., MARTINEZ-FRANCO, E., AGUADO, J., SANCHEZ, E. & AMAT-TARDIU, L. 2015. Pelvic organ prolapse and stress urinary incontinence, do they share the same risk factors? *Eur J Obstet Gynecol Reprod Biol,* 190**,** 52-7.

ROLFE, B., MOONEY, J., ZHANG, B., JAHNKE, S., LE, S.-J., CHAU, Y.-Q., HUANG, Q., WANG, H., CAMPBELL, G. & CAMPBELL, J. 2011. The Fibrotic Response to Implanted Biomaterials: Implications for Tissue Engineering. *Regenerative Medicine and Tissue Engineering - Cells and Biomaterials.*

ROMAN, S., MANGIR, N., HYMPANOVA, L., CHAPPLE, C. R., DEPREST, J. & MACNEIL, S. 2019. Use of a simple in vitro fatigue test to assess materials used in the surgical treatment of stress urinary incontinence and pelvic organ prolapse. *Neurourol Urodyn,* 38**,** 107-115.

RUTMAN, M. P. & BLAIVAS, J. G. 2009. Surgery for Stress Urinary Incontinence: Historical Review. *In:* BADLANI, G. H., DAVILA, G.W., MICHEL, M.C., DE LA ROSETTE, J.J.M.C.H. (ed.) *Continence.* London: Springer.

SCARPERO, H. M., DMOCHOWSKI, R. R. 2007. Pelvic Anatomy for the Surgeon. *In:* CHAPPLE, C. R., ZIMMERN, P. E., BRUBAKER, L., SMITH, A. R. B., BO, K. (ed.) *Multidisciplinary Management of Female Pelvic Floor Disorders.* 1 ed. Philadelphia: Churchill Livingstone Elsevier.

SEIFALIAN, A., BASMA, Z., DIGESU, A. & KHULLAR, V. 2023. Polypropylene Pelvic Mesh: What Went Wrong and What Will Be of the Future? *Biomedicines,* 11.

SETTEN, E., CASTAGNA, A., NAVA-SEDENO, J. M., WEBER, J., CARRIERO, R., REPPAS, A., VOLK, V., SCHMITZ, J., GWINNER, W., HATZIKIROU, H., FEUERHAKE, F. & LOCATI, M. 2022. Understanding fibrosis pathogenesis via modeling macrophage-fibroblast interplay in immune-metabolic context. *Nat Commun,* 13**,** 6499.

SHEIKH, Z., BROOKS, P. J., BARZILAY, O., FINE, N. & GLOGAUER, M. 2015. Macrophages, Foreign Body Giant Cells and Their Response to Implantable Biomaterials. *Materials (Basel),* 8**,** 5671-5701.

SIME, P. J., XING, Z., GRAHAM, F. L., CSAKY, K. G. & GAULDIE, J. 1997. Adenovector-mediated gene transfer of active transforming growth factor-beta1 induces prolonged severe fibrosis in rat lung. *J Clin Invest,* 100**,** 768-76.

SMITH, T. M., SMITH, S. C., DELANCEY, J. O., FENNER, D. E., SCHIMPF, M. O., ROH, M. H. & MORGAN, D. M. 2013. Pathologic evaluation of explanted vaginal mesh: interdisciplinary experience from a referral center. *Female Pelvic Med Reconstr Surg,* 19**,** 238-41.

SONG, E., OUYANG, N., HORBELT, M., ANTUS, B., WANG, M. & EXTON, M. S. 2000. Influence of alternatively and classically activated macrophages on fibrogenic activities of human fibroblasts. *Cell Immunol,* 204**,** 19-28.

SPILLER, K. L., ANFANG, R. R., SPILLER, K. J., NG, J., NAKAZAWA, K. R., DAULTON, J. W. & VUNJAK-NOVAKOVIC, G. 2014. The role of macrophage phenotype in vascularization of tissue engineering scaffolds. *Biomaterials,* 35**,** 4477-88.

SPILLER, K. L., NASSIRI, S., WITHEREL, C. E., ANFANG, R. R., NG, J., NAKAZAWA, K. R., YU, T. & VUNJAK-NOVAKOVIC, G. 2015. Sequential delivery of immunomodulatory cytokines to facilitate the M1-to-M2 transition of macrophages and enhance vascularization of bone scaffolds. *Biomaterials,* 37**,** 194-207.

SRIDHARAN, R., CAMERON, A. R., KELLY, D. J., KEARNEY, C. J. & O'BRIEN, F. J. 2015. Biomaterial based modulation of macrophage polarization: a review and suggested design principles. *Materials Today,* 18**,** 313-325.

STEDMAN'S 2012. *Stedman's Medical Dictionary*, Lippincott, Williams and Wilkins.

STEEN, E. H., WANG, X., BALAJI, S., BUTTE, M. J., BOLLYKY, P. L. & KESWANI, S. G. 2020. The Role of the Anti-Inflammatory Cytokine Interleukin-10 in Tissue Fibrosis. *Adv Wound Care (New Rochelle),* 9**,** 184-198.

STOFFEL, J. T., BRESETTE, J. F. & SMITH, J. J. 2002. Retropubic surgery for stress urinary incontinence. *Urologic Clinics of North America,* 29**,** 585-596.

SUBAK, L. L., WAETJEN, L. E., VAN DEN EEDEN, S., THOM, D. H., VITTINGHOFF, E. & BROWN, J. S. 2001. Cost of pelvic organ prolapse surgery in the United States. *Obstet Gynecol,* 98**,** 646-51.

TALLEY, A. D., ROGERS, B. R., IAKOVLEV, V., DUNN, R. F. & GUELCHER, S. A. 2017. Oxidation and degradation of polypropylene transvaginal mesh. *J Biomater Sci Polym Ed,* 28**,** 444-458.

TANG, L., JENNINGS, T. A. & EATON, J. W. 1998. Mast cells mediate acute inflammatory responses to implanted biomaterials. *Proc Natl Acad Sci U S A,* 95**,** 8841-6.

TARIQUE, A. A., LOGAN, J., THOMAS, E., HOLT, P. G., SLY, P. D. & FANTINO, E. 2015. Phenotypic, functional, and plasticity features of classical and alternatively activated human macrophages. *Am J Respir Cell Mol Biol,* 53**,** 676-88.

THIERY, J. P. & SLEEMAN, J. P. 2006. Complex networks orchestrate epithelial-mesenchymal transitions. *Nat Rev Mol Cell Biol,* 7**,** 131-42.

THOMAS, D., DEMETRES, M., ANGER, J. T. & CHUGHTAI, B. 2018. Histologic Inflammatory Response to Transvaginal Polypropylene Mesh: A Systematic Review. *Urology,* 111**,** 11-22.

TRINCHIERI, G. 1995. Interleukin-12: a proinflammatory cytokine with immunoregulatory functions that bridge innate resistance and antigen-specific adaptive immunity. *Annu Rev Immunol,* 13**,** 251-76.
TURNER, D. A., SHAW, C., MCGROTHER, C. W., DALLOSSO, H. M., COOPER, N. J. & TEAM, M. R. C. I. 2004. The cost of clinically significant urinary storage symptoms for community dwelling adults in the UK. *BJU Int,* 93**,** 1246-52.
ULMSTEN, U. & PETROS, P. 1995. Intravaginal slingplasty (IVS): an ambulatory surgical procedure for treatment of female urinary incontinence. *Scand J Urol Nephrol,* 29**,** 75-82.
VASCONCELOS, D. P. 3D chitosan scaffolds impair NLRP3 inflammasome response in macrophages.
VASCONCELOS, D. P., AGUAS, A. P. & BARBOSA, J. N. 2022. The inflammasome in biomaterial-driven immunomodulation. *J Tissue Eng Regen Med,* 16**,** 1109-1120.
VASCONCELOS, D. P., AGUAS, A. P., BARBOSA, M. A., PELEGRIN, P. & BARBOSA, J. N. 2019. The inflammasome in host response to biomaterials: Bridging inflammation and tissue regeneration. *Acta Biomater,* 83**,** 1-12.
WAKEFIELD, L. M. & HILL, C. S. 2013. Beyond TGFbeta: roles of other TGFbeta superfamily members in cancer. *Nat Rev Cancer,* 13**,** 328-41.
WALTERS, M., KARRAM, M. 2007. *Urogynaecology and Reconstructive Pelvic Surgery,* Philadelphia, Mosby Elsevier.
WALTERS, M. D. & RIDGEWAY, B. M. 2013. Surgical treatment of vaginal apex prolapse. *Obstet Gynecol,* 121**,** 354-374.
WANG, A. C., LEE, L. Y., LIN, C. T. & CHEN, J. R. 2004. A histologic and immunohistochemical analysis of defective vaginal healing after continence taping procedures: a prospective case-controlled pilot study. *Am J Obstet Gynecol,* 191**,** 1868-74.
WANG, H., KLOSTERHALFEN, B., KLINGE, U., MULLEN, A. & JOCKENHOEVEL, S. 2023. Influence of polypropylene mesh degradation on tissue inflammatory reaction. *J Biomed Mater Res A,* 111**,** 1110-1119.
WARD, K. L., HILTON, P., UK & IRELAND, T. V. T. T. G. 2008. Tension-free vaginal tape versus colposuspension for primary urodynamic stress incontinence: 5-year follow up. *BJOG,* 115**,** 226-33.
WESTMAN, J. & GRINSTEIN, S. 2020. Determinants of Phagosomal pH During Host-Pathogen Interactions. *Front Cell Dev Biol,* 8**,** 624958.
WILSON, L., BROWN, J. S., SHIN, G. P., LUC, K. O. & SUBAK, L. L. 2001. Annual direct cost of urinary incontinence. *Obstet Gynecol,* 98**,** 398-406.
WILSON, M. S., MADALA, S. K., RAMALINGAM, T. R., GOCHUICO, B. R., ROSAS, I. O., CHEEVER, A. W. & WYNN, T. A. 2010. Bleomycin and IL-1beta-mediated pulmonary fibrosis is IL-17A dependent. *J Exp Med,* 207**,** 535-52.
WIPFF, P. J., RIFKIN, D. B., MEISTER, J. J. & HINZ, B. 2007. Myofibroblast contraction activates latent TGF-beta1 from the extracellular matrix. *J Cell Biol,* 179**,** 1311-23.
WITHEREL, C. E., ABEBAYEHU, D., BARKER, T. H. & SPILLER, K. L. 2019. Macrophage and Fibroblast Interactions in Biomaterial-Mediated Fibrosis. *Adv Healthc Mater,* 8**,** e1801451.
WITHEREL, C. E., GRANEY, P. L. & SPILLER, K. L. 2018. In Vitro Model of Macrophage-Biomaterial Interactions. *In:* CHAWLA, K. (ed.) *Biomaterials for Tissue Engineering: Methods and Protocols.* Springer Nature.

WITHEREL, C. E., SAO, K., BRISSON, B. K., HAN, B., VOLK, S. W., PETRIE, R. J., HAN, L. & SPILLER, K. L. 2021. Regulation of extracellular matrix assembly and structure by hybrid M1/M2 macrophages. *Biomaterials,* 269**,** 120667.

WOHLRAB, K. J., EREKSON, E. A. & MYERS, D. L. 2009. Postoperative erosions of the Mersilene suburethral sling mesh for antiincontinence surgery. *Int Urogynecol J Pelvic Floor Dysfunct,* 20**,** 417-20.

XU, J., LAMOUILLE, S. & DERYNCK, R. 2009. TGF-β-induced epithelial to mesenchymal transition. *Cell Research,* 19**,** 156-172.

YU, T., WANG, W., NASSIRI, S., KWAN, T., DANG, C., LIU, W. & SPILLER, K. L. 2016. Temporal and spatial distribution of macrophage phenotype markers in the foreign body response to glutaraldehyde-crosslinked gelatin hydrogels. *J Biomater Sci Polym Ed,* 27**,** 721-42.

ZHOU, G., LIEDMANN, A., CHATTERJEE, C. & GROTH, T. 2017. In vitro study of the host responses to model biomaterials via a fibroblast/macrophage co-culture system. *Biomaterials Science,* 5**,** 141-152.

ZHU, L. M., SCHUSTER, P. & KLINGE, U. 2015. Mesh implants: An overview of crucial mesh parameters. *World J Gastrointest Surg,* 7**,** 226-36.

ZHU, Z., DING, J., MA, Z., IWASHINA, T. & TREDGET, E. E. 2017. Alternatively activated macrophages derived from THP-1 cells promote the fibrogenic activities of human dermal fibroblasts. *Wound Repair Regen,* 25**,** 377-388.

ZHU, Z., HOMER, R. J., WANG, Z., CHEN, Q., GEBA, G. P., WANG, J., ZHANG, Y. & ELIAS, J. A. 1999. Pulmonary expression of interleukin-13 causes inflammation, mucus hypersecretion, subepithelial fibrosis, physiologic abnormalities, and eotaxin production. *J Clin Invest,* 103**,** 779-88.